

Some Fundamental Achievements in EEG Analytics

Alexey Kulaichev

This monograph includes eight fundamental studies on EEG analysis: 1) disadvantages and errors of coherent analysis; 2) errors in spectral estimates of EEG amplitude compared to direct amplitude measurements; 3) the new method for analyzing EEG synchrony by envelope correlation which is very effective for differentiating various diseases and functional states; 4) differentiation of norm and schizophrenia by analysis of EEG correlation synchrony; 5) the changes in EEG synchrony at depressive deviations; 6) the analysis of EEG synchronism and amplitude relationship in all-night sleep; 7) the solution to the problem of choosing the optimal reference electrode for EEG recording; 8) the free available software tools for EEG complex group analysis. The book contains various materials suitable for students, researchers and academicians.

Dr Alexey Kulaichev is a Professor at the Biological department of Moscow State University, Russia. He has 52 years of research and academic experience. His research area includes applied mathematics, systems analytics, programs development, physiology, cardiology, psychology, psychiatry, set theory, gravity theory, history, philosophy, religion, oriental studies, indology, and sport. He has published over 100 articles, 15 monographs and textbooks, have 4 patents. He has received two state medals, two state certificates of appreciation, and an honorary academic title from Moscow University.

**Cambridge
Scholars
Publishing**



9 781036 415976

978-1-0364-1597-6

www.cambridgescholars.com

Cover art: *CSP CDi (180)*, by CSP

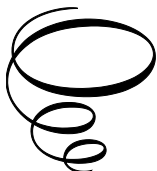
Some Fundamental Achievements in EEG Analytics

Some Fundamental Achievements in EEG Analytics

By

Alexey Kulaichev

Cambridge
Scholars
Publishing



Some Fundamental Achievements in EEG Analytics

By Alexey Kulaichev

This book first published 2024

Cambridge Scholars Publishing

Lady Stephenson Library, Newcastle upon Tyne, NE6 2PA, UK

British Library Cataloguing in Publication Data

A catalogue record for this book is available from the British Library

Copyright © 2024 by Alexey Kulaichev

All rights for this book reserved. No part of this book may be reproduced, stored in a retrieval system, or transmitted, in any form or by any means, electronic, mechanical, photocopying, recording or otherwise, without the prior permission of the copyright owner.

ISBN: 978-1-0364-1597-6

ISBN (Ebook): 978-1-0364-1598-3

CONTENTS

Abstract	vi
Chapter 1	1
Disadvantages and Errors of Coherence Analysis	
Chapter 2	19
Inaccuracy of EEG Estimates based on Power Spectrum	
Chapter 3	34
Correlation of EEG Envelopes is the Best Method for Identifying Mental Diseases, Functional States, Individual and Intergroup Differences	
Chapter 4	53
Effective Differentiation of Norm and Schizophrenia by Analysis of EEG Correlation Synchrony	
Chapter 5	78
The Changes of EEG Correlation Synchrony at Depressive Deviations of Advanced Age	
Chapter 6	92
Comparative Analysis of EEG Correlation Synchronism and EEG Amplitude Relationship in All-night Sleep	
Chapter 7	111
Optimal Choice of Reference Electrode for EEG Recording	
Chapter 8	123
Software Tools for EEG Complex Group Analysis	

ABSTRACT

This monograph includes eight fundamental studies on EEG analysis: 1) disadvantages and errors of coherent analysis; 2) errors in spectral estimates of EEG amplitude compared to direct amplitude measurements; 3) the new method for analyzing EEG synchronicity by envelopes correlation which is very effective for differentiating of various diseases and functional states; 4) differentiation of norm and schizophrenia by analysis of EEG correlation synchrony; 5) the changes in EEG synchrony at depressive deviations; 6) the analysis of EEG synchronism and amplitude relationship in all-night sleep; 7) the solution the problem of choosing the optimal reference electrode for EEG recording; 8) the free available software tools for EEG complex group analysis. The book contains various materials suitable for students, researchers and academicians.

Keywords: EEG; metrology; coherence; spectral analysis; amplitude and power spectrum, amplitude modulation; filtration, discriminant classification; envelopes correlation; schizophrenia; depression, sleep stages, reference electrode.

CHAPTER 1

DISADVANTAGES AND ERRORS OF COHERENCE ANALYSIS

ABSTRACT

Methodological and computational errors that are common in EEG coherence analysis are described. A comprehensive review of the fundamental problems in coherence functions reveals that this metric cannot be trusted as a reliable and effective predictor of EEG synchronization.

Keywords: Coherence; spectral analysis; EEG non-stationarity; amplitude modulation.

INTRODUCTION

The first application of mathematical methods into electroencephalography is traditionally associated with N. Viner, who proposed the use of correlation analysis in 1936, taking the EEG to be a stationary wave process. The intensive application of mathematical methods characterized the first stage in the development of computerized electrophysiology [1, (pp. 20–32)]. This was taken up by physiologists and the engineers working with them with great enthusiasm. However, professional mathematicians, who do not see any great scientific prestige from immersing themselves deeply in this field, generally restrict themselves to overall theoretical positions expressed in general terms. The introduction of mathematical methods by technical specialists led to the diffusion of a wide range of incorrect and even erroneous methods, viewpoints, and concepts among physiologists. In particular, the two fundamental differences between EEG signals and most other physical signals are not considered: a) fundamental non-stationarity; b) amplitude modulation at all frequency ranges. This applies to a particularly critical extent to coherence analysis, to which attention has been drawn previously [2].

SOURCES

According to [3, (p. 138)], “Goodman first proposed the so-called coherence function in 1960 [4] and studies reported in [5] its first use in the analysis of brain bioelectrical activity.” On the one hand, studies in [4] did not consider or mention coherence, while spectral analysis methods had been developed long before this and were resumed in basic monographs from well known authors such as Bartlett (1955), Bendat (1958), Blackman and Tewkey (1959), and others. On the other hand, the coherence formula as applied to electrophysiology was introduced and commented on (without source references) by one of the authors of [5] in later studies [6].

It should also be noted that the extensive specialist literature on coherence has a number of deficiencies. Thus, the coherence function for processes $x(t)$ and $y(t)$ (some- times termed coherence squared) is usually stated as:

$$\gamma^2(f) = \frac{|G_{xy}(f)|^2}{G_x(f)G_y(f)}, \quad (1)$$

where $|G_{xy}(f)|$ is the modulus of the complex-valued cross spectrum, and $G_x(f)$ and $G_y(f)$ are the power spectra of processes $x(t)$ and $y(t)$.

Most sources [7, p. 146; 3, p. 138; 8, p. 342; 9, p. 36; 6, p. 172], apart from citing Equation (1), which gives a value of unity, provide no elaboration. Only a few monographs [10, p. 271] clarify that the numerator and denominator are *averaged for the ensemble* (averaged spectra calculated for sequential analysis epochs). However, nowhere is it stated which of the several possible types of averaging should be used in Equation (1).

Subsequently, after first defining Equation (1) on p. 146 in [7], it was repeated many times in the text, though the need for averaging across the ensemble is explained (and then quite indirectly) only in a special addendum of terms on p. 517. An even more confused situation is found in [11]: on p. 138 of volume 2, i.e., long after Equation (1) on p. 112, the discussion of smoother evaluations of coherence makes reference to correlational and spectral windows on p. 294 of volume 1, which in turn refers to the previous description (p. 289) of the Bartlett smoothing method. In [12, p. 463], there is an analogous coherence equation, whose numerator is defined by a previous Fourier transformation from a correlational function with an erroneous reference to chapter 3, though it is in fact defined in chapter 4, p. 43, using averaging over a time interval,

which should also be recognized as a very confused way of explaining the need for the numerator of Equation (1) to include complex-valued averaging of the ensemble in a frequency range, which is far from obvious in relation to matching of the results. In [8, p. 330], the unquoted coherence Equation (1) is given immediately after exposition of various methods of averaging spectra, including averaging using a sliding frequency window (the Daniel method [8, p. 322]), which creates the false illusion that this averaging can also be applied to calculating coherence. It remains possible that calculation of this “pseudocoherence” has been used. Furthermore, most specialist monographs make wide use of mathematical computation in an integral form, far from real cases of time-limited and sampled signals.

With respect to this confused situation, there is a need for a brief discussion of the basic mathematical relationships using a simplified example.

MATHEMATICAL DEFINITIONS

Let there be two monoharmonic and centered processes with some frequency f

$$\begin{aligned} x(t) &= a\cos 2\pi ft + b\sin 2\pi ft; \\ y(t) &= c\cos 2\pi ft + d\sin 2\pi ft. \end{aligned} \tag{2}$$

If a whole number of the periods of these processes fall within an analysis epoch, then the coefficients a , b , c , and d will be (in complex-valued spectra $X(f)$, $Y(f)$) the real and imaginary parts of the discrete Fourier transform (DFT) for frequency f

$$X(f) = a + ib; \quad Y(f) = c + id \tag{3}$$

where i is the imaginary term.

The power spectra of these processes are the squares of the moduli of $X(f)$ and $Y(f)$, i.e., the squares of their amplitude spectra $A_x(f)$, $A_y(f)$.

$$\begin{aligned} G_x(f) &= A_x(f)^2 = a^2 + b^2; \\ G_y(f) &= A_y(f)^2 = c^2 + d^2; \end{aligned} \tag{4}$$

and the phase spectra are given by

$$\varphi_x(f) = \arctan(b/a); \quad \varphi_y(f) = \arctan(d/c). \quad (5)$$

We note that on the complex plane, any spectral component, for example $X(f)$, is represented by a vector whose length is defined by the modulus $|X(f)|$ and the angular position by the phase $\phi_x(f)$, its components a and b being the projections of the vector onto the real and imaginary axes.

The complex-valued cross spectrum of processes $x(t), y(t)$ is defined by

$$G_{xy}(f) = e + ig, \quad (6)$$

where $e = ac + bd$, $g = bc - ad$.

The modulus of the cross spectrum is given by the product of the amplitude spectra of the two processes

$$\begin{aligned} |G_{xy}(f)| &= \sqrt{e^2 + g^2} = \\ &= \sqrt{(ac + bd)^2 + (bc - ad)^2} = \\ &= \sqrt{G_x(f)} \sqrt{G_y(f)}, \end{aligned} \quad (7)$$

and its phase spectrum is given by the difference between the phase spectra of the two processes

$$\varphi_x(f) = \arctan(g/e) = \varphi_x(f) - \varphi_y(f). \quad (8)$$

We will use $E[\dots]$ to indicate the operation of averaging for the ensemble for non-overlapping epochs (Bartlett method). One possible averaging formula for calculating the square of the coherence will then be of the form

$$\gamma^2(f) = \frac{|E[G_{xy}(f)]|^2}{E[G_x(f)]E[G_y(f)]}, \quad (9)$$

Where

$$\begin{aligned}
 |E[G_{xy}(f)]| &= \sqrt{E[e]^2 + E[g]^2} = \\
 &= \sqrt{E[ac + bd]^2 + E[bd - ad]^2}, \\
 E[G_x(f)] &= E[a^2 + b^2].
 \end{aligned}$$

In relation to the vagueness noted above, it is of note that Equation (9) does not occur in the widely available literature.

Discussion of the significance of coherence in EEG studies continues to the present day, for example in [13] (contemporary “improvements” in coherence analysis require separate evaluation), where in contrast to Equation (1), as in the physiological primary source noted previously [6], a non-squared coherence formula is presented.

COHERENCE IN TECHNICAL ADDENDA

Methods for spectral analysis were initially used for signals of physical origin and were only later applied to EEG investigations. In technical addenda, coherence is used as a particularly second-degree characteristic – only for evaluating the significance of other cross-spectral characteristics and for defining measures of the influence on them of noise and/or nonlinearity. Decreases in coherence values can result from the following main causes [7, p. 179; 10, p. 271]: 1) presence of non-correlating noises in signals determining instability in the phase of the cross spectrum over time; 2) the presence of nonlinear relationships between processes; 3) leakage of power determined by inadequate frequency resolution, i.e., observation periods of insufficient duration; 4) the presence of time delays on transfer of interactions between two processes commensurate with the observation interval.

Small coherence values can indicate the insignificance, at the frequency being addressed, of other cross-spectral characteristics or can indicate the need to increase the number of averagings to eliminate the effects of noise.

The cardinal difference is that signals of physical origin often *truly have* stationary harmonics created by *real* sources: radio stations operating at their characteristic frequency; errors in the geometry of the moving part of a mechanism inducing vibration, etc. By recording the radio background at different locations at the frequency of a given radio station, we will at any

time point have a fixed phase difference (determined by the distance of the measuring points from the source). If there is radio noise at this frequency, then the cross-phase of this harmonic will show some degree or other of change; coherence allows this variability to be evaluated and increases in the number of averagings allow it to be decreased.

In the brain there are *actually no* harmonic oscillators or anything producing stationary reflections in the EEG. Arbitrarily dividing the frequency band into spectral lines (defined by the duration of the analysis epoch), Fourier transformation yields pseudoharmonics as a result of interference between a multiplicity of uncontrolled and unknown factors, and these harmonics change from epoch to epoch. This is reflected primarily on instantaneous autospectra, where each harmonic does not have a smooth transition at the boundary of two neighboring analysis epochs, but rather sharp, random jumps in amplitude, and, consequently, in phase. These jumps are then reproduced in the cross- phase of the two processes and hence in coherence values.

In summary, we can conclude that the large and unique value that coherence has acquired in EEG studies as compared with its background position in primary sources is ungrounded. Coherence was developed to solve other tasks and is based on other premises, so efforts should have been made to find and construct more appropriate and reliable measures at the very beginning of its EEG application.

THE NEEDS OF ELECTROPHYSIOLOGY

In the physiology of higher nervous activity, it is important to have reliable assessments of different aspects of the synchronicity of EEG processes. When high synchronicity is present, the presence of different types of physiological relationships between processes can be proposed and verified: the effects of one process on the other, the influence of a common source on both processes, and detection of topographical patterns of highly synchronized relationships with the aim of differentiating functional states, personal characteristics, normal and pathological, the effects of drugs, etc.

The attraction of coherence for these purposes appears largely to result from the repeatedly published and insufficiently discussed proposition that coherence in a frequency range is an analog of the Pearson correlation coefficient over a time period [11, p. 112; 8, p. 342; 10, p. 270; 9, p. 36; 6, p. 172]. As will be shown twice, these propositions are quite far from

reality. Here, in particular, we will note that a) coherence (Equation (1)) can relate only to the square of the correlation coefficient, which in practice is extremely rarely used; b) unlike coherence, the range of values of the correlation coefficient is from -1 to $+1$.

INTERPRETATION OF COHERENCE

Equation (9) does not give a direct and clear informative interpretation of coherence. We will therefore consider another acceptable version of Equation (1) [1, p. 196], whose denominator is a transformation using Equation (7):

$$\begin{aligned}\gamma^2(f) &= \frac{|E[G_{xy}(f)]|^2}{E[G_x(f)G_y(f)]} = \\ &= \frac{|E[G_{xy}(f)]|^2}{E[|G_{xy}(f)|^2]},\end{aligned}\tag{10}$$

which, to distinguish it from γ^2 , we will henceforth term *phase coherence* (we note that this order of averaging comes from an illustration [10, p. 270] of the addition of cross- spectrum vectors in the complex plane).

This assessment is a good approximation to γ^2 : a) the correlation between them in the range $\gamma^2 = 0-1$ is greater than 0.95; b) the mean difference between values is less than 0.074. In addition, evaluation of $\square \square 2$ has a clear interpretation [10, p. 270]: the numerator contains the geometric sum of the cross- spectrum vectors for sequential analysis epochs and the denominator contains the arithmetic sum of the vector lengths. Therefore, the more randomly the phase of the cross-spectrum changes, the smaller the numerator will be in comparison with the denominator. The stable the cross- spectrum phase, the closer the numerator will be to the denominator. Thus, *phase coherence* is a better indicator of the stability/instability of the phase difference (Equation (8)) between two processes.

$\square 2$ coherence partially inherits this property of reflecting synchronicity, but its significance depends not only on the stability of the phase difference between the two processes, but also on their amplitude stability, this being quite complex. Despite the equivalence of the denominators in Equations (9) and (10) in relation to Equation (7), they differ in terms of

the order of averaging. Thus (as illustrated by the numerical example in Table 1.1), the denominator in Equation (9) decreases not proportionally to the numerator, but to progressively lesser extents, in response to increases in the amplitude variability of the processes; in this it contrasts with the denominator in Equation (10).

Table 1.1. Relationship between coherence and amplitude-phase ratios of the spectra of two monoharmonic signals

Nº	Epochs	a	b	$G_x(f)$	c	d	$G_y(f)$	$e = ac + bd$	$g = ad - bc$	Results
1	1	4	0	16	0	4	16	0	16	$ E[G_{xy}(f)] ^2 = 128$
	2	0	4	16	0	4	16	16	0	$E[G_x(f)]E[G_y(f)] = 256, \gamma^2 = 0.5$
	$E[...]$			16			16	8	8	$E[G_x(f)G_y(f)] = 256, \gamma^2 = 0.5$
2	1	4	0	16	0	4	16	0	16	$ E[G_{xy}(f)] ^2 = 68$
	2	0	2	4	0	2	4	4	0	$E[G_x(f)]E[G_y(f)] = 100, \gamma^2 = 0.68$
	$E[...]$			10			10	2	8	$E[G_x(f)G_y(f)] = 136, \gamma^2 = 0.5$
3	1	4	0	16	0	4	16	0	16	$ E[G_{xy}(f)] ^2 = 64.25$
	2	0	1	1	0	1	1	1	0	$E[G_x(f)]E[G_y(f)] = 72.25, \gamma^2 = 0.889$
	$E[...]$			8.5			8.5	0.5	8	$E[G_x(f)G_y(f)] = 128.5, \gamma^2 = 0.5$

Table 1.1 shows a simple example in which we consider two sequential epochs in processes $x(t)$ and $y(t)$ using three different amplitude ratios (versions 1–3). In all cases, epoch 2 shows a 90° phase change in the cross-spectrum (the autospectrum vectors of process $x(t)$ are 0° and 90° in epochs 1 and 2, while the autospectrum vector of process $y(t)$ remains at 90° in both epochs). If the amplitudes of the processes are the same in both epochs (version 1), then both Equations (9) and (10) give the same result, $\gamma^2 = \gamma_2 = 0.5$, which comprehensively reflects a jump of 90° in the phase difference between the processes at the two sequential epochs. When the amplitudes of the process are halved in epoch 2 (version 2), we obtain $\gamma^2 = 0.68$, while a four-fold reduction (version 3) gives $\gamma^2 = 0.889$ (compared with the constant $\gamma^2 = 0.5$).

Thus, γ^2 coherence gives an increased assessment in relation to the extent of synchronicity of the processes, with a complex relationship with the extent of their amplitude variability. This coherence is fundamentally different from the correlation coefficient as a stable indicator of a linear relationship between two paired values which are not dependent on the ratio of the ranges of their values.

As the amplitude of the spectral harmonics of EEG processes vary significantly even over short time periods, we can conclude that γ^2 coherence is a poor numerical indicator of the degree of synchronicity of EEG processes (we note that γ^2 phase coherence is no better than \square^2 because of other errors as discussed below).

ERRORS IN SPECTRAL ANALYSIS

One of the main errors in discrete Fourier transformation (DFT) arises from leakage or drainage of power from spectral peaks to neighboring spectral lines. In technical addenda, this is decreased by using a variety of correcting windows and this method has been transported uncritically into electrophysiology. However, studies reported in [1, p. 200] showed that windows have a double effect on spectral peaks: they compress broad peaks but broaden well localized peaks. Therefore, it is more correct to calculate the mean and maximum amplitudes of a spectrum after preliminary filtration of the signal in the range being analyzed, which excludes leakage and modulating peaks from neighboring ranges.

However, the leakage effect depends on the ratio of the harmonic period and the analysis epoch [1, p. 200]: there is no leakage when there is a whole number of harmonic periods per analysis epoch and leakage is maximal when there is a half-integer number of harmonic periods per analysis epoch. Furthermore, even in the latter case, leakage decreases in inverse proportion to increases in distance from the main peak. However, there is a further, not previously noted, but important distortion to spectra, associated with the amplitude modulation present in all EEG signals. This effect [1, p. 187] results in the appearance of two symmetrical side peaks of 40% or more of the amplitude of the central peak and separated from it by a number of spectral lines equal to the number of signal modulation periods observed (this applies to monoharmonic signals, and the situation with real EEG traces will be significantly more complex).

These two main errors produce additional (to the above-noted) random fluctuations in spectra, which are particularly clear visually when frequency resolution is high. Phase spectra are more subject to these fluctuations than amplitude spectra.

Fig. 1.1, *a* shows a small fragment of a typical and prolonged EEG trace with a high alpha-rhythm content in the two occipital leads. Fig. 1.1, *b* shows the amplitude cross-spectrum between these two processes for an 8-sec analysis epoch, which reveals a high-amplitude peak at the fundamental

frequency of the alpha rhythm, 9 Hz. The presence of low-amplitude random fluctuations throughout the frequency range should also be noted. Fig. 1.1, *c*, *d* shows the phase cross-spectrum and the coherence spectrum, which are already completely dominated by random fluctuations and no clear frequency pattern can be discriminated. Fig. 1.2 shows a plot of changes in cross-spectrum phase at the fundamental alpha-rhythm frequency of 9 Hz for 32 sequential epochs. This shows that the phase (whose stability significantly reflects coherence) shows random and large epoch-by-epoch variations over the wide range $\pm 160^\circ$. This randomly fluctuating nature of oscillations in coherence and phase is typical of illustrations presented in physiology reports [15, pp. 68–82; 14, p. 29; 9, pp. 134–137, and others]. The situation with averaged coherence values is no better (see below).

Sharp reductions in the accuracy of calculations for small signal amplitudes should be noted, these being characteristic of high-frequency ranges and due to the limited data element length resulting from the integer-based representation of the output of analog-to-digital converters – low-amplitude harmonics are represented by the least significant bits. This affects first the accuracy of calculations of autospectrum and cross-spectrum amplitudes and then, to a greater extent, coherence values. This effect is a further source of error in coherence analysis.¹

¹ In this regard we must not criticize modern ACD with high bit coding (up to 24-bit) which use delta-sigma conversion; these ACD record all signals from the surrounding space and particularly the high-amplitude network noise. After its removal by digital filtration, the extracted EEG signal is generally located in the 8–12 least significant bits.

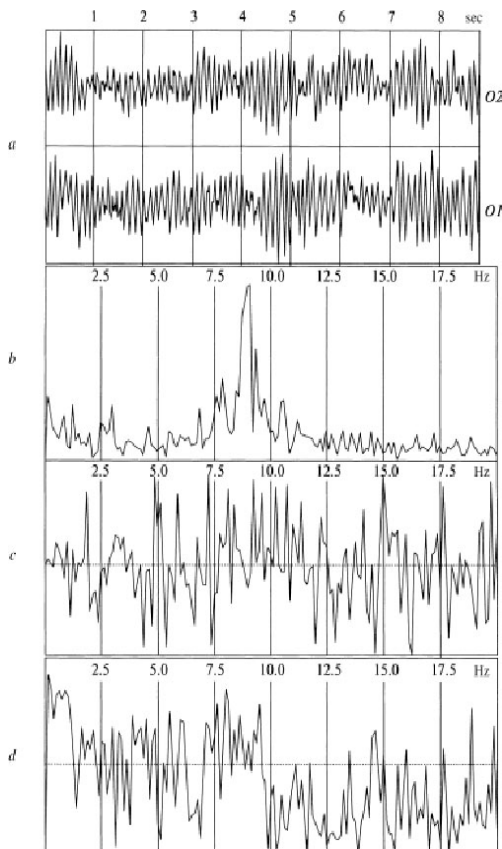


Fig. 1.1. Typical EEG spectra. *a*) Occipital EEG lead with a high alpha-rhythm content (9-sec trace), sampling frequency 128 Hz, analog filters with bandpass 0.5-32 Hz, total trace duration 64 sec; *b*) amplitude cross-spectrum (one 8-sec epoch); *c*) phase crossspectrum (one 8-sec trace); *d*) coherence spectrum (average of 8 epochs)

Thus, coherence is extremely dependent on random fluctuations resulting from fundamental instrument errors associated with DFT and the properties of the EEG processes themselves. This also has the result that coherence cannot be regarded as an informative measure for evaluating the levels of synchronicity of EEG processes. According to the popular expression: anything can be extracted from Gaussian noise.

DEPENDENCE ON NOISE LEVEL

An important question, ignored in the literature, is that of elucidating the relationship between coherence and the levels of noise in the signals being analyzed. We will address this using a statistical modeling method, which is based on a very simple concept. The instantaneous spectra $X(f)$ and $Y(f)$ of monoharmonic processes $x(t)$ and $y(t)$ are generated by geometrical summation of two components: a) a defined vector of length r with a range of values $r = 01$ with a fixed phase angle (for example, 0°), and b) a random vector of length $1r$ with a phase angle selected randomly in the range 0 – 360° . Each coherence value is calculated by averaging 30 pairs of such instantaneous spectra and the mean value is calculated using 1000 $\square 2$ values calculated in this way.

The relationship between the mean value of $\square 2$ and the noise content in the signal $(0-r)\%$ is shown in Fig. 1 . 3, and this plot leads to the following conclusions: 1) The S-shaped nature of this relationship fundamentally distinguishes coherence from the correlation coefficient, whose relationship with the noise level is essentially linear; 2) at noise levels exceeding 60%, the relationship is largely flattened, so over this range $\gamma 2$ cannot serve as a measure of the noise content or the extent of desynchronization of EEG processes; 3) $\gamma 2$ can only be a satisfactory indicator of noise content in the narrow range over which the curve shows an essentially linear relationship with noise, i.e., 20–60%; 4) when signals contain more than 30–40% noise it becomes difficult to claim a high level of synchronicity between EEG processes, such that only $\gamma 2$ values of >0.7 are acceptable for this.

These conclusions are supplemented by data reported in [7, p. 308] on the number of averagings n required to obtain significant values of $\gamma 2$ with errors levels of less than ± 0.1 depending on the true value of $\gamma 2$ (Table 1 . 2). As the non-stationarity of EEG processes over prolonged periods of time has the result that the number of averagings available for coherence calculations is generally no more than 10, it follows that only values of $\gamma 2$ of >0.8 can be regarded as satisfactorily significant.

However, scientific reports generally discuss experimental assessments of coherence in the range 0.1–0.8 and use these to draw physiological conclusions. These conclusions may therefore be extremely mediocre evaluations of the levels of synchronicity of EEG processes.

COMPUTER ANALYZERS

What situation applies to the various commercialized programs for coherence calculations? We asked several leading and senior EEG analyzer producers (in Moscow, St. Petersburg, Taganrog, Ivanovo, Kharkov) about their algorithms for calculation of coherence and received responses whose agreement was far less than 100%.

Testing of a number of program bundles using identical EEG traces showed (uniformity of testing was hindered by the incompatibility of the programs in terms of loading traces in the international EDF format) that the correspondence of coherence spectra applies only in relation to their integral characteristics (one comparison example is shown in Fig. 1.4): plots were monotonic or multipeak, had neighboring high or low values at particular frequencies, and had approximate coincidence of the frequency values of certain peaks. Other qualitative characteristics, as well as quantitative evaluations, showed significant differences. This would appear to result from the relationship between coherence values and a multitude of parameters undeclared on the packaging and uncontrolled: squared or non-squared versions of the computations, the length of the analysis epoch, the number of epochs averaged, the magnitude of the time shift between epochs, the use of a correcting window, the type of final smoothing of the coherence function, etc.

An example of the dependence of a coherence spectrum on the duration of the epochs being averaged and the correcting window is shown in Fig. 1.5. This clearly shows that the results are significantly different in terms of the positions, shapes, and amplitudes of the dominant peaks.

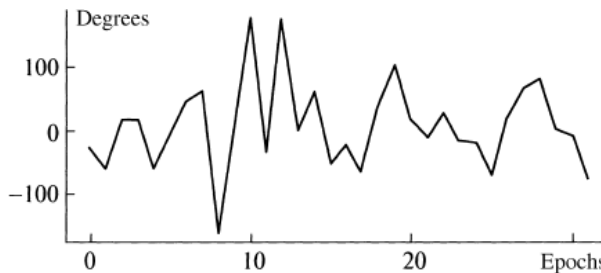


Fig. 1.2. Changes in cross-spectrum phase (Fig. 1.1, c) for the dominant alpha rhythm frequency of 9 Hz (Fig. 1.1, b) at 32 sequential 2-sec epochs.

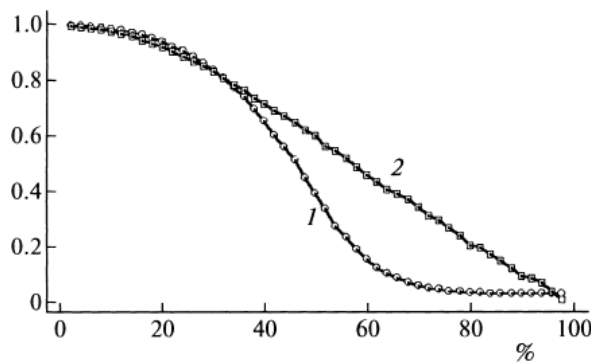


Fig. 1.3. Relationship between coherence values (1) and correlation coefficients (2) and the proportion of noise in the signal

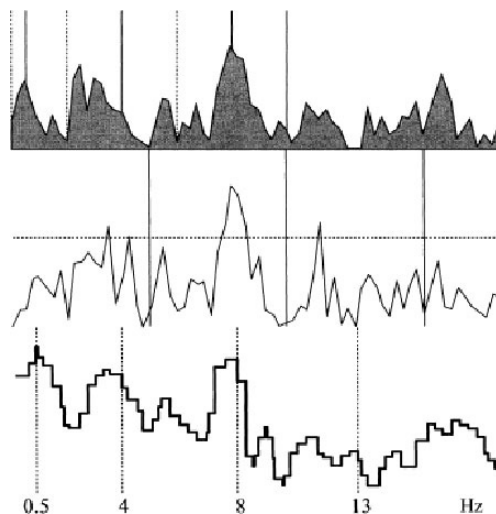


Fig. 1.4. Coherence spectra calculated using three EEG analyzers, epoch length 4 sec, average of 16 epochs

Table 1.2. True γ^2 coherence values and numbers of ensembles needing to be analyzed n to obtain true \square^2 values with errors not exceeding ± 0.1

γ^2	0.3	0.4	0.5	0.6	0.7	0.8	0.9
n	327	180	100	54	26	10	3

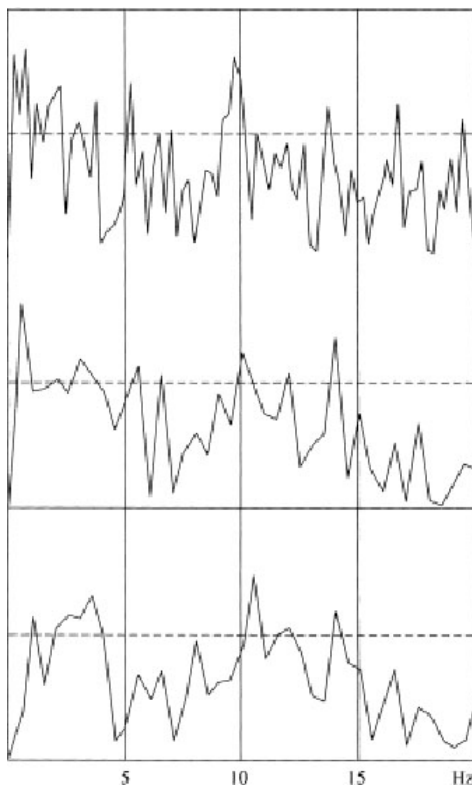


Fig. 1.5. Relationship between coherence and analysis epoch duration T and use of a correcting window (average of 16 epochs); above downwards: $T = 4$ sec; $T = 2$ sec; $T = 2$ sec + Hann correcting window

Fig. 1.6 shows plots of the mean coherence values in standard frequency ranges calculated for the spectra of Fig. 1.5. The range of variation of coherence values is very large – amounting to 28–36% of the maximum value (in the delta, theta, and beta1 ranges). Thus, the mean coherence calculated using different values for the parameters are not comparable in quantitative terms. The variability increases even more when we calculate mean coherence for a group of subjects [15, pp. 71, 74], when most paired differences in coherence, on the background of large standard deviations, are statistically insignificant.

It should also be noted that recent years have seen the increasing introduction of new spectral analysis methods based on wavelets, which

produce results even more fundamentally (both quantitatively and qualitatively) different from the results obtained using traditional DFT and, thus, from the whole assemblage of data accumulated over many decades.

Thus, coherence analysis results obtained using different program bundles and with different values for the parameters are poorly comparable in qualitative and quantitative terms, as are any scientific conclusions based on these results.

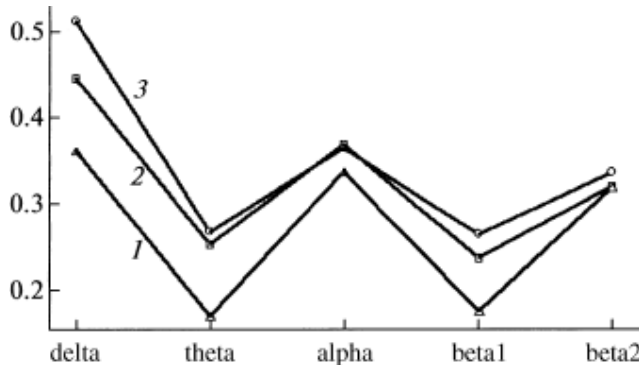


Fig. 1.6. Variability of mean coherence values in frequency ranges in relation to analysis epoch duration and use of a correcting window (average of 16 epochs): 1) $T = 4$ sec; 2) $T = 2$ sec; 3) $T = 2$ sec + Hann correcting window

CONCLUSIONS

This multilateral analysis of the fundamental disadvantages of coherence functions (identification of the influences of a multitude of uncontrolled random factors, inapplicability to EEG analysis, dependence on a number of adjusting factors, the nonlinearity of the dependence on the noise level, dependence on phase and amplitude variability, the non-comparability of the results obtained, etc.) indicates that this numerical characteristic cannot, on the basis of metrological considerations, be supported as an analytical tool in the current understanding of this term.

ALTERNATIVES

Many investigators have in recent years recognized the stationary-segments paradigm of EEG structure [16], such that various approaches can be applied to EEG traces using relatively stationary segments with a

criterion for the synchronicity of the time dynamics of such structures. One potential approach in this direction [17 and others] is based on segmentation for areas of increased/ decreased amplitude modulation of signals, with evaluation of the synchronicity of two leads in terms of the proportion of coinciding intersegment transitions (an algorithmic approach to this method is presented in [1, pp. 227–230, 251–254]. Another approach consists of using Pearson correlation coefficients to assess the synchronicity of EEG modulation rhythms in a selected time period. Both of these methods have now been verified and the results obtained using them demonstrate their applicability to many problems and their potential.

REFERENCES

1. A. P. Kulaichev, Computerized Electrophysiological and Functional Diagnosis [in Russian], FORUM-INFRA-M, Moscow (2007).
2. A. P. Kulaichev, “Some methodological problems of EEG frequency analysis,” *Zh. Vyssh. Nerv. Deyat.*, 47, No. 5, 918–926 (1997).
3. M. N. Livanov, Temporospatial Organization of Potentials and Systems Activity in the Brain [in Russian], Nauka, Moscow (1989).
4. N. R. Goodman, “Measuring amplitude and phase,” *J. Franklin Inst.*, 270, 437–450 (1960).
5. W. R. Adey and D. O. Walter, “Application of phase detection and averaging techniques in computer analysis of EEG records in the cat,” *Exper. Neurol.*, 7, 186–209 (1963).
6. D. O. Walter, “Spectral analysis for electroencephalograms: Mathematical determination of neurophysiological relationships from records of limited duration,” *Exper. Neurol.*, 8, 155–181 (1963).
7. J. Bendat and A. Pirsol, Measurement and Analysis of Random Processes [Russian translation], Mir, Moscow (1971).
8. R. Otnes and L. Enoxon, Applied Analysis of Time Series [Russian translation], Nauka, Moscow (1978).
9. V. D. Trushch and A. V. Korinevskii, Computers in Neurophysiological Studies [in Russian], Nauka, Moscow (1978).
10. R. B. Randall, Frequency Analysis, Brüel and Kjaer, Copenhagen (1989).
11. G. Jenkins and D. Watts, Spectral Analysis and its Applications [Russian translation], Mir, Moscow (1971).
12. S. L. Marple, Jr., Digital Spectral Analysis and its Applications [Russian translation], Mir, Moscow (1990).
13. G. Nolte, O. Bai, L. Wheaton, Z. Mari, S. Vorbach, and M. Hallett, “Identifying true brain interaction from EEG data using the imaginary part of coherency,” *Clin. Neurophysiol.*, 115, 2292–2307 (2004).

14. V. S. Rusinov, O. M. Grindel, G. N. Boldyreva, and E. M. Vakar, *Biopotentials in the Human Brain* [in Russian], Meditsina, Moscow (1987).
15. M. N. Livanov, V. S. Rusinov, P. V. Simonov, M. V. Frolov, O. M. Grin-del, G. N. Boldyreva, E. M. Vakar, V. G. Volkov, T. A. Maiorchik, and N. E. Sviderskaya, *Diagnosis and Prognosis of the Functional State of the Brain* [in Russian], Nauka, Moscow (1988).
16. A. Ya. Kaplan, "EEG nonstationarity: methodological and experimental analysis," *Usp. Fiziol. Nauk.*, 29, No. 3, 35–55 (1998).
17. A. Ya. Kaplan, S. V. Borisov, S. L. Shishkin, and V. A. Ermolaev, "Analysis of the segment structure of human EEG alpha activity," *Ros. Fiziol. Zh.*, 4, 84–95 (2002).

CHAPTER 2

INACCURACY OF EEG ESTIMATES BASED ON POWER SPECTRUM

ABSTRACT

This work performs the metrological comparison of two groups of indicators estimating the average level of EEG– potentials. The indirect spectral indicators (ISI) based on amplitude spectrum and power spectrum are contrasted with natural indicators (NI) based on period-amplitude analysis, on EEG absolute value and on EEG envelope. Five major results were obtained: 1) NI give almost equivalent estimates that differ from ISI significantly; 2) NI demonstrate smooth dynamics of their value change at successive epochs whereas ISI are subject to drastic and casual fluctuations; 3) ISI unlike NI do not possess the additivity property of statistical averaging, their estimates depending on number and length of averaged epochs can differ over 3 times in their values; 4) ISI at simulated signals with a known amplitude ratio give estimates that differ 1.4–1.55 times from true value whereas NI show the proper estimates; 5) ISI depending on differences between EEG spectral distribution give estimates which differ over 5 times in their ratios while NI show the same ratios which differ 1.38–3.7 times from ISI. The least reliable results in all comparisons are related to the power spectrum. These conclusions do not allow to qualify metrologically ISI as an analytical tool that is adequate for the nature and peculiarities of EEG potentials. Their use may lead to incompatibility of the results obtained by different researchers and clinicians.

Keywords: EEG amplitude; amplitude spectrum; power spectrum; period-amplitude analysis; envelope; filtration; metrology

INTRODUCTION

In this work we examine and discuss one of the major questions for the field of metrology. It is concerned with those criteria, estimates and standards in computing or quantitative EEG (QEEG) that were not

generally formulated for a number of reasons [1]. As follows from the special monographic review [2] as well as from many papers on QEEG, metrological questions still remain beyond the scope of interest of EEG researchers. The newly proposed mathematical methods are not compared with their previous analogues, their efficiency in solving typical physiological tasks is not estimated, compared, and neither it is statistically verified. The methods traditionally used in practice are not critically examined and reviewed. Moreover, there is still no global normative EEG database.

Only a fraction of literature on the topic [3,1,4-5,6] focuses on special metrological aspects. A separate branch is represented by 65 years long discussion about an optimal EEG reference which still has not led to the development of some universally estimated quantitative criteria and standards (cf. reviews in [7,8]). The lack of metrological support and standards leads to incompatibility and inconsistency of results and conclusions drawn by different researchers (cf. literature reviews in [9-11]).

More favourable situation developed in traditional clinical EEG diagnostics which focused entirely on visual studying of records and where clear criteria and standards for both symptomatology and drawing clinical conclusions were formulated [12]. Another positive example is concerned with heart rate variability analysis where the permanent international working group established by European cardiological society and North American society of stimulation and electrophysiology several decades ago provides metrological standardization and regulation of computing methods and estimated indicators [13].

One way or another, the scientific EEG investigations during many decades mainly followed the physical and technical applications of mathematical methods of signal analysis which were often directly and noncritically transferred by invited engineering specialists without any consideration given to fundamental nonstationarity of bio-signals and nonharmonic nature of their sources [1]. Indeed, there isn't any widely known pure or applied mathematician who developed special methods of EEG analysis.

However, there will hardly be objections against the vital necessity to seek better accuracy and more adequate measurement as well as analytical tools in any field of science or domain of knowledge. If a researcher has two analytical tools with different measurement errors, then being responsible for the evidence and consultations he presents, he will definitely choose

the tool of higher measuring accuracy and reliability, otherwise scientific community can qualify his results and conclusions as insufficiently convincing. Furthermore, fundamental questions of accuracy and adequacy of measuring and analytical means are undoubtedly methodically significant, actual and primary in any scientific area including EEG studies.

Based on the aforesaid, our aim is to compare metrologically the direct measurements of average EEG amplitude in frequency domains to indirect estimates obtained from amplitude and power spectra. The following analysis reveals the numerous errors peculiar to spectral EEG amplitude estimates.

THE ESTIMATES OF EEG AVERAGE AMPLITUDE

From the very beginning of the computer era, especially due to FFT algorithm developed in 1965, EEG amplitude in chosen frequency domain began to be estimated via amplitude spectrum or power spectrum as squared amplitude spectrum [14,15].

However, in case of insufficient professional mathematical intuition a nonlinear relationship between power spectrum estimates is difficult to perceive in comparison with linear relationship between amplitude spectrum estimates. Moreover, it is not easy to realize the physiological meaning of estimations expressed in squared microvolts when EEG biopotentials are initially measured rather than their squares or volumes. As a result of its nonlinearity the power spectrum is characterized by dominant high-amplitude peaks with leveled and even disappearing medium-amplitude and low-amplitude details. This is expressed in ratios of frequency domains in chosen derivation and in ratios of derivations in chosen domain but it is visually-hypertrophied and evident for topographic maps displaying only two areas on a scalp in blue and red colours. And finally, let us speculate about the mathematical meaning of power spectrum average value. It is the dispersion of EEG amplitude spectrum with respect to zero as the mean value [14]. The rhetorical question immediately arises: what physiological meaning can be associated with this indicator?

Moreover, the results of spectral analysis are characterized by a number of errors, the most famous one is the power leakage from the main peaks. However, this effect is narrowed by increased frequency resolution and it is accounted for signals with powerful monoharmonic sources. That does

not correspond to EEG where this kind of generators does not exist. So, if the phenomenon does not exist, any ways of dealing with it [16] make no sense. Less known error is caused by the influence of amplitude modulation which is inherent in EEG signals. It leads to appearance of side peaks in spectrum which can be at a considerable distance from the main peak [1].

Notably, at frequency resolution of 0.25 Hz and better distribution of EEG, spectral harmonics appears to be a chaotic sequence of high and low amplitude components which are also highly variable in their amplitude and frequency through epochs (Fig. 2.1). Therefore, separate harmonics are not viable for analysis and they make no physiological sense. And that is why the averaged spectral estimates within a selected frequency domain are commonly used in practice for they are more statistically stable indicators. These indicators will be considered as indirect estimates based on amplitude spectrum (As) and power spectrum (Ps).

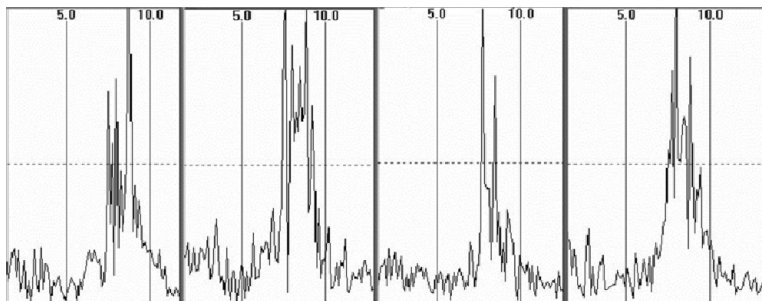


Fig. 2.1. The amplitude spectra in four successive 8-second epochs in O2 derivation, "closed eyes" test

Now let us discuss what is meant by "average signal amplitude". For monoharmonic signals the answer seems to be obvious - it is the difference between maximum and minimum of oscillations. In case of polyharmonic character of signal the answer is not so obvious. During the pre-computer era this problem was solved by period-amplitude analysis when the measurements of amplitudes and periods of consecutive oscillations were performed manually on paper record, then the average amplitude was calculated (it is designated as Ap), as well as other descriptive statistics. With the profound use of computers this method was fulfilled by a preliminary digital signal filtration in a chosen frequency domain and subsequent automatic measurements of differences between ascending and descending amplitude extrema (Fig. 2.2B). Under these conditions,

however, there are two options depending on a critical decision: to consider or not to consider the amplitude differences relating to periods which are beyond the analyzed frequency domain (such periods usually belong to the low-amplitude oscillations). Furthermore, averaging of amplitude differences usually is not corrected taking into account variability of their temporary duration.

Another method comparatively simple for application consists in calculating the mean of EEG absolute value (Fig. 2.2C, this indicator is designated as Am). Indeed, as such measurements are preceded by EEG filtration in a frequency domain, then the transformed record is centered around zero and both positive and negative EEG extrema are quite symmetric and their dynamics are sufficiently smooth. Therefore, averaging of amplitudes of the signal through all time samples gives a stable and balanced measure of average EEG amplitude. As the simple calculations can show, this indicator also considers the temporal variability of EEG periods.

The third alternative estimation can be a mean value of EEG envelope (Fig. 2.2D) which reflects the signal amplitude modulation (this indicator will be denoted as Ae). In this connection Ae is similar to 0.5 of Ap but it is disposed of quantization of EEG extrema in time and of variability of their periods.

These three indicators are referred below as “natural measures” of average EEG amplitude and they are compared with indirect spectral estimates.

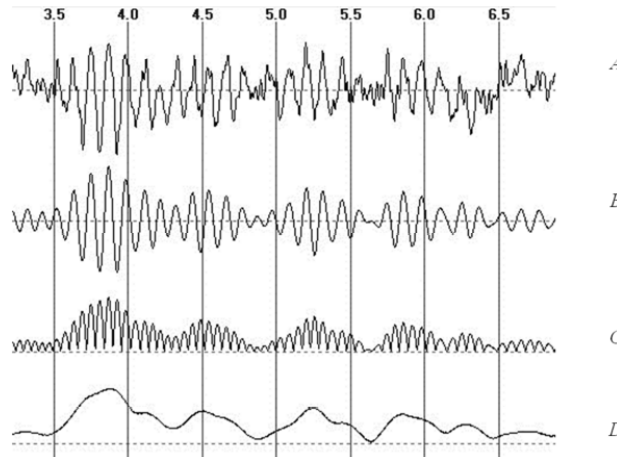


Fig. 2.2. From top to bottom: the EEG fragment, its filtering in alpha domain, the module of filtered signal, the EEG envelope

METHODS AND RESULTS

Integral Differences

Here let us estimate distinctions between Ps , As , Ap , Am , Ae indicators using 32-seconds EEG record for "closed eyes" test, 10-20% system of derivations, 256 Hz sampling rate, and analysis in alpha domain. Since the values of indicators vary significantly then Z-normalization of values of each indicator throughout all derivations should be performed for comparability of results.

Fig. 2.3 shows the evaluation of Ps , As , Ae estimates through four derivation meridians (Ap and Am values by reason of their proximity to Ae are not shown). As it can be easily seen, this record demonstrates classical consecutive reduction of alpha rhythm amplitude from occipital to frontal derivations with noticeable left- and right-handed asymmetry in parietal and occipital areas. Furthermore, it is obvious a number of differences between three indicators changing their sign in some derivations.

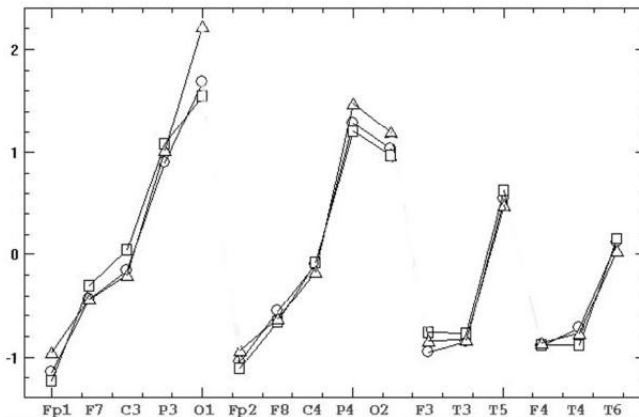


Fig. 2.3. Z-normalized estimates of EEG average amplitude based on amplitude spectrum (squares), power spectrum (triangles) and EEG envelope (circles)

First of all, let us calculate descriptive statistics (variation range, mean standard deviation) for absolute values of differences of As , Ap , Am indicators relative to Ae :

$$|As-Ae|: 0.009 \ 0.21, 0.101 \ 0.058;$$

$$|Am-Ae|: 0.0001 \ 0.012, 0.0036 \ 0.003;$$

$$|Ap-Ae|: 0.0004 \ 0.07, 0.003 \ 0.002.$$

The greater difference occurs for As , it reaches 21% of $Z-$ value and its average difference exceeds 10%. The differences of Ap and Am from Ae are minimal, average difference does not exceed 0.36% of Z -value. The divergences between the mean values of $|As-Ae|$ and $|Am-Ae|$ as well as of $|As-Ae|$ and $|Ap-Ae|$ are verified by t-test with high confidence $p=0.000007$. Nevertheless, the difference between $|Am-Ae|$ and $|Ap-Ae|$ is not significant at $p=0.46$, thus Ap and Am indicators may be regarded as equivalent.

Let us calculate similar statistics for the differences of three natural indicators relative to As :

$|Ae-As|$: 0.009 0.21, 0.101 0.058;

$|Am-As|$: 0.019 0.26, 0.12 0.066;

$|Ap-As|$: 0.004 0.21, 0.102 0.033.

The null hypothesis of pairwise differences between $|Ae-As|$, $|Am-As|$, $|Ap-As|$ are accepted with high confidence $p=0.95$, 0.95, 0.96, thus these three natural indicators can be considered as equivalent.

Finally, let us perform calculations for Ps relative to Ae and As :

$|Ps-Ae|$: 0.003 0.54, 0.115 0.126;

$|Ps-As|$: 0.02 0.67, 0.169 0.157.

Thus, power spectrum gives estimates greater than above-considered ones with respect to their variation ranges and mean values as compared to amplitude spectrum and envelope indicators.

Summary: Three natural indicators of EEG average amplitude practically do not differ and may be regarded as equivalent ones, but they are significantly different from the indirect estimates based on amplitude spectrum. Even greater differences with the other four parameters are valid for the power spectrum.

Differential Differences

Several methodological approaches can be applied for a more detailed numerical study of adequacy of considered indicators. As the equivalence of free natural estimates has been shown above then in further comparisons the measure based on an envelope will be mainly used.

The idea of the first approach is as follows. If we divide a hole EEG record onto overlapping epochs with a small-time shift between themselves, the dynamics of adequate indicator values through epochs should become sufficiently smooth.

Now let us consider the occipital O2 derivation with a high amplitude of alpha rhythm and the frontal F3 derivation with a low representation of alpha rhythm. Total 32-seconds time interval will be divided onto 150th epochs of 2-seconds duration and shifted at 0.2-seconds between themselves. For each i -th epoch ($i=1-150$) let us calculate As_i and Ae_i estimates. To make their comparison possible Z-normalization of each indicator should be performed for all epochs. Since the time shift between epochs amounts to 10% of their duration, temporal dynamics of adequate estimates through epochs should be sufficiently smooth without sharp fluctuations.

Significant differences between the time dynamics of two indicators is illustrated in Fig. 2.4: the dynamics for Ae is smoother compared to a high-amplitude random fluctuations for As .

Besides, comparing O2 and F3 graphs reveals a whole series of episodes of opposite tendencies between two indexes, i.e. differences in their topographical relations. For example, As_i and Ae_i estimates differ significantly in O2, but they are equal or their ratio changes to opposite in F3. Such topographic differences are extremely disturbing because they can lead to incompatibility of results and conclusions for intergroup comparisons estimating influence of various factors such as age, sex, occupation, pathology, functional condition, motivation, social or professional affiliation, etc.

The numerical estimation of the degree of "smoothness" of dynamics can be made if to calculate absolute differences for each X -indicator between pairs of subsequent epochs $X_i=|X_{i+1}-X_i|$ (i.e. absolute derivative) and then evaluate the mean value X . The results of the quantitative comparison are given in the Table 2.1 the columns of which include derivation, frequency domain, As or Ae indicator, mean absolute difference between As and Ae (i.e. mean values of $|As_i-Ae_i|$) with its standard deviation, mean value As or Ae (i.e. absolute derivative) with its standard deviation, a significance level of null-hypothesis "no distinction between As and Ae ".

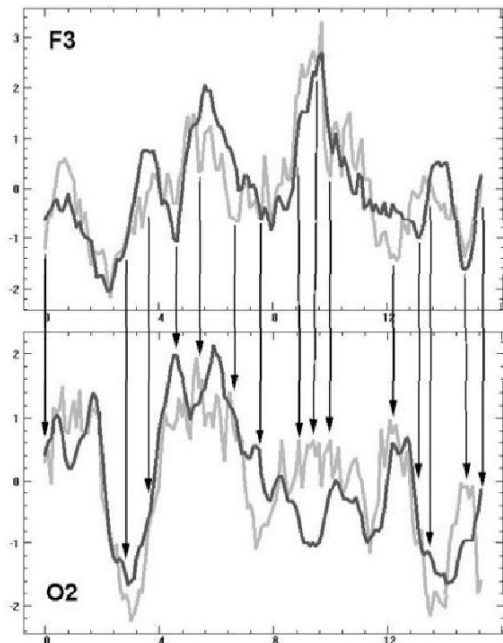


Fig. 2.4. Dynamics of average EEG amplitude in alpha domain at 150th 2-seconds epochs (x-axis) shifted by 0.2-seconds among themselves for F3 and O2 derivation, gray – amplitude spectrum estimates, black – EEG envelope estimates, the arrows mark the obvious episodes of topographical distinctions

Table 2.1. The results of the analysis of differential distinctions between average EEG amplitude estimates based on amplitude spectrum and EEG envelope

Deri- vation	Domain	Epoch	Measure	Difference	Deri- vative	Signifi- cance
F3	Alpha	2 s	Spectrum	0.53	0.11	0.31
			Envelope			0.21
O2	Alpha	2 s	Spectrum	1.0	0.54	0.30
			Envelope			0.16
F3	Beta1	2 s	Spectrum	0.45	0.36	0.46
			Envelope			0.24
O2	Alpha	4 s	Spectrum	0.31	0.24	0.23
			Envelope			0.12
O2	Alpha	8 s	Spectrum	0.39	0.27	0.20
			Envelope			0.08

As anyone can see from the Table 2.1 the average absolute difference between As_i and Ae_i is up to 31–100% of Z-value that much more exceeds the differences mentioned in the previous section. This situation is quite alarming because any researcher due to random factors can perform EEG recording in an error-prone time period.

The mean values and standard deviations for Ae are 1.5–2 times smaller compared to As and the differences between Ae and As are highly significant statistically. Similar conclusions are also reproduced for higher frequency beta1-domain and for longer 4- and 8-seconds epochs. Thus, the revealed regularities are stable and reproducible regardless of derivation, frequency domain and epoch duration.

Finally, let us asses the power spectrum estimates for alpha domain in O2 derivation and 2-seconds epoch. The average absolute differences between Ps and Ae are characterized by statistics 0.54 ± 0.45 and between Ps and As by statistics 0.29 ± 0.25 . Statistics for Ps derivative is 0.25 ± 0.21 . It is significantly different from Ae at $p=0.0001$ and differs from As at $p=0.02$ by a statistical trend.

Summary: The natural estimates of average EEG amplitude provide a smoother dynamic of their changes during neighbouring epochs whereas the spectral amplitude and power estimates are the subject to sharp and casual fluctuations. Furthermore, they do not coincide with each other by a statistical trend.

Additivity of Averaging Results

The statistical averaging operation has the property of additivity, namely: the mean value of the sample is equal to averaging of averaged values of its consistent subsamples. Natural estimates of EEG average amplitude possess those properties by definition.

Let us examine this property for spectral estimates. Let us take the same F3 and O2 derivations in alpha and beta1 domains and calculate As and Ps at 32-seconds epoch. Then this interval is divided into 2, 4, 8 epochs, calculate As_i and Ps_i at each i -epoch and average those estimates. The results are given in the Table 2.2 which implies a consistent increase in As and Ps estimates depending on the number and size of epochs.

This situation is also quite alarming because different researchers analyze EEG records of different lengths, so their results and conclusions may be incomparable and even contradictory in some cases. This property is not

inherent to a particular frequency characteristic (amplitude spectrum, power spectrum, etc.) but to FFT method itself applied for EEG signals. By increasing the analysis period and frequency resolution in EEG spectra more harmonics with low amplitude appear and such harmonics make no physiological sense. It results in the systematic reduction of average values with increasing of epoch length according to the law very close to the linear one (Table 2.2).

Table 2.2. Alterations of average EEG amplitude estimates based on amplitude and power spectrum depending on the number and size of averaged epochs.

Destination	Domain	Measure	Epoch 32s	2 epochs	4 epochs	8 epochs	4s
			16s	8s			
O2	alpha	amplitude	3.5	4.96	6.9	10.11	
F3	alpha	amplitude	2.43	3.4	4.76	6.9	
O2	beta1	amplitude	1.46	2.04	2.82	4.16	
F3	beta1	amplitude	1.07	1.56	2.24	3.21	
O2	alpha	power	26.46	48.09	81.05	169.8	

Summary: The indirect spectral estimates of average EEG amplitude do not possess the property of additivity of statistical averaging operations. The resulting estimates depending on the number and length of averaged epochs can differ over 3 times in their values.

Comparison on Simulated Signals

Now let us compare natural and indirect estimates of average EEG amplitude using two synthesized signals (Fig. 2.5).

As anyone can see, the ratio of the original harmonic amplitudes is $184/122=1.508$. The similar ratio is for means of variations range of synthesized signals: $(548.3+19.2)/2=283.8 \mu\text{V}$, $(367.4+6.3)/2=186.8 \mu\text{V}$, the ratio is 1.512. It is obvious that an adequate measure should give the same ratio of two estimates.

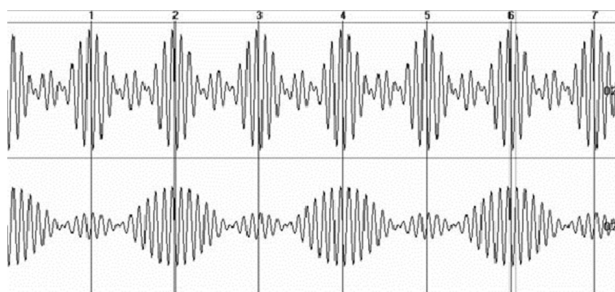


Fig. 2.5. Two synthesized signals of 32-seconds length: 1) the sum of 3 harmonics of $184 \mu\text{V}$ amplitude and 9, 10, 11 Hz frequencies; 2) the sum of 3 harmonics of $122 \mu\text{V}$ amplitude and 9.5, 10, 10.5 Hz frequencies. As gives 8.64 and $4.1 \mu\text{V}$, ratio=2.11. Ps : gives 492.2 and $220.2 \mu\text{V}^2$, ratio=2.34, Ap gives 249.5 and $168.1 \mu\text{V}$, ratio=1.48, Am gives 83.1 and $55.5 \mu\text{V}$, ratio=1.5; Ae gives 88.04 and $132.1 \mu\text{V}$, ratio=1.5.

Summary: The indirect spectral indicators of EEG average amplitude on simulated signals with known amplitude ratio produce estimates $2.11/1.511=1.4$ and $2.34/1.511=1.55$ times different from the correct values, whereas the natural indicators show correct ratio of mean amplitude of signals.

Dependence on Spectral Distribution

As it has been shown above, the natural indicators give correct amplitude estimation for known model signals. Therefore, they can be used as a reference point to continue the comparison on real EEG records varying in the shape of distribution of spectral harmonic amplitudes (Fig. 2.6).

As anyone can see, two examiners differ considerably in their EEG spectral distribution. For the first of them the frequency range of predominant alpha rhythm amplitudes is quite narrow 9.2–10 Hz, while for the second the range is wider 8–12 Hz. The resulting estimates are:

Ae : 31.3 and $118 \mu\text{V}$, ratio=0.26;
 Am : 20 and $75.3 \mu\text{V}$, ratio=0.267;
 Ap : 227.1 and $60.4 \mu\text{V}$, ratio=0.266;
 As : 4.1 and $11.29 \mu\text{V}$, ratio=0.36;
 Ps : 25 and $351.3 \mu\text{V}^2$, ratio=0.07.

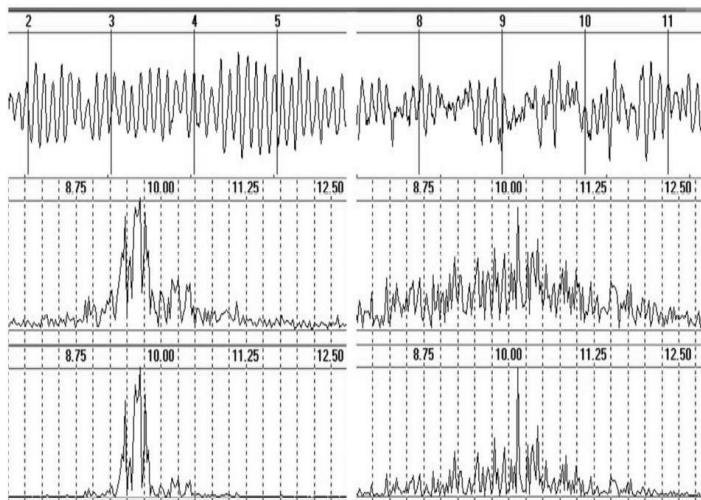


Fig. 2.6. Two subjects with different spectral distribution in alpha domain, from top to bottom: EEG in O2 derivation, amplitude spectrum, power spectrum

Note that the latest result would be a consequence of *Ps* quadratic suppression of harmonics on the lateral frequencies of the first examiner.

Thus, the natural indicators demonstrate almost the same proportion (the difference between them is $0.267 - 0.26 = 0.007$ or $0.007/0.26 = 2.7\%$ of ratio value) while the spectral estimations $0.36/0.26 = 1.38$ and $0.26/0.07 = 3.7$ times differ from the natural ones according to their ratios respectively. In addition, the spectral indicators demonstrate even a greater difference between the ratio values ($0.36/0.07 = 5.1$ times). So as compared to correct natural indicators, *As* estimations for two examiners are closer between themselves whereas *Ps* estimations diverge considerably. This situation is rather disturbing since for intergroup comparisons it can lead to displacement of mean values and standard deviations. This may prevent statistically reliable detection of real differences or lead to identification of pseudo-differences.

Summary: *As* and *Ps* indicators depending on differences between subjective EEG spectral distribution give estimates which differ over 5 times in their ratios while the natural indicators show the same relation of values 1.38–3.7 times different from spectral estimates ratios.

CONCLUSION

As it follows from the findings in sections 3.1–3.5, the spectral estimates of average EEG amplitude in frequency domains possess a number of significant and fundamental errors. In addition, the measures based on amplitude and power spectra differ in their estimates. These results and findings do not allow to qualify metrologically the spectral estimates as a viable (reliable) analytical tool adequate to the nature and specificity of EEG potentials. Their use may lead to inconsistency and thus incompatibility of results obtained by different researchers and clinicians. Therefore, applying the natural estimates of average EEG amplitude seems to be more preferable and sustainable.

REFERENCES

1. Kulaichev A. P. (2007) Computer electrophysiology and functional diagnostics, 4th edition. INFRA M, Moscow, 640 pp.
2. Tong S., Thankor N. V. (2009) Quantitative EEG analysis methods and clinical applications. Artech House, 421 pp.
3. Ivanov L. B. (2011) On informativeness of use of coherent analysis in clinical electro- encephalography. Zh Vyssh Nerv Deiat Im I P Pavlova. 61 (4): 499–512.
4. Kulaichev A. P. (2009) The informativeness of coherence analysis in EEG studies. Neurosci Behav Physiol. 59 (6): 757–767.
5. Kulaichev A. P. (2011) The method of correlation analysis of EEG synchronism and its possibilities. Zh Vyssh Nerv Deiat Im I P Pavlova. 61 (4): 485-498.
6. Orihovskaya K. B., Antonova-Rafi U. V. (2014) The effect of EEG spectrum leakage when using Barletta filter and at his absence. Int research J. (22) 3–2: 42–43.
7. Kayser J., Tenke C. E. (2010) In search of the Rosetta Stone for scalp EEG: Converging on reference-free techniques. Clin. Neurophysiol. 121: 1973–1975.
8. Ng S. C., Raveendran P. (2007) Comparison of different montages on to EEG classification. Biomed 06, IFMBE Proceedings 15, 365–368.
9. Kulaichev A. P. (2012) Comparative analysis of EEG correlation synchronism and EEG amplitude relationships in all-night sleep. Zh Vyssh Nerv Deiat Im I P Pavlova. 62 (1):108-119.
10. Kulaichev A. P., Gorbachevskaya N. L. (2013) Differentiation of norm and disorders of schizophrenic spectrum by analysis of EEG correlation synchrony. J. Exp. Integr. Med. 3 (4): 267–278.
11. Kulaichev A. P., Iznak A. F., Iznak E., Kornilov V. V., Sorokin S. A.

(2014) The Changes of EEG correlation synchrony at depressive deviations of advanced age. *Zh Vyssh Nerv Deiat Im I P Pavlova*. 64 (2): 1–9.

12. Deuschl G., Eisen A. (1999). Recommendation for the practice of clinical neurophysiology: Guidelines of the International Federation of clinical neurophysiology. Elsevier, Amsterdam,304 pp.
13. Malik M., BiggerJ. T., Camm A. J., Kleiger R. E., Mallian i A., Moss A. J., Schwartz. P. J. (1996) Heart rate variability. Standards of measurement, physiological interpretation, and clinical use. *Eur Heart J.* 17 (3): 354–381.
14. Otnes R. K., Enochson L. (1987) Applied time series analysis, vol. 1: basic techniques. N. Y., 428 pp.
15. Randall R. B. (1987) Frequency Analysis, 3rd edition. Brüel & Kjaer, 344 pp.
16. Harris F. J. (1978) On the use of windows for harmonic analysis with the discrete Fourier transform. *IEEE proceedings*. (66) 1:51–83.

CHAPTER 3

CORRELATION OF EEG ENVELOPES IS THE BEST METHOD FOR IDENTIFYING MENTAL DISEASES, FUNCTIONAL STATES, INDIVIDUAL AND INTERGROUP DIFFERENCES

ABSTRACT

The principal errors of spectral and coherent analysis are discussed, and the mathematics of these methods is not related to EEG nature. In this regard, in 2011, the new method was developed for evaluating EEG synchrony by the correlation of envelopes, which has a direct and fundamental physiological meaning. The basics of this method and the methodology of subsequent multilateral statistical analysis are considered. The effective use of the method for identifying individual and intergroup differences in the norm and several types of schizophrenia, depressive diseases, five stages of sleep, and similar functional states are presented.

Keywords: EEG, metrology, amplitude and power spectra, coherency, envelope, correlation, statistical analysis, schizophrenia, depression, sleep stages, functional states.

Introduction

Unfortunately, in the field of computational or quantitative EEG (qEEG), metrological criteria, assessments and standards have not been formed globally for several of reasons [1]. As evidenced by the content of the special fundamental monograph [2] and many journal publications on qEEG, metrological issues almost do not attract the attention of EEG researchers. The new proposed mathematical methods are not compared with analogs; their effectiveness in solving typical physiological problems is not evaluated, is not compared and is not statistically verified. Traditional methods are not critically examined and rethought. Periodically, attempts are made to introduce completely exotic and unrelated brain physiology methods from the theories of chaos, information, and entropy, fractals,

attractors, automatic regulation, nonlinear dynamics, wavelets, etc.

One way or another, but scientific research of EEG mainly followed in the wake of physical and technical applications of mathematical methods of signal analysis which were often directly and uncritically transferred by involved engineering and physical specialists without due consideration of a) the fundamental non-stationarity of biosignals; b) the inharmonic nature of their sources; c) the presence of amplitude modulation. Indeed, there is not a single well-known a pure or applied mathematician who has contributed to the development of special methods of EEG analysis. As a result, many methods that were inadequate in this field were transferred, which, in the absence of metrological criticism, leads to incompatibility and inconsistency of the results and conclusions obtained by different researchers. Such a situation can in no way be recognized as the scientific one.

It is no exaggeration to say that the main means of qEEG are [2] spectral estimates of EEG amplitude in frequency domains and estimates of synchrony between pairs of derivations using the coherence function.

EEG amplitude estimates

During the pre-computer era, EEG amplitude was estimated by direct measurements (DM) of EEG waves. After the FFT algorithm appearance in 1965, EEG amplitude was indirectly estimated (IdE) from the amplitude and power spectra. There is no doubt that DM acts as an indisputable standard, and IdM may differ from them in the resulting values. The corresponding comparison was carried out in the special metrological study [3], and it showed the following differences:

- 1) The three studied in [3] DM indicators give almost equivalent estimates that highly significantly differ from IdE;
- 2) DM demonstrate the smooth dynamics of their value change at successive epochs, whereas IdE are subject to drastic and casual fluctuations;
- 3) IdE, unlike DM, don't possess the property of additivity, which is inherent for statistical averaging, its values depending on the number and length of averaged epochs can differ in 3 or more times;
- 4) IdE on simulated signals with known amplitude ratio give estimates by 1.4–1.55 times different from true value whereas DM proper correlations of average amplitudes;

- 5) IdE depending on the shape of spectrum amplitude distribution, may vary in its ratio to a variety of subjects more than five times while DM show the same relation of values which differ from IdE in 1.38–3.7 times;
- 6) The largest errors were found for the power spectrum.

These conclusions do not allow metrologically qualify IdE as the analytical tools adequate to the nature and specifics of EEG potentials. Their use may lead to the incompatibility of results obtained by different researchers.

In addition, the spectra have an extremely distant relation to EEG nature since, unlike sound and electromagnetic signals, EEG is not the sum of harmonics. EEG is the sum of postsynaptic potentials under the electrode whose short-time changes take the form of asymmetric bell-shaped functions. Therefore, individual spectral harmonics have no physiological meaning. They change arbitrarily both when the length of the analysis epoch changes, as well as on neighboring epochs.

Coherence

The poorly known history of EEG coherence is a vivid example of the mass spread of pseudoscientific misconception. The coherence function was formulated in 1930 by Norbert Wiener [4], implementing the idea previously expressed by David Hilbert that it would be good to have something similar to Pearson correlation in the spectral region. Wiener intended this function for problems of quantum mechanics and nonlinear optics, which are obviously extremely far from EEG studies. Subsequently, coherence became widespread in the analysis of physical signals but as a purely auxiliary indicator for assessing the significance of other cross-spectral characteristics [5].

Many years have passed when in 1963, the newly minted young Ph.D. [6], without any reference to sources and predecessors, proposed coherence as the main indicator of EEG synchrony. This PhD published 2–3 more articles on this topic, after which he lost interest in it. But the growing snowball of coherency rolled around the world, capturing the minds of many thousands of followers like a mass pandemic.

The special metrological analysis of the weaknesses and errors of coherence was carried out in the study [7], which gave the following results:

- 1) the coherence mainly evaluates the degree of phase instability of the cross-spectrum of two EEG signals, which to an even greater extent than spectral harmonics has no physiological meaning;
- 2) at the same time, the coherence also changes depending on the ratio of the values of the cross-spectrum vectors at neighboring epochs², and such a dual sensitivity is unacceptable for a measuring instrument;
- 3) the coherence dependence on phase instability has a highly nonlinear snake-like character, which is unacceptable for accurate measurements;
- 4) the coherence values are strongly influenced by choice of four setting parameters which is also unacceptable for a measuring instrument;
- 5) different EEG analyzers secretly use different settings of these parameters, so the obtained coherence values are incompatible.

Thus, coherence evaluates unknown what, unknown how, and unknown why, being an example of pseudoscientific anachronism. As the literature reviews, performed in the three main areas of scientific and medical research, show [9–11], the use of coherence leads to a total incompatibility of results on the localization of inter-individual and intergroup differences. Thus, these numerous publications do not belong to the field of science, which is designed to search for and finds objective laws in natural phenomena, but to the category of random noise or pseudoscientific garbage.

Correlation of EEG envelopes

In connection with the numerous and fundamental errors of coherence considered, another and adequate assessment of EEG synchrony was proposed in 2011 [8] by calculating the Pearson correlation coefficient between the envelopes of two EEG derivations. Unlike coherence, this assessment has a direct and fundamental physiological meaning. Indeed, since the envelope represents a change in EEG amplitude modulation (fig. 1)³, it increases with increasing synchrony in the change of postsynaptic

² As the difference in values of vectors increases, the coherence increases, which is directly opposite to the Pearson correlation property. Thus, Wiener, in his algorithm, distorted Hilbert's original idea.

³ Mathematically, the envelope is a module of an analytical (complex-valued) signal, the real part of which is equal to the signal itself, and the imaginary part is obtained from the signal by the Hilbert transform. In turn, Hilbert transform is

potentials under the electrode. Therefore, the envelopes correlation evaluates the degree of synchrony in the dynamics of postsynaptic synchrony between two EEG derivations.

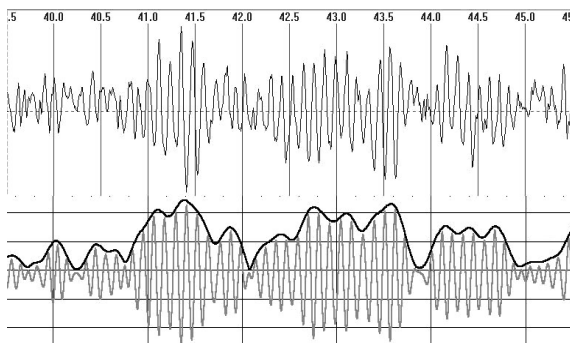


Fig. 1. Example of an envelope: *above* – EEG with a high content of alpha rhythm; *below* – the result of filtering in alpha domain⁴ with an overlay of the envelope.

It was found that in more than 42% of cases, there are high correlations between the envelopes of closely located (neighboring) derivations from 0.6 to 0.99 at the median = 0.42, while for more distant derivations, 98.5% of the envelope correlations do not exceed 0.6 at the median = 0.17. At the same time, highly correlated connections between the envelopes form distinct topographic patterns on the scalp, which are largely preserved in neighboring EEG frequency domains.

This allows us to reduce the amount of significant information, limiting ourselves only to the grid of connections between nearby pairs of derivations; for the 10–20% scheme, such pairs will be 43 (Fig. 2, a). The use of such a standard grid, in particular, contributes to the comparability of the results obtained by different researchers. Within the framework of such a grid, it is easy to visualize highly correlated connections between envelopes (Fig. 2, *a–c*), obtaining well-visually detectable topographic patterns.

equivalent to the double Fourier transform, when before the reverse transformation, all spectral harmonics are shifted in phase by 90°.

⁴ Preliminary filtering of the signal in the selected frequency domain is preferably performed by the double FFT method, characterized by minimal amplitude and phase distortions compared to classical filters.

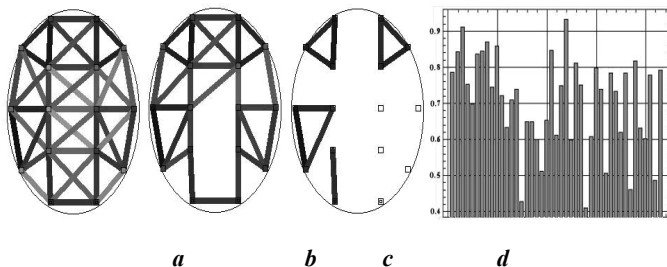


Fig. 2. The three topograms of EEG synchrony of chosen subject for standard grid of channels depending on correlation value r_{xy} : a — $r_{xy}>0.2$; b — $r_{xy}>0.6$; c — $r_{xy}>0.8$; d — profile of synchrony for chosen subject: *vertical axis* — correlation values; *horizontal axis* — the nearby pairs of derivations ordered from left to right and from top to bottom according to its arrangement on a scalp.

The sequence of correlation coefficients between EEG envelopes for pairs of derivations in their ordered sequence in such a standard grid is called the profile of synchrony (PS) of the subject. It is convenient to depict PS in the form of a bar chart (Fig. 2, d), which provides the researcher with an additional visual pattern. It is precisely such profiles that are the source material for the further areas of analysis.

In the case of a group of subjects, we will have a PS matrix (Fig. 3): columns are pairs of derivations from the standard grid, rows are the subjects. Such matrices can be obtained: 1) for different time intervals of the same functional state; 2) for different functional states; 3) for different frequency ranges; 4) for different groups of subjects that differ in certain characteristics, etc. And such matrices in further directions of analysis can be compared in pairs (Fig. 3): 1) by the same pairs of derivations (by columns); 2) by the same subjects (by rows); 3) for all subjects, each with each; 4) for pairs of derivations each with each.

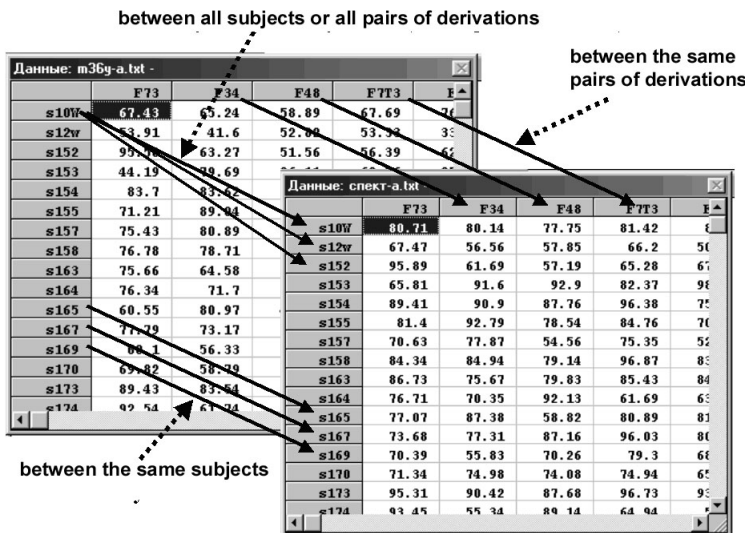


Fig. 3. The example of two matrices with profiles of synchrony for two groups of subjects and three variants of its comparison.

Methodology of the subsequent analysis

After calculating PS of two or more groups of subjects, it is necessary to identify and reliably statistically justify the existence of differences of interest to the researcher [8]. For individual pairwise comparisons, there are several options (Fig. 3). The similarity of the compared pairs is estimated by the correlation coefficients of Pearson, Spearman, Kendall, etc., and the differences are estimated by the parametric and nonparametric criteria of Student, Fisher, Wilcoxon, signs, Ansari Bradley, Klotz, Kolmogorov–Smirnov, etc. Thus, it is possible to identify completely different PS patterns characteristic of *pathology* and *norm* groups (Fig. 4). Simultaneously, it should be remembered that with several paired comparisons at the same time, it is necessary to adjust the critical level of significance of null hypotheses using the Bonferroni correction.

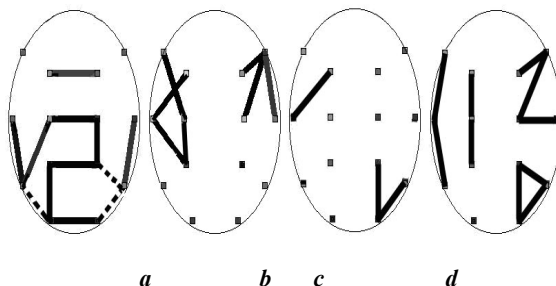


Fig. 4. Differences in EEG synchrony of alpha domain among two groups of examinees: *a* — the differences between pairs of EEG-channels on significance level $p < 0.05$ (solid lines — more EEG-synchrony in the *norm* group, dotted lines — more EEG-synchrony in the *schizophrenia* group); *b* — statistically undistinguished pairs of EEG-channels on significance level $p > 0.6$; *c* — the differences between symmetric pairs of EEG channels (dominating pairs are shown) in *norm* group; *d* — the differences between symmetric pairs of EEG-channels in the *schizophrenia* group.

Further, it is possible to study the difference and similarity of PS of each subject in different frequency domains and at different time intervals to assess the stability of the functional state. Here, according to the correlation coefficients r_{ij} between PS of each j -th subject in two adjacent frequency domains or on neighboring time intervals (Fig. 3), it is possible to make inter-individual comparisons and ranking of the subjects.

The next direction is the use of multidimensional statistical methods to identify intergroup differences. The differences of the matrices in the average PS values are estimated using the 2-ways ANOVA method.

The next step may be to use factor analysis for each matrix to identify PS, mainly projected on the principal factor axes. As follows from Fig. 5, these projections are fundamentally different for the *norm* and *pathology* groups. To quantify the differences, it is possible to calculate correlations between the factor loadings of PS for each factor performed between the two groups of subjects. As a result, the correlations for the three principal factors are obtained at a minimum of 0.106–0.328, which indicates a fundamental difference in factor structures and intergroup differences.

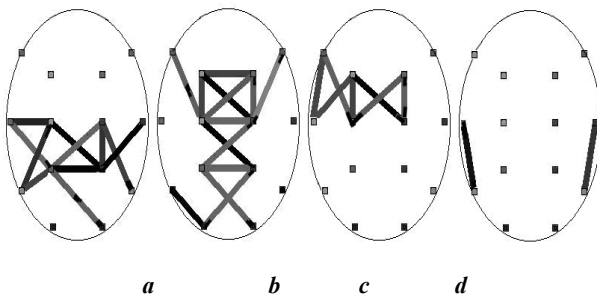


Fig. 5. The pairs of EEG derivations which PS has preferential projections on the first (*a, b*) and second (*c, d*) of main factors for the *norm* (*a, c*) and *schizophrenia* (*b, d*) groups.

One of the most important methods is to use the discriminant analysis, which allows us to construct a classifying function for a statistically reliable and stable division of subjects into two analyzed groups. Such a function can be practically used to assign new individuals to a particular group, that is, as a means of preliminary medical or functional diagnostics.

Identification of highly consistency groups of subjects

One of the important statistical tasks is the identification and processing of outliers and the selection of homogeneous groups of subjects, which, unfortunately, are almost not taken into account in EEG studies. Such outliers are the result of the action of extraneous and accidental causes that can mask really existing patterns. Inattention to these issues may lead to the identification of *pseudo-significant* or *pseudo-not-significant* individual and intergroup differences.

Since in the method under consideration, we do not have samples of variable values, but PS are the sets of measurements, so we do not apply the usual method of detecting outliers by large deviations from the average value. Therefore, a special method of averaged correlations of PS was developed [8]. In this case, for each group, paired correlations r_{jk} between PS of all j, k -subjects are calculated at a given time interval. Then we get a square correlation matrix $|r_{jk}|$ by which the average value $M_j(r_{jk})$ from its correlation with all other k -th subjects is determined for each j -th subject. Then, using the obtained $M_j(r_{jk})$, variation series or Quetelet graphs are constructed (Fig. 6), on which subjects with low consistency or outliers are distinguished. They may be the result of uncontrolled features of current functional and mental state or errors in diagnosis. Therefore, they should

be removed from further analysis.

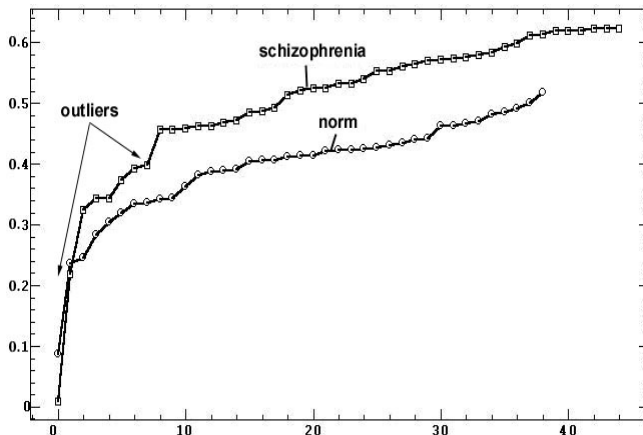


Fig. 6. The diagram of the distribution of average correlation between PS of alpha domain in two groups of subjects: *vertical axis* — correlation values; *horizontal axis* — the subjects ordered on increase of average correlation.

Fig. 6 also shows a higher value of average consistency in *pathology* group $M_j(r_{jk})=0.505\pm 0.12$ in comparison with *norm* group $M_j(r_{jk})=0.397\pm 0.084$ with their significant difference at the significance level $p<0.00005$. This confirms a well-known rule: «*every healthy person is healthy in his own way, but all the "sick" persons are sick in the same way*». This is a real confirmation of the effectiveness and adequacy of the envelope correlations method.

Results of the method application

The described method of envelope correlations (MEC) was used to assess various mental diseases and functional states. EEG recordings were carried out in a state of relaxation with closed eyes according to 10–20% system of derivations.

Schizophrenia [8]

The material included adolescents aged 10–14 years: 39 schoolchildren without mental disorders (the control or *norm* group) and 45 patients with schizophrenic disorders in categories F20, F21, F25 according to ICD-10.

The following significant results were obtained: 1) numerous topographic patterns that are far from a random distribution (Fig. 2, 5); 2) proximity of topographic patterns in neighboring frequency ranges (Fig. 7, 8); 3) higher stability of functional state over time in the *norm* group; 4) higher interindividual consistency of *pathology* group (Fig. 6); 5) difference of pairs of derivations with high synchrony in the two groups of subjects (Fig. 8); 6) higher synchrony in the *norm* group (Fig. 7); 7) a consistent decrease in synchrony from the frontal interhemispheric connections to the occipital ones in both groups (Fig. 7); 8) a difference in topography of hemispheric dominance with its wider spatial representation in *pathology* group (Fig. 8); 9) a strong factor structure of PS in both groups with the predominance of four main factors; 10) a qualitative and quantitative difference in the factors acting in two groups (Fig. 5).

Further, the MEC results were compared with five other well-known synchrony estimates in the literature: coherence [7], inter-segment synchrony [12], correlations between the frequency parts of amplitude and phase spectra [13] and between filtered EEG. According to the indicators of descriptive statistics, MEC differed favorably from other methods in terms of centering and uniformity of its values distribution in 0–1 region.

The discriminant classification gave the best results in θ , α , β_1 domains with 2–3% errors for each group compared to 5.5–28.2% errors when using other methods [14–17]. Statistical modeling showed that the resulting small percentage of MEC errors differs significantly from the random one at the significance level $p < 0.005$. Then, EEG measurements of amplitudes in derivations were added to the PS matrices, which led to 100% reliable, error-free classification.

To substantiate the practical significance of the results obtained, a control check was carried out. To do this, the *pathology* group was randomly divided into two ones in a ratio of 3:2 – the *learning* and *classified* samples. The discriminating function was calculated from *learning* sample, which was then used to assign to a particular group of *classified* subjects. Using of α domain and consistent subgroups of subjects gave the best result: 1.5% of errors in *learning* classification and 6.2% of errors in *control* classification. It should be noted that such important control checks have never been carried out anywhere and by anyone.

Schizophrenia [9]

The material included three groups of 8–15-year-old adolescents: 36 schoolboys without mental disorders (the *norm N* group), the group of 45 patients with the diagnosis of F20 *schizophrenia*, and the group of 80 patients with the diagnosis of F21 *schizotypal disorder*.

The results of the performed complex analysis reveal the complicated picture of regional, interhemispheric differences in EEG synchrony between two schizophrenic disorders and the norm. In particular, most of the patterns listed at the beginning of Section 7.1 were confirmed.

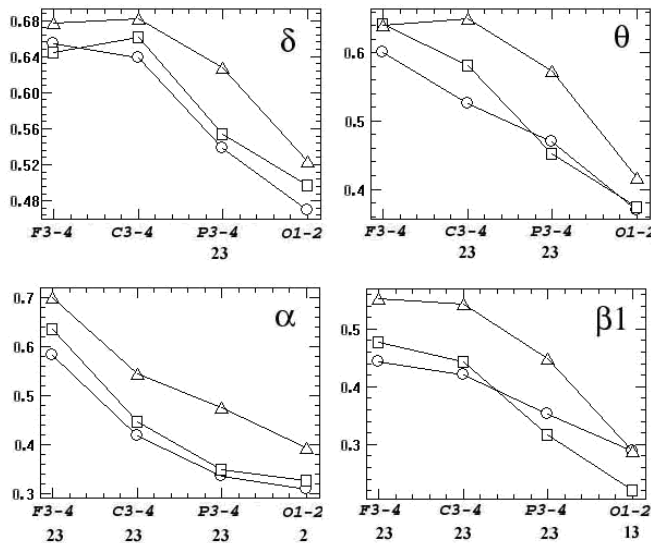


Fig. 7. Differences in interhemispheric synchrony for five frequency domains ($p=0.04-0.0004$). The values averaged for each group, synchrony (vertical axes) are shown for derivation pairs: $F3-F4$, $C3-C4$, $P3-P4$, $O1-O2$ (horizontal axes). Group markers: circles – F20, squares – F21, triangles – N. Below graphics, the designation of reliable intergroup differences is shown in number notation: 1 – F20–F21, 2 – F20–N, 3 – F21–N

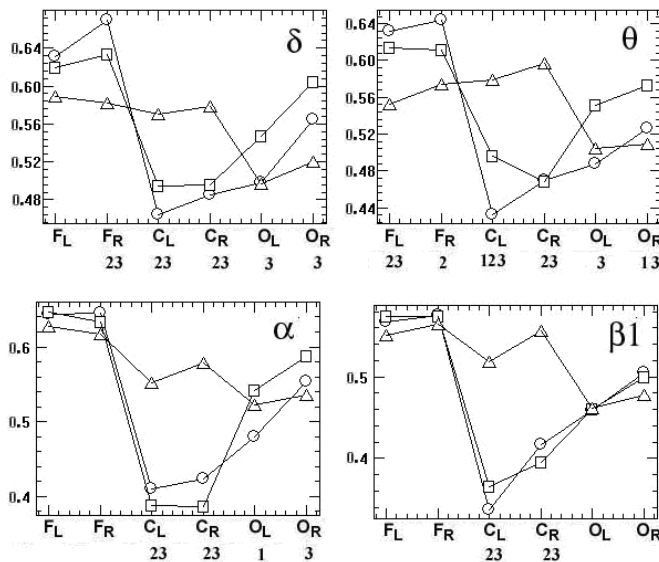


Fig. 8. Regional intra-hemispheric differences in frequency domains ($p=0.033-10^{-8}$). The averaged values of synchrony for each group (vertical) in order of regions (horizontal): F_L , F_R (frontal left and right), C_L , C_R (central left and right), O_L , O_R (occipital left, right)⁵, other notations are similar to Fig. 7.

It is necessary to emphasize, that in this study not only the usual problem of differentiation of norm and pathology was considered, but at the same time also the non-depicted earlier in literature more complex task of detection of subtle differences between the two close nosologies. The significant differences between F20 and F21 groups appear mainly in frontal and occipital areas in certain frequency domains. Besides, in occiput, interhemispheric and intra-hemispheric synchrony for schizophrenia (F20) in some cases was closer to normal. In contrast, for schizotypal disorder (F21), intrahemispheric synchrony is higher than normal, but interhemispheric synchrony is below than normal. Certain relationships of this kind are also observed in parietal, temporal, and central areas.

One the distinctive and stable component of mental disorders in comparison with the norm is the presence of the vast areas of low

⁵ e.g., F_L region comprising the synchrony values between $F7$, $F3$, $T3$, $C3$ derivations; C_L , region including synchrony between $T3$, $C3$, $T5$, $P3$; O_L region including synchrony between $T5$, $P3$, $O1$, etc.

ynchrony separating isolated frontal and occipital intrahemispheric areas with synchrony near to normal level (Fig. 8). The presence of such a reduction and detection of right-sided asymmetry can indicate a substantial violation of interhemispheric and frontal-occipital relationships for the schizophrenic and schizotypal disorder, which fits into the framework of the well-known theory of disintegration of cortical electrical activity.

The intergroup comparison reveals the crosswise area of the sharp decrease in synchrony of pathology groups ("downfall") in comparison with the norm, including sagittal-interhemispheric and axial-central segments (Fig. 8). It's possible that this indicates significant violations of interhemispheric and frontal-occipital relationships at disorders of the schizophrenic spectrum. When comparing two pathology groups (F20–F21), in many frequency domains we also observe distinctive regional and interhemispheric areas of increase-decrease of synchrony.

Four psychometric tests were performed on all patients: volume of direct reproduction defined by the technique of memorization of 10 words under verbal presentation; volumes of simple and difficult paired associates; runtime of Schulte tables execution. Indeed, violation of cognitive functions is one of the main consequences of schizophrenia. Several high correlations between psychometric indicators and local estimates of synchrony for each of F20 and F21 groups were revealed.

The main results of discriminant classification are the following: 1) θ domain provides the lowest percentage of classification errors; 2) $\beta 2$ domain is the next one by its discriminant sensitivity; 3) association of PS of these two frequency domains gives the exact classification of three groups without any errors. The obtained results favorably differ from several alternative approaches using other indicators and more sophisticated methods – see in Section 7.1. It should also be emphasized, that the efficiency for classification of θ domain was also found in the previous study.

Numerous confirmations of the results of the previous study in different groups of patients indicate the stability and effectiveness of MEC compared to the above-mentioned randomness of the coherent analysis results.

Depression [10]

The material included two groups of older adults aged 49–82 years: 1) 11 men and 40 women with the psychogenically provoked depressive

reaction of bereavement: category F43.21 according to ICD-10, HDRS=22±5.09 on Hamilton scale; 2) a control group of 18 men and 11 women without depressive disorders.

The results of the analysis revealed a complex picture of regional and interhemispheric differences in EEG synchrony between the norm and depressive deviations, including different ratios of greater — less or the same synchrony in activity of different cortical zones.

One of the principal features of the obtained integral picture is the presence of extended zones of sharply reduced synchrony of neurophysiological activation processes in depression, covering the entire pre-medial region in the forehead-occipital direction, including interhemispheric connections, as well as lateral frontotemporal connections in both hemispheres. In the same time, a single topographic picture of changes in EEG synchrony during depression is reproduced in general terms in all frequency domains. This indicates a deep deprivation in depressions of frontal-occipital, frontal-temporal and interhemispheric interactions throughout in sagittal direction.

There is a general decrease in sagittal directions with signs of left-sided asymmetry. This indicates that greater activation of right hemisphere, which causes the predominance of negative emotions in depression, maybe enhanced with a greater discoordination of processes in the right hemisphere.

In addition, an increase in synchrony was revealed in several axially directed intra-hemispheric pairs of derivations primarily in temporo-central and temporo-parietal ones. This may indicate an increase in systemic coordination between auditory and somatosensory sensitivity in the primary projection areas and in the associative posterior temporal and parietal zones. On the other hand, a decrease in synchrony in sagittal anterior-posterior-temporal and central-parietal pairs of derivations may indicate a deprivation of systemic coordination between the processes in the areas of primary projection of the auditory and tactile analyzers and the associative processes of integrated perception of corresponding sensations. About the primary and associative visual areas, such synchronization-desynchronization phenomena are not observed.

It should be particularly noted that a similar picture of differences in norm and pathology was also revealed in the study of schizophrenia, where there was also an extended interhemispheric and pre-medial-sagittal zone of

decreased synchrony from the forehead to the back of the head with a compensatory increase in correlation synchrony in axially conjugated pairs of derivations. This indicates the similarity of changes in synchrony of neurophysiological activation processes in these two types of mental disorders.

This similarity of changes looks even more convincing considering that the topography of correlation synchrony distribution in the group of healthy adolescents had significant differences from the group of healthy older adults. This suggests that MEC detects similar changes in different forms of pathology and in different age groups. This stability compares favorably with the heterogeneity of the results obtained when using coherence function in studies of depression and schizophrenia.

In discriminant classification, the use of δ , θ , β_2 frequency domains allows to accurately separate the records of two studied groups without any errors. Recall that θ , β_2 domains were also the best ones for classification of schizophrenia, which once again confirms the stability of MEC results. The only alternative classification of norm and depression using estimates of spectral power and coherence [18] was accompanied by 8.7% of errors.

Sleep stages [11]

The material included many hours of sleep recordings for 15 right-handed men aged 18–34. Seventy-five 20-second fragments were visually selected for each of 5 sleep stages W, 1, 2, 3/4, REM according to Rechtshafen—Kale criteria. The five PS matrices calculated from these fragments were the source material for subsequent cross-analysis.

In addition to numerous particular regularities, the following significant results were obtained: 1) left-hemisphere dominance in all stages of sleep, which is natural for right-handed subjects and indicates the effectiveness of MEC; 2) the dominance of the frontal regions over the occipital ones; 3) differences in the synchrony ratios for sleep stages in different frequency domains; 4) differences in the patterns of synchrony changes in interhemispheric connections from the forehead to the occipital ones; 5) topographic features of localization of highly synchronous connections by sleep stages and frequency domains; 6) significant topographic difference of W stage from other stages; 7) close topography is observed: in θ

domain for all stages; as well as in stages 2 and 3/4 for all frequency domains.

Discriminant classification with expanded data matrices, when amplitude indicators were added to PS matrices, revealed an average of 11% errors, and classification errors of individual stages were in the range of 3–20%. This is significantly better than the results of four similar publications using other methods, where the classification errors of various stages were 5–42% [19–22].

Additionally, a control check was performed when the records of each sleep stage were divided into two groups in the ratio of 80 to 20% – a learning and a classified sample. The number of classification errors of the learning sample was 7%, and the attribution errors of the classified sample were 18.3%. This seems to be a completely acceptable result, which is absent in other publications.

Conclusion

The results presented in Sections 7.1–7.4 exhaustively and comprehensively substantiate the thesis formulated in the title of the article.

REFERENCES

1. Kulaichev A. P. Metrology of computational EEG analysis. Actual problems of the humanities and natural sciences. 2018. 8(115):17-22.
2. Tong S., Thankor N.V. Quantitative EEG analysis methods and clinical applications. Boston. Artech House. 2009. 421 pp.
3. Kulaichev A.P. Inaccuracy of Estimates of Mean EEG Amplitude in Frequency Domains Based on Amplitude and Power Spectrum. Int J Psychol Brain Sci. 2016. (1) 2: 21-28.
4. Wiener N. Generalized harmonic analysis. Acta Math. 1930. 55: 182-195.
5. Randall R.B. Frequency Analysis. Brüel & Kjaer, Copenhagen. 1989. 344 pp.
6. Walter D.O. Spectral analysis for electroencephalograms: Mathematical determination of neurophysiological relationships from records of limited duration. Exper. Neurol. 1963. 8: 155-181.
7. Kulaichev A.P. The Informativeness of Coherence Analysis in EEG Studies. Neurosci. Behav. Physiol. 2011. 41(3): 321-328.
8. Kulaichev A. P. Method of analysis of EEG correlation synchrony and its possibilities. Zh Vyssh Nerv Deiat I P Pavlova. 2011. 61(4): 485-498.

9. Kulaichev A.P., Gorbachevskaya N.L. Differentiation of norm and disorders of schizophrenic spectrum by analysis of EEG correlation synchrony. *J Exp Integr Med.* 2013. (3): 267-278.
10. Kulaichev A. P., Iznak A. F., Iznak E. V., Kornilov V. V., Sorokin S. A. Changes in EEG correlation synchrony in depressive disorders of psychogenic type. *Zh Vyssh Nerv Deiat I P Pavlova.* 2014. 64(2): 1-9.
11. Kulaichev A. P. Comparative analysis of correlation synchrony and EEG amplitude ratios in night sleep. *Zh Vyssh Nerv Deiat I P Pavlova.* 2012. 62(1): 108-119.
12. Borisov S.V., Kaplan A.Ya., Gorbachevskaya N.L., Kozlova I.A. Analysis of EEG structural synchrony in adolescents with schizophrenic disorders. *Human Physiology.* 2005. 31(3): 255-261.
13. Sterman, M.B., Kaiser, D.A. Comodulation: A new QEEG analysis metric for assessment of structural and functional disorders of the CNS. *J. Neurotherapy.* 2001. 4(3): 73-83.
14. Boostani R., Sadatnezhad K., Sabeti M. An efficient classifier to diagnose of schizophrenia based on the EEG signals. *Expert systems with applications.* 2009. 36(3): 6492-6499.
15. Ince N.F., Stephane M., Tewfik A.H., Pellizzer G., McClannahan K. Schizophrenia classification using working memory MEG ERD/ERS patterns. *Proc. of 3rd int. IEEE/EMBS conf. on neural eng.* 2007. 457-460.
16. Sakoglu U., Michael A.M., Calhoun V.D. Classification of schizophrenia patients vs healthy controls with dynamic functional network connectivity. *NeuroImage.* 2009. 47(1): S39-S41.
17. Winterer G., Ziller M., Dorn H., Frick K., Mulert C., Wuebben Y., Herrmann W. M. Frontal dysfunction in schizophrenia – a new electrophysiological classifier for research and clinical applications. *Europ. archives of psychiatry and clin. neuroscience.* 2000. 250(4): 207-214.
18. Knott V., Mahoney C., Kennedy S., Evans K. EEG power, frequency, asymmetry and coherence in male depression. *Psychiat. Res.* 2001. 106(2): 123-140.
19. Fell J., Roschke J., Mann K., Schaffner C. Discrimination of sleep stages: a comparison between spectral and nonlinear EEG measures. *EEG Clin. Neurophysiol.* 1996. 98(5): 401-410.
20. Park Hae-Jeong, Oh Jung-Su, Jeong Do-Un, Park Kwang-Suk. Automated sleep stage scoring using hybrid rule and case-based reasoning. *Comput. Biomed. Res.* 2000. 33(5): 330-349.

21. Susmakova K., Krakovska A. Selection of measures for sleep stages classification. Proc. 7th Int. Conf. Measurement. Smolenice. 2009:86-89.
22. Susmakova K., Krakovska A. Discrimination ability of individual measures used in sleep stages classification. Art. Intel. Med. Arch. 2008. 44(3): 261-277.

CHAPTER 4

EFFECTIVE DIFFERENTIATION OF NORM AND SCHIZOPHRENIA BY ANALYSIS OF EEG CORRELATION SYNCHRONY

ABSTRACT

Objectives: The goal of the study was to discover the integrated differences in electroencephalography (EEG) synchrony between healthy people and patients with schizophrenia illnesses.

Methods: In this investigation, EEG recordings were made under a state of quiet wakefulness with eyes closed for three groups of 8–15-year-old adolescents: normal group and two groups of mental disorders in nosological categories F20 and F21 according to International Classification of Diseases (ICD)-10. We employed an alternate approach for assessing EEG synchrony based on correlation between EEG signal envelopes. This method has been shown to be a highly sensitive tool for distinguishing between psychopathological and functioning states in the past.

Results: The investigation revealed a complicated picture of major topographical, inter-hemispheric, regional, and age distinctions, in which many of the fragmentary results previously received by other researchers were confirmed. One of the basic features of the received integrated picture of pathology is existence of extended zones of sharply lowered EEG synchrony dividing local and isolated areas in frontal and occipital regions mainly of normal or sometimes increased EEG synchrony. The obtained results are perfectly consistent with the notion of cortical electric activity disintegration in schizophrenia spectrum diseases.

Conclusion: The technique used provides nearly 100 percent reliability of tripartite classification of norm and two pathology groups individually, it allows for the discovery of many authentic correlations between EEG synchrony estimations and psychometric indices, and its results are consistently reproducible for different groups of patients and examinees,

opening up opportunities and prospects for its use as an auxiliary quantitative differential indicator.

Keywords: Discriminant classification; electroencephalography; envelope correlation; schizophrenia; schizotypal disorder.

INTRODUCTION

According to the special review [1] among the numerous papers devoted to electroencephalography (EEG) differences between norm and schizophrenia, relatively few studies relate to differences in EEG synchrony in a state of quiet wakefulness. However, when compared to amplitude spectrum [2-4], power spectrum [1], and certain other metrics [4], the classificatory sensitivity of EEG synchrony estimations is substantially higher. To a large extent, this is due to the fact that EEG synchrony estimates have significantly lower intra-individual variability, which is 8-12 percent compared to 23-41 percent for average amplitude spectrum and 86-95 percent for power spectrum, according to our data obtained at various experimental materials and estimated by variation coefficient. So, by EEG synchrony estimations it is possible to receive reliability of comparable distinctions at smaller sample volumes and reliability of smaller distinctions under comparable sample volumes. In general, synchronous cortical rhythms support the idea of intact functional and anatomical connection between different brain areas. This is of particular importance as disturbed oscillatory activity, alterations in synchronization and dysfunctional intra- and interhemispheric connectivities are an important feature in schizophrenia [5-7].

Results obtained by different researchers are rather fragmentary and contradictory, that was noted in the discussion [8]. Some researchers have found that compared with the norm at schizophrenia a coherence is lower, namely: (a) intra- and inter-hemispheric coherence in all domains [9]; (b) violated left hemispheric $F-T$ connections [10]; (c) a coherence in delta (δ) and theta (θ) domains at $Fp1-F7$ derivations and in alpha (α) domain at $F7-F8$ [11]; (d) a coherence in δ domain in temporal lobe [12]. Other studies on the contrary have shown that for schizophrenia compared with the norm a coherence is higher, namely: (a) intra- and inter-hemispheric one in θ domain and intra-hemispheric one in α domain [13]; (b) inter-hemispheric one in δ and beta (β) domains at $O1-O2$ and in δ domain at $T5-T6$ [14]; (c) intra-hemispheric one in general [15] or only in δ domain [16]. It is significant that most of the cited works were published about ten and more years ago. Probably, such a situation is caused by the fact that

coherence function is unstable indicator of EEG synchrony [17- 20]. The observed inconsistency of results makes it actual to use alternative approaches for the evaluation of EEG synchrony in this field.

MATERIALS AND METHODS

EEG recording was carried out in a state of quiet wakefulness with eyes closed. The electrodes were placed according to 10-20% system in 16 cortex areas ($O1, O2, P3, P4, C3, C4, F3, F4, T5, T6, T3, T4, F7$ and $F8$); united ears electrodes were used as referents ($A1+A2$); the bandwidth was 0.5- 35 Hz; sampling rate was 200 Hz. For the analysis we selected the fragments free of artifacts with a duration of 41 seconds (8196 discrete time slots). The analysis was carried out in five standard frequency domains: δ 0.5-4 Hz, θ 4-8 Hz, α 8-13 Hz, β -1 13-20 Hz, β -2 20-32 Hz.

The group of patients with disorders of schizophrenic spectrum was diagnosed according to International Classification of Diseases (ICD)-10 in Mental Health Research Center, Moscow and it consisted of 125 boys (8-15 years old). For 45 of them (age 11.5 ± 2.2 years), the diagnosis made was schizophrenia, childlike type (F20), and for 80 adolescents (age 11.9 ± 2.5 years) schizotypal disorder (F21). Control group (N, norm) included 36 pupils from Moscow's schools without documented mental deviations (age 12.2 ± 2 years). Parents of all examinees gave the written permission for carrying out researches and publication of their results.

In this study we used the alternative approach to similarity estimation between bioelectric activity of different cerebral areas: the analysis of EEG correlation synchrony (ACS) was proposed and detailed previously [4]. It estimates the degree of EEG synchrony by correlation coefficient between envelopes of EEG records preliminary filtered in a given frequency range. Here it is appropriate to emphasize that as an envelope representing a change of EEG amplitude modulation, the synchrony estimation constructed on its basis has the direct and important physiological sense (unlike coherence). Indeed, the EEG amplitude increases with increase of synchrony of postsynaptic potentials, so the correlation of EEG envelopes estimates the degree of synchrony in change of such intra-neuronal synchronism.

An ordered sequence of such correlations between nearby derivations (in our case, between 36 EEG derivation pairs) have been named 'profile of synchrony' (PS) and such profiles as topographic patterns of EEG synchrony (for group of subjects we have an array or a matrix of profiles)

are the source material for the further analysis. This method has already demonstrated its high efficiency for a similar problem [4] as well as for differentiation of night sleep stages, i.e. functional states [3].

Below for evaluation of pairwise sample differences we use the nonparametric Wilcoxon test since a large part of sample distributions differs from normal law. For evaluation of group differences, we also apply the two-way analysis of variance (ANOVA) with repeated measures design (number of repeated measures is equal to number of subjects in compared groups). We also use the designations of groups: F20, F21, N and the designation of frequency domains: δ , θ , α , β -1, β -2.

RESULTS

Analysis of Records on Consistency

In any statistical sample, due to the influence of casual, uncontrolled factors in an experiment, there are outliers, and also among measurements there are some which are more and some which are less consistent. For reliable separation of prevailing parties, it is desirable preliminarily to clear samples of outliers as well as of less consistent measurements. In our case, a role of random factors can be acted by: (1) instrumental factors such as differences in position of electrodes concerning anatomic cortex structures, changes in inter-electrode resistance, etc; (2) personal factors such as differences in individual EEG characteristics, differences in current physiological and psychological state, etc; (3) classifying factors such as patients belonging to nosology not differentiated or not clearly differentiated in ICD-10 [21], subjective judgments of psychiatrists, etc. Therefore, in each of two groups of patients it is desirable to get rid of influence of such extraneous casual factors by extracting among each of groups a central compact “kernel” of highly consistent measurements. In connection with the representative statistical volume of available samples, such selection of compact “kernel” is considered to be possible to perform.

For this purpose, we used the method, which was proposed previously [4] and showed its effectiveness for a similar task as well as for differentiation of functional states [3]. Its essence is calculation of the average correlation of PS of each subject with profiles of synchrony of all other subjects. This average correlation estimates the average personal consistency of topographic distribution of EEG synchrony on scalp. As a result, a growing sequence of such estimates (rank- ordered sample) is formed. Using this chart we select subjects, averaged correlations of which exceed 0.4-0.5 and number

of which is not less than 50% of original sample.

Since our analysis is carried out in 5 frequency domains, in order to perform the abovementioned selection, the estimates should be used that averaged over 5 domains. In the variational series for F20 and F21 groups (Fig. 3.1a) we can see the presence of outliers and of several subgroups of different degree of consistency. Fig. 3.1b presents variational series of highly consistency subgroups of F20, F21 and N subjects. The fact draws the attention that N subgroup is characterized by less averaged consistency (0.5) compared with F20 and F21 subgroups (0.52 and 0.55, respectively). This confirms the conclusion [18] that a sample from a less representative general population related to a particular type of pathology turns out to be more consistent than a sample from a much larger population related to psychological norm, or in other words according to winged expression: every “healthy” man is healthy in its own way but every “sick” one is sick alike.

It is necessary to emphasize, that in this study not only the usual problem of differentiation of norm and pathology was considered, but at the same time also the non-depicted earlier in literature more complex task of detection of subtle differences between the two-close nosology. Such a formulation of the task proves advisability and necessity for the following analysis of use of the highly consistent EEG records (Fig. 3.1b): (1) F20 subgroup included 23 patients in age of 11.2 ± 2.1 ; (2) F21 subgroup included 41 patients, in age of 12.2 ± 2 . As anyone can see, the selected subgroups reproduce the age ratio of initial groups in a well-balanced way, and on this basis, they are also quite suitable for the further analysis.

In a case of larger volume of experimental data, the second stage could be completed of the source material purification, which consists in removal of records, synchrony profiles of which contain two or more values exceeding three standard deviations. A simple statistical calculation shows that probability of occurrence of such a “complex” outlier among 36 variables of synchrony profile is 0.054.

Discriminant Classification

The results of some our researches, in particular [3,4], have shown that linear discriminant classification of groups of subjects corresponding to different nosology, therapeutic treatment, functional states, social, age and sexual categories is the effective primary indicator of prospectivity of further research. If such a classification of originally specified groups

gives a significant number of errors (over 20-30%), then such groups are slightly differing by their EEG indicators or are strongly internally heterogeneous, and if so, further detailed analysis of their differences is, as a rule, unproductive.

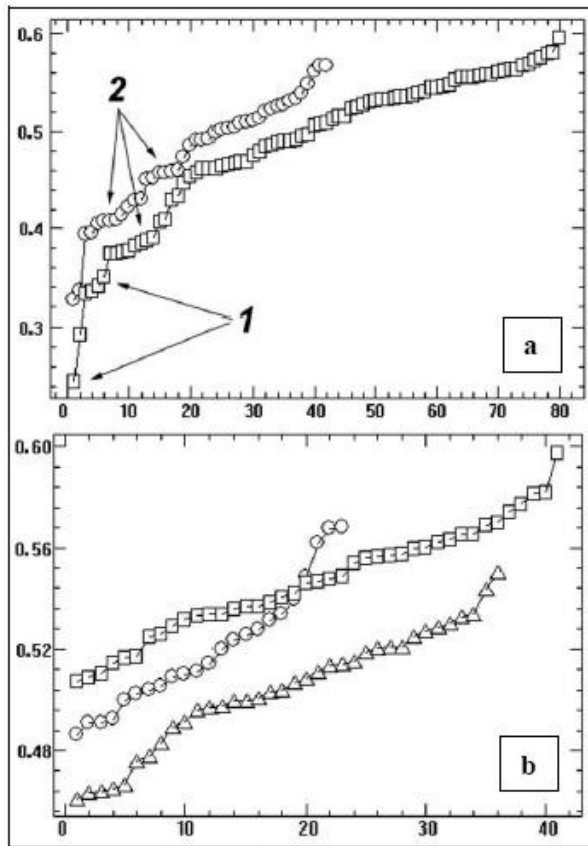


Fig. 3.1. Average inter-individual correlations of synchrony profiles of EEG records (vertical) in its ascending order (horizontal): (a) all records of F20 and F21 groups; circles, F20 group; squares, F21 group; (b) highly consistent records of F20 and F21 groups, and all records; triangles, N group; (1) outliers, (2) less harmonized subgroups

The results of the classification are given in Table 3.1. Let us note the following: (1) θ domain provides the lowest (on average) percentage of classification errors, which confirms the previous results [4]; (2) β -2

domain is the next one by its discriminant sensitivity; (3) association of indicators of these two frequency domains gives the exact classification of three groups; (4) presence of small errors of classification shows that: (a) the performed selection of subjects assured sufficient consistency of each pathology group; (b) a detailed analysis of intergroup differences promises fruitful results.

The obtained results favorably differ from a number of alternative approaches using other indicators and more sophisticated methods for classification by normal and schizophrenic patterns of EEG, where the number of errors makes: 23% [22], 12.5% [23], 5.5-13.5% [24], 25-28.2% [25], 18.6% [26]. Only in the study by Kaplan et al. [27] the accuracy of classification has been achieved close to 100%, however, the revealed there set of rules was able to achieve a unidirectional separation of schizophrenia from the norm, but not vice versa.

Table 3.1. Errors of discriminant classification (in percentage) between the norm and the pathology ($F20_m + F21_m \leftrightarrow N_m$) and between two pathology categories ($F20_m \leftrightarrow F21_m$) depending on a frequency domain

Frequency domain	$F20_m + F21_m \leftrightarrow N_m$	$F20_m \leftrightarrow F21_m$	Mean value
δ	4	7	5.5
θ	4	3	3.5
α	2	10	6
β-1	3	10	6.5
β-2	1	9	5
θ + β-2	0	0	0
Mean value	2.3	6.5	

It is also interesting to compare these results with discrimination by usage of spectral estimations. Let's restrict ourselves to θ domain which is the best one for minimizing errors. The usage of spectrum amplitude averaged in frequency domain [mcV] gives '(9 + 25) / 2 = 17%' classification errors

in average (9%, 25% and 17% correspond to three columns of Table 3.1); a usage of averaged power estimates [mcV2] gives ' $(15 + 29) / 2 = 22\%$ ' errors; the logarithm of power [2log(mcV2)] often used in studies gives ' $(10 + 22) / 2 = 16\%$ ' errors. This once again confirms the above given conclusion on the higher discriminating sensitivity of EEG synchrony estimates.

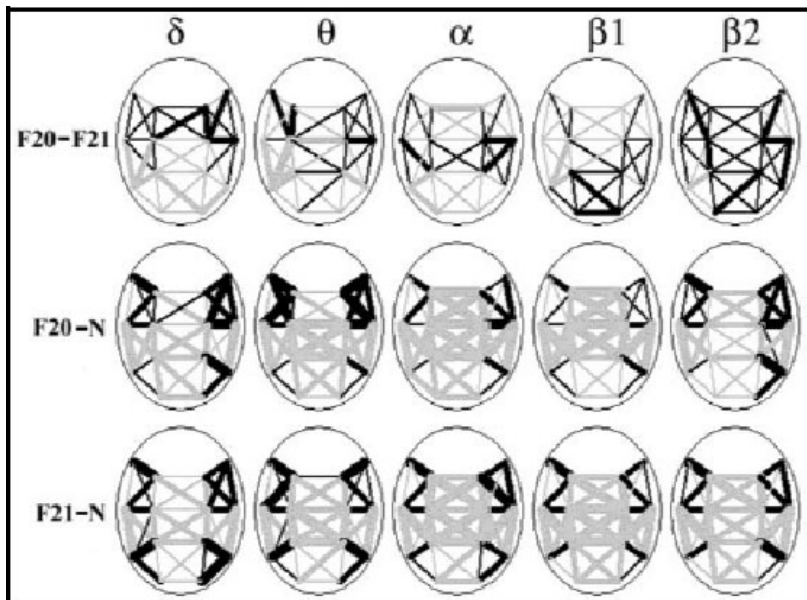


Fig. 3.2. Topographic maps of intergroup differences (compared groups are designated at the left) in averaged synchrony for all derivation pairs in 5 frequency domains (specified at top). Black lines specify the higher synchrony in the first of two compared groups; gray lines, the smaller synchrony; three gradation of lines thickness specify the absolute difference in averaged synchrony (ΔS) between two compared groups as it increases: $\Delta S < 0.05$; $\Delta S < 0.1$; $\Delta S > 0.1$

Local Relations of Synchrony

In order to determine directions and prospects for further analysis it is necessary, first of all, to examine the overall detailed picture of relations of EEG synchrony between normal and pathological groups. For each of three groups we compute the average values of synchrony in each derivation pair and scrutinize intergroup ratios of greater/lesser synchrony (Figs. 3.2 & 3.3).

At the topograms in Figs. 3.2 & 3.3, first of all, our attention is drawn to the crosswise area of sharp decrease in synchrony of pathology groups ("downfall") in comparison with the norm, including sagittal inter-hemispheric and axial-central segments. It's possible that this indicates significant violations of inter-hemispheric and frontal-occipital relationships at disorders of schizophrenic spectrum. At comparison of two pathology groups (F20-F21), in many frequency domains, we also observe distinctive regional and inter-hemispheric areas of increase/decrease of synchrony.

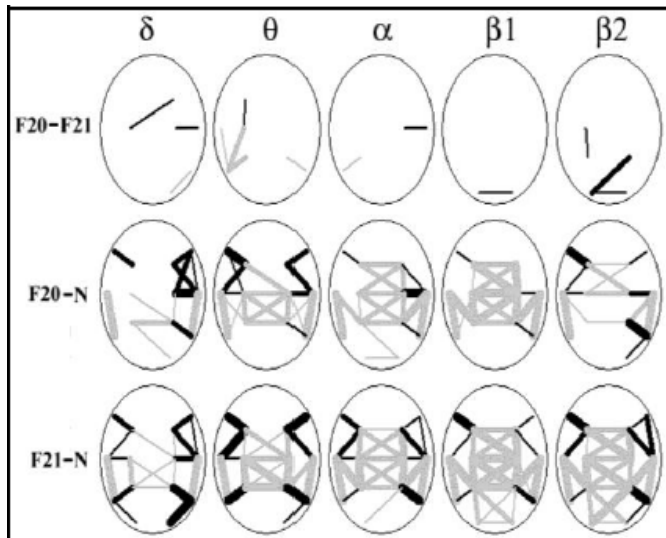


Fig. 3.3. Topographic maps of intergroup differences reliability in averaged synchrony for derivation pairs in 5 frequency domains. Three gradation of lines thickness specify the significant level of null hypothesis: $0.01 < P < 0.05$; $P < 0.01$; $P < 0.001$. Other notations are similar to Fig. 3.2

Due to observed regional structure of intergroup synchrony relations with a purpose of identification of statistically significant patterns it is more appropriate now to consider separately inter-hemispheric and averaged regional intra-hemispheric ratios.

Interhemispheric Synchrony

For each group and each frequency domain there were calculated average values of synchrony between derivations $F3-F4$, $C3-C4$, $P3-P4$ and $O1-$

O2. The results are presented in Fig. 3.4. From comparison of the charts and the statistical distinctions, first of all, it should be noted that;

- (1) In most cases, there can be observed a reduction of synchrony in ‘**center** → **vertex** → **occiput**’ direction. Jonckheere test, which takes an orientation of factor effect into account, reveals the existence of such trends at $P = 0.03-10-7$ for all groups and domains (except for F20 group in β -2 domain). The reduction of synchrony in ‘**front** → **center**’ direction is observed for all groups in α domain ($P = 0.0002-10-7$) and for pathology groups also in θ domain ($P = 0.016-0.0012$). This conclusion coincides with the results of Borisov et al [8].
- (2) In most cases (68% from 40 comparisons, $P = 0.04-0.0004$) there is observed the higher synchrony in N group in relation to F20 and F21 groups, and in 23% cases this ratio is manifested in a form of trend of mean values. This conclusion coincides with the results of Borisov et al. [8] and Strelets et al. [9] being opposite to some fragmentary conclusions [13, 14]; the latter ones however are distinguished by statistically small volumes of samples included 8 and 11 patients.
- (3) Local differences between F20 and F21 groups are observed only in *O1-O2* occipital pair in β -1 ($\delta = 0.04$) and β -2 ($\delta = 0.03$) domains, and in both cases, the synchrony values for F20 group do not differ from the norm ($\delta = 0.46$), but for F21 group these values are significantly lower ($P = 0.043$).
- (4) However, in Fig. 3.4 for F20 and F21 groups in sagittal neighboring derivation pairs we see systematic differences between them that the analysis of variance allows to reveal when the second factor is regional one (2 factor gradations): **(a)** increase of synchrony in F21 group (with the convergence to the norm) in *F-C* region in θ domain ($P = 0.00005$); **(b)** increase of synchrony in F20 group (with the convergence to the norm) in *F-C* region in β -1 ($P = 0.00001$) and β -2 ($P = 0.004$) domains.
- (5) For differences between front-occiput regional synchrony (*F-O*) there is only one distinction between F20 and F21 groups in β -1 domain ($P = 0.01$)

Regional Intra-hemispheric Differences

For each group and for each frequency domain there were calculated average values of synchrony for six regions: for the left and right frontal regions (FL and FR, respectively) comprising the values of synchrony

between $F7, F3, T3, C3$ and $F8, F4, C4, T4$ derivations; for the left and right central ones (CL and CR) including synchrony between $T3, C3, T5, P3$ and $C4, T4, P4, T6$ derivations; for left and right occipital ones (OL and OR) including synchrony between $T5, P3, O1$ and $P4, T6, O2$ derivations. The results are presented in Fig. 3.5.

From comparison of the charts and shown statistical differences, first of all, it should be noted that;

- (1) In N group there is observed: **(a)** approximate equality of synchrony in frontal-central FL, FR, CL, CR regions (except its decrease in α domain, $P = 0.02-0.0007$); **(b)** reduction of synchrony in the occipital OL, OR area ($P = 0.048-10-5$, except $\beta-2$ domain).
- (2) In F20 and F21 groups it is observed a sharp decrease of synchrony in central region compared with frontal and occipital ones. In most cases the differences between FL-CL, FR- CR, CL-OL, CR-OR manifest itself with high confidence (76% reliable differences from 50 comparisons, $P = 0.033-10-8$).
- (3) Synchrony in N group compared with F20 and F21 groups is as follows: **(a)** it is significantly higher in central region (95% reliable differences from 20 comparisons, $P = 0.01-10-7$), which coincides with the results of Borisov et al [8], Strelets et al [9] and Winterer et al [12]; **(b)** in some cases it is lower in frontal and occipital regions (30% reliable differences from 40 comparisons, $P = 0.049-0.001$), which partially coincides with the results of Mann et al [15], Merrin et al [13], Strelets et al [9] and Wada et al [16].
- (4) Local intraregional differences between F20 and F21 groups are detected in CL and OR regions in θ domain ($P = 0.04$) and in OL region in α domain ($P = 0.047$). Additionally, in Fig. 3.5, the macro regional intergroup differences (for both hemispheres) are also observed, and analysis of variance allows to reveal those differences in case that as a second factor we use left and right regions: **(a)** reduction of synchrony in F20 group in occipital OL-OR area in δ ($P = 0.007$), θ ($P = 10-6$) and α ($P = 0.0002$) domains with its convergence to the norm and increase of synchrony in central CL-CR area in $\beta-2$ domain ($P = 0.008$); **(b)** reduction of synchrony in F21 group in frontal FL-FR area in $\beta-2$ domain ($P = 0.004$) with its convergence to the norm.
- (5) Comparing of the difference between frontal synchrony and occipital one reveals differences between F20 and F21 groups in δ domain for FR-OR remainder ($P = 0.03$) and for remainders between FL-OL ($P = 0.02$) and FR-OR ($P = 0.03$) regions in θ

domain.

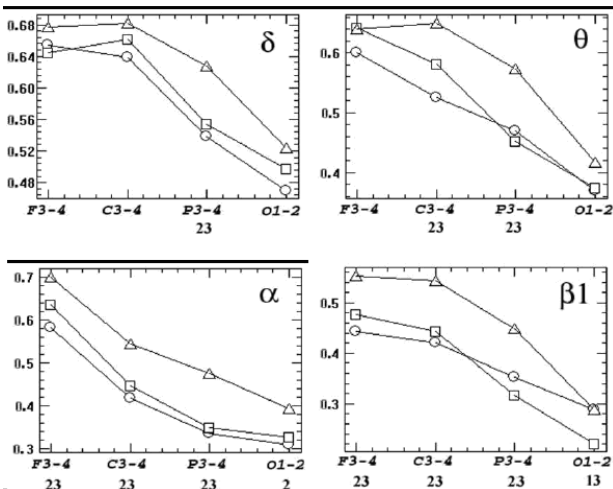


Fig. 3.4. Differences in inter-hemispheric synchrony for 5 frequency domains ($P = 0.04-0.0004$). The values averaged for each group synchrony (vertical axes) are shown for derivation pairs: $F3-F4$, $C3-C4$, $P3-P4$ and $O1-O2$ (horizontal axes).

Group markers: circles, F20; squares, F21; triangles, N. Below graphics, the designation of reliable intergroup differences is shown in number notation: 1, F20-F21; 2, F20-N; 3, F21-N

Regional Asymmetry

Visually, in Fig. 3.5 we can note some signs of right-sided asymmetry; most distinctly they appeared in F20 and F21 groups. Statistical comparison of mean values for left and right regions reveals the presence of right-sided asymmetry ($P = 0.048-0.007$) in occipital OL-OR area for F20 group in δ , α and $\beta-2$ domains and for F21 group in α , $\beta-1$ and $\beta-2$ domains, and also in central CL- CR area for F20 and N groups in $\beta-1$ domain. Differences in asymmetry coefficient calculated by the formula ' $(L \times R) / (L + R)$ ' are detected in central CL- CR area in θ domain ($P = 0.035-0.018$) between F20 and N groups and between F20 and F21 groups.

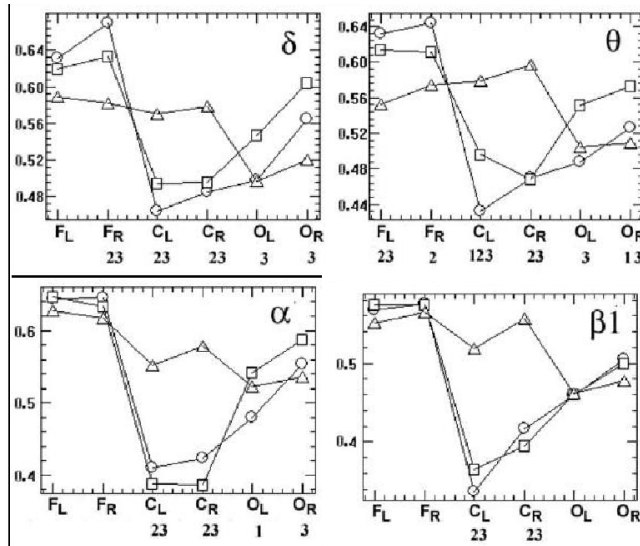


Fig. 3.5. Regional intra-hemispheric differences in frequency domains ($P = 0.033-10-8$). The averaged values of synchrony for each group (vertical) in order of regions (horizontal): FL, FR (frontal left and right), CL, CR (central left and right), CL, CR (occipital left, right); other notations are similar to Fig. 3.4

On the one hand, these asymmetries are not that numerous so to indicate a general pattern; on the other hand, no case of asymmetry is revealed in N group.

Age and Sex Differences

In order to identify age-related differences, we divide each group into two subgroups in age ranges of 8-11 and 12-15 years (the respective number of subgroups is 16 and 7 boys for F20 category, 16 and 20 boys for F21, category and 22 and 19 boys for N category). Now let's make a comparison of these subgroups. The results are presented in Table 3.2, from a consideration of which we can make the following conclusions:

- (1) In all detected cases, the differences are associated with an increase in synchrony with age, and this indicates a presence of systematic tendency;
- (2) Intraregional changes of synchrony are most representative in N group and intra-hemispheric ones in F20 group;

- (3) In a case of the pair comparison of three N, F20, F21 groups, most of the changes in synchrony topographically do not coincide, except for in the following cases: in α domain in FR region for N, F21 groups, in β -1 and β -2 domains in CL region for N, F20 groups, in α domains for C3-C4 derivation pair for F20, F21 groups and for P3-P4 derivation pair for N, F20 groups;
- (4) If we compare the results of Table 3.2 with the charts at Figs.3.4 & 3.5, then the convergence of EEG synchrony with the age to the norm is observed in pathology groups in inter-hemispheric connections predominantly in α domain, whereas as for relative intra-hemispheric relations, the situation is reversed: in CR region differences increase and in FL, FR, OR regions the higher synchrony observations are leveled in pathology groups in relation to norm.

Revealed age differences may indicate an identification feasibility of the differences between norm and pathology within specific age categories in a case of presence of much more voluminous experimental material.

The scope of this article does not allow us to consider our available results of analysis of female adolescents, which topography of EEG synchrony distribution in control and pathology groups has a number of significant local differences and yet maintains the marked phenomenon of cross-shaped "downfall" in EEG synchrony at pathology. However, it certainly indicates that such studies should be performed while taking the gender into account.

Comparison with Psychometric Measures

For assessment of cognitive functions of patients, violation of which is one of the main consequences of schizophrenia, the following four psychometric indices were used:

Volume of direct reproduction (VDR); defined by the technique of memorization of 10 words under verbal presentation (developed by A.R. Luria in 1962). This technique is intended to assess the status of voluntary verbal memory, fatigue, activity of attention, storing, preservation, reproduction, voluntary attention, etc.

Volume of simple and difficult paired associates (VSA, VDA)/paired-associates learning (PAL); this technique is intended to study the memory and memory processes;

Runtime of Schulte tables execution (TS); this technique is applied to research a rate of sensorimotor reactions and characteristics of attention, level of intellectual working capacity.

Table 3.2. Authentic age changes in intra-hemispheric and inter-hemispheric EEG synchrony in frequency domains δ , θ , α , $\beta-1$ and $\beta-2$. Remainders are represented between average values of synchrony in subgroups of 8-11 and 12-15 years old; the significance values are shown in brackets

Group	Localisation	δ	θ	α	$\beta-1$
F20	FR				0.13 (0.01)
F21	FL			0.1 (0.005)	
F21	CR			0.07 (0.01)	
N	FL	0.09 (0.02)	0.11 (0.001)	0.09 (0.02)	
N	FR	0.1 (0.01)	0.1 (0.004)	0.12 (0.001)	0.05 (0.04)
N	CR	0.1 (0.01)	0.07 (0.02)	0.09 (0.03)	0.06 (0.02)
N	OR	0.1 (0.006)			0.09 (0.002)
F20	<i>F3-F4</i>				0.13 (0.03)
F20	<i>C3-C4</i>			0.15 (0.047)	
F20	<i>P3-P4</i>		0.1 (0.04)	0.17 (0.02)	
F20	<i>O1-O2</i>	0.16 (0.02)			
F21	<i>F3-F4</i>			0.1 (0.01)	
F21	<i>C3-C4</i>			0.11 (0.04)	
F21	<i>O1-O2</i>			0.12 (0.006)	
N	<i>P3-P4</i>			0.1 (0.01)	

Between these indices for both groups of patients there were found no significant correlations (except VDA and TS, $P = 0.49$), which indicates that there are no strong functional dependencies between those indices for analyzed samples of patients.

The proximity of estimates of EEG synchrony to psychometric indices was assessed by Pearson correlation coefficient r critical value of which for those samples is $r_{cr} < 0.31$ at $P = 0.05$. Fig. 3.6 shows the identified significant correlations with local estimates of EEG synchrony between derivation pairs in the range of average and above average correlation values ($r = 0.45-0.75$, $P = 0.03-0.008$). In addition, it is interesting to calculate correlations with the average estimates of regional intra-hemispheric synchronicities as well as of differences between them that characterize the magnitude of decrease of EEG synchrony in CL, CR regions in relation to neighboring FL, FR, OR, OL regions. These correlations are presented in Table 3.3. The received results allow making the following conclusions:

- (1) The greatest number of significant correlations with the psychometric indices is revealed for F20 group (25 vs 9 for F21 group); it is quite consistent with the fact that for schizophrenia category (F20) the violations of cognitive processes estimated by these psychometric indices are more expressed.
- (2) The greatest number of significant correlations belongs to the “downfall” of synchrony for pathology groups in central axial area and to its remainders with neighboring regions: 19 significant correlations against 11 for other areas and derivation pairs.
- (3) In rank-order of total numbers of significant correlations, the frequency domains are ranked as follows: β -2 = 11, θ = 9, α = 9, δ = 4 and β -1 = 4 correlations. With respect to local correlations (Fig. 3.6) β -2 and θ domains have the obvious advantage as well as in a case of discriminant classification; the leading place of β -2 domain can be determined by its greater relationship with cognitive activity.
- (4) In rank-order of significant correlations, the psychometric indicators are ranged as follows: VDA = 13, VSA = 11, TS = 10 and VDR = 8 correlations. According to average value of correlations, the TS index has a considerable advantage ($r = 0.7$) in comparison with VDR (0.49), VSA (0.48) and VDA (0.5). The last would seem to indicate that in F20 group (which shows the highest number of correlation), the features of attention and mental performance are more vulnerable compared with the capabilities of memorizing and reminiscence

- (5) Signs of correlations for VDA, VSA are opposite to ones for TS, which corresponds to their psychometric ratio.
- (6) In high-frequency domains (β -1, β -2) compared with mid-frequency domains (θ , α), in most cases there are inversion of signs of correlations, which can be a result of opposite relationship between the activity of these domains and the cognitive abilities.

Let us note that in recent years we can see an increasing interest of researchers to comparison of different estimates of EEG synchrony on one hand and psychometric and syndromic indicators of schizophrenic spectrum disorders on the other hand. These studies reveal the following significant correlations: 0.36-0.52 [28], 0.27-0.39 [29], 0.37-0.82 [30] for a small group of 14 patients, 0.37-0.55 [31], 0.38-0.49 [32]. In this comparison, the numerous received by us significant correlations between EEG synchrony estimates and psychometric indices in a range of 0.45-0.75 look rather perspective.

Reproducibility of Results

In order to test the stability of our results obtained on the basis of the here stated methodology, we analyzed another EEG data which has been recorded in 2001-2004 and discussed earlier [8]. Two groups of male adolescents 10-12 years old include: F20 group of 18 patients (in age range of 12.1 ± 0.93) and control group of 25 pupils (in age range of 12.1 ± 0.53). The results turned out to be similar to Figs. 3.4 & 3.5; they are shown in Fig. 3.7 (identified significant differences showed $P = 0.047-10^{-5}$). As you can see, these charts are in good agreement with Figs. 3.4 & 3.5 with the exact reproduction of the phenomenon of cross-shaped “downfall” in EEG synchrony for F20 group. The separate and not numerous distinctions can be a consequence of narrower age range of the used groups. The discriminant classification gives an unmistakable separation of normal and pathological groups in all frequency domains. Thereby, the ACS-method possesses sufficient accuracy and stability, yielding almost identical results on various groups of examinees and patients.

Table 3.3. Correlations between psychometric measures with intra-hemispheric regional synchrony and with remainders between regional synchrony for frequency domains δ , θ , α , β -1 and β -2

Indice	δ	θ	α	β -1	β -2
VDR		-0.41 $F_R \cdot C_R$		-0.53 F_R	
				-0.50 $F_R \cdot C_R$	
VSA				-0.50 $F_R \cdot C_R$	
VDA	-0.47 $O_L \cdot C_L$	-0.43 $F_R \cdot C_R$		-0.54 $O_L \cdot C_L$	-0.47 $O_R \cdot C_R$
				-0.52 F_R	
TS	-0.56 C_L			-0.57 C_L	
	-0.47 C_R			-0.49 C_R	
				+0.48 $O_R \cdot C_R$	

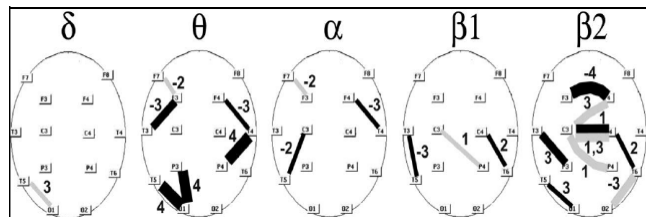


Fig. 3.6. Significant correlations between synchrony estimates and psychometric measure ($P = 0.03-0.008$) with the following numbering notation: (1) volume of direct reproduction by technique of memorization of 10 words under verbal presentation; (2) volume of simple binary associations; (3) volume of complex binary associations; (4) runtime of Schulte tables execution. Color of lines indicates the group of patients: black F20, gray F21; three grades of lines thickness indicate the absolute value of correlations: 0.45-0.49, 0.5-0.59, 0.6-0.75. The figures at lines indicate the numbering notation of psychometric measure; minus indicates a negative correlation

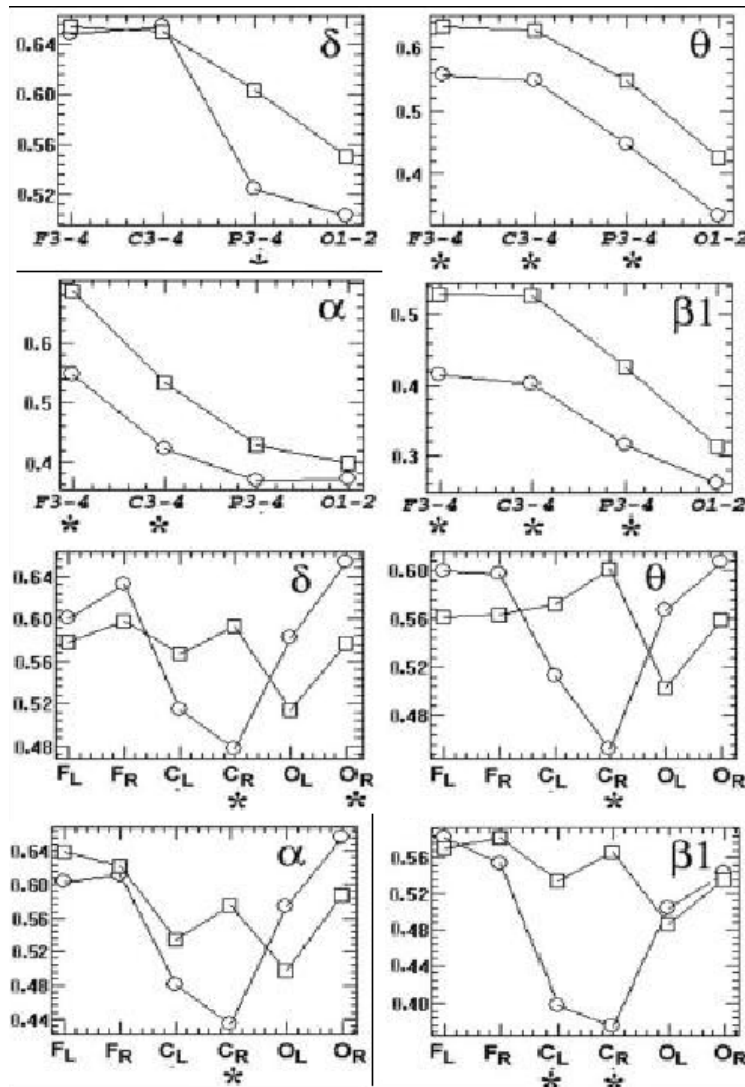


Fig. 3.7. Differences between synchrony for N and F20 group records as discussed earlier [8]; asterisks denote cases of significant group differences ($P = 0.47 \cdot 10^{-5}$): at top - Inter-hemispheric synchrony, below - regional intra-hemispheric synchrony. Remaining notation is similar to Figs. 3.4 & 3.5

DISCUSSION

The results of our complex analysis reveal the complicated picture of regional, inter-hemispheric and age differences in EEG synchrony between two disorders of schizophrenic spectrum and the norm, including interchanging cortical areas with oppositely directed ratios of higher, lesser or equal synchrony. Apparently, this is caused the apparent inconsistency of fragmentary results obtained by other researchers as noted in the introduction. Disclose of complete picture of EEG synchrony relations in these studies could be prevented by: **(a)** uncertainties of coherent analysis [18]; **(b)** small volume of experimental data [13,14,30]; **(c)** absence of selection of EEG records on consistency; **(d)** absence of separation of groups according to nosological type, age and sex. However, many of particular conclusions of other researchers find their counterparts in the considered complex picture: local cases of increase of intra-hemispheric coherence in schizophrenics [9,13,15,16], its decline in central region [8,12], reduced inter-hemispheric synchrony [8,9], a violation of frontal-temporal relationships [10].

One of distinctive and stable components of above considered picture of mental disorders in comparison with the norm is the presence of the vast areas of low synchrony separating isolated intra-hemispheric (frontal and occipital) areas with synchrony near to normal level. The presence of such a reduction and detection of right-sided asymmetry can indicate a substantial violation of inter-hemispheric and frontal-occipital relationships for schizophrenic and schizotypal disorder, which fits into framework of the well-known theory of disintegration of cortical electrical activity [33,34] ascending to Bleuler's studies (1911, 1913). Apparently, in schizophrenic process, a tendency to disintegration comprises cortical neuronal substrate at different levels, *i.e.* from local neuronal ensembles to spatially separated neural networks, which causes serious disturbances in their interaction [8]. It is considered that one of direct consequences of this disintegration is represented by observed violations of cognitive and behavioral functions at patients with schizophrenic disorders.

Our additional task of differentiation of two closely related F20 and F21 categories among the block of disorders of schizophrenic spectrum is especially complicated because among experts there is still no consensus on a safe separation criterion for schizophrenia and schizotypal disorder [21]. The significant differences between F20 and F21 groups appear mainly in frontal and occipital areas in certain frequency domains. With this in occiput an inter- and intra-hemispheric synchrony for schizophrenia

(F20) in some cases was closer to normal, whereas for schizotypal disorder (F21) intra-hemispheric synchrony is higher than normal, but inter-hemispheric synchrony is below than normal. Certain relationships of this kind are also observed in parietal, temporal and central areas. Apparently, this is due to the fact that criteria of schizotypal disorder include, in particular, the presence of unusual phenomena of perception including somatosensory, auditory and visual illusions or hallucinations, and as a result there can be more drastic deviations of EEG synchrony from the norm in areas of primary projection of corresponding analyzers.

On the other hand, in frontal and some central cortex areas in F20 group there are observed greater deviations of inter-hemispheric and intra-hemispheric synchrony estimates from the norm than in the case of schizotypal disorder. This is consistent with the concept of greater safety of frontal cortex at patients of F21 categories [21]. It is significant that most such deviations in intra-hemispheric synchrony manifest themselves in β -2 domain, whose activity is directly related to cognitive activity, and namely violations of cognitive processes are most typical just for schizophrenia pathology [21].

We note also that most of patterns on charts like Figs. 3.2-3.5 also appear when we analyze full amount of data (125 patients), but the performed selection of highly consistency subgroups (64 patients) improved considerably the reliability of conclusions about observed differences. Moreover, re-calculating of previous EEGrecords [8] by the here used methodology confirms all the above mentioned inter-hemispheric and regional relationships with high numerical accuracy. That proves the stable reproducibility of results in different groups of patients by the use of ACS-method.

These results demonstrate the high efficiency of ACS- method in differentiation of normal examinees from patients of different mental disorders by EEC and according to its classifying efficiency θ and β -2 frequency domains have noticeable advantage. It should also be emphasized that the efficiency for classification of θ domain was found in our previous paper [4]; in the same paper there was shown an advantage of ACS-method in comparison with other methods of classification and with other EEG indices.

The present study also showed that for the reliable differentiation on EEG of various subcategories within such the complex and multidimensional nosology as psychiatric disorders of schizophrenic spectrum, it is necessary

to use: (1) a bigger volume of experimental data than it takes place in most cited studies; (2) separate study of different nosology, age categories and sexual groups; (3) preliminary extraction of highly consistent EEG records for elimination of extraneous factors influence.

Apparently, the real progress towards development and implementation of efficient numerical methods for differentiation of norm and various forms of mental pathology by EEG is possible upon condition of international cooperation and coordination of researches. It also requires a formation of an integrated bank of EEG records from the data of various research and clinical centers differentiated by separate nosology, functional states, sex, age and other characteristics. One of possible mechanisms for this integration may be obligation to upload EEG records in standard European Data Format (EDF) in such a bank and do it for all articles published in leading scientific journals. In addition, such publicly-accessible bank will make the results and theoretical conclusions of EEG studies to be the falsifiable in sense of Karl Popper. For the purification of such a bank from influence of extraneous random factors a technique can be used similar to above discussed extraction of highly consistent EEG records.

CONCLUSION

The considered multidimensional results on distinctions of the norm and two groups of deviations of schizophrenic spectrum confirm in particular; (a) the revealed numerous significant correlations of EEG synchrony estimates with psychometric indices, (b) the high classifying sensibility of the used ACS-method, near 100% reliability, and (c) the reproducibility of results for different groups of patients and examinees. All this shows that EEG correlation synchrony measures can be perspective for the use as auxiliary quantitative estimates (in addition to ranking expert estimates) at diagnostics of mental deviations of schizophrenic spectrum.

REFERENCES

1. Mel'nikova TS, Lapin IA, Sirkosyan VV. The review of use of the coherent analysis in psychiatry. *Soc Clin Psychiatr* 2009; 19:90-4.
2. Ford MR, Goethe JW, Dekker DK. EEG coherence and power in the discrimination of psychiatric disorders and medication effects. *Biol Psychiat* 2005; 21:1175-88.
3. Kulaichev AP. Comparative analysis of EEG correlation synchronism and EEG amplitude relationships in all-night sleep. *Zh Vyssh Nerv Deiat Im I P Pavlova* 2012; 62:108-19.

4. Kulaichev AP. The method of correlation analysis of EEG synchronism and its possibilities. *Zh Vyssh Nerv Deiat Im I P Pavlova* 2011; 61:485-98.
5. Schmitt A, Hasan A, Gruber O, Falkai P. Schizophrenia as a disorder of disconnectivity. *European archives of psychiatry and clinical neuroscience*. 2011 Nov;261(2):150-4.
6. Na SH, Jin SH, Kim SY, Ham BJ. EEG in schizophrenic patients: mutual information analysis. *Clinical Neurophysiology*. 2002 Dec 1;113(12):1954-60.
7. Uhlhaas PJ, Singer W. Abnormal neural oscillations and synchrony in schizophrenia. *Nature reviews neuroscience*. 2010 Feb;11(2):100-13.
8. Borisov SV, Kaplan Ala, Gorbachevskaya NL, Kozlova IA. Analysis of EEG structural synchrony in adolescents with schizophrenic disorders. *Fiziol Cheloveka* 2005; 31:16-23.
9. Strelets VB, Garakh ZhV, Novototskii-Vlasov VYu, Magomedov RA. Relationship between EEG power and rhythm synchronization in health and cognitive pathology. *Neurosci Behav Physiol* 2006; 36:655-62.
10. Norman RM, Malla AK, Williamson PC, Morrison-Stewart SL, Helmes E, Cortese L. EEG coherence and syndromes in schizophrenia. *Br J Psychiat* 1997; 170:411-5.
11. Tauscher J, Fischer P, Neumeister A, Rappelsberger P, Kasper S. Low frontal electroencephalographic coherence in neuroleptic-free schizophrenic patients. *Biol Psychiatry* 1998; 44: 438-47.
12. Winterer G, Egan MF, Radler T, Hyde T, Coppola R, Weinberger DR. An association between reduced interhemispheric EEG coherence in the temporal lobe and genetic risk for schizophrenia. *Schizophr Res* 2001; 49:129-43
13. Merrin EL, Floyd TC, Fein G. EEG coherence term in unmedicated schizophrenic patients. *Biol Psychiatry* 1989;25: 60-6.
14. Nagase Y, Okubo Y, Matsuura M, Kojima T, Torua M. EEG coherence in unmedicated schizophrenic patients: topographical study of predominantly never medicated cases alert. *Biol Psychiatry* 1992; 32:1028-34.
15. Mann K, Maier W, Franke P, Roschke J, Gansicke M. Intra- and interhemispheric electroencephalogram coherence in siblings discordant for schizophrenia and healthy volunteers. *Biol Psychiatry* 1997; 42: 655-63.
16. Wada Y, Nanbu Y, Kikuchi M, Koshino Y, Hashimoto T. Photic stimulation in drug-naive patients. Aberrant functional organization in schizophrenia: analysis of EEG coherence during rest.

Neuropsychobiology 1998; 38:63-9.

- 17. Guevara MA, Corsi-Cabrera M. EEG coherence or EEG correlation? *Int J Psychophysiol* 1996; 23:145-53.
- 18. Kulaichev AP. The informativeness of coherence analysis in EEG studies. *Neurosci Behav Physiol* 2011; 41:321-8.
- 19. Kulaichev AP. Some methodical problems of the frequency analysis of EEG. *Zh Vyssh Nerv Deiat Im I P Pavlova* 1997; 47:918-26.
- 20. Leocani L, Comi G. EEG coherence in pathological conditions. *J Clin Neurophysiol* 1999; 16:548-55.
- 21. Siever L, Koenigsberg H, Harvey P, Mitropoulou V, Laruelle M, Abi-Dargham A, Goodman M, Buchsbaum M. Cognitive and brain function in schizotypal personality disorder. *Schizophr Res* 2002; 54:157-67.
- 22. Winterer G, Ziller M, Dorn H, Frick K, Mulert C, Wuebben Y, Herrmann WM. Frontal dysfunction in schizophrenia - a new electrophysiological classifier for research and clinical applications. *Eur Arch Psychiatry Clin Neurosci* 2000; 250:207-14.
- 23. Boostani R, Sadatnezhad K, Sabeti M. An efficient classifier to diagnose of schizophrenia based on the EEG signals. *Exp Syst Appl* 2009; 36: 6492-99.
- 24. Lastochkina NA, Puchinskaya LM. Correlation analysis of EEG rhythms and functional asymmetry of the hemispheres in children with the hyperdynamic syndrome. *Neurosci Behav Physiol* 1992; 2:251-8.
- 25. Sakoglu U, Michael AM, Calhoun VD. Classification of schizophrenia patients vs healthy controls with dynamic functional network connectivity. *Neuroimage* 2009; 47: S39- 41.
- 26. Morrison-Stewart SL, Williamson PC, Corning WC, Kutcher SP, Merskey H. Coherence on electroencephalography and aberrant functional organisation of the brain in schizophrenic patients during activation tasks. *Br J Psychiatr* 1991; 159:636-44.
- 27. Kaplan Ala, Borisov SV, Zheligovskii VA. Classification of the adolescent EEG by the spectral and segmental characteristics for normals. *Zh Vyssh Nerv Deiat Im I P Pavlova* 2005; 55:478- 86.
- 28. Bob P, Palus M, Susta M, Glaslova K. EEG phase synchronization in patients with paranoid schizophrenia. *Neurosci Lett* 2008; 447:73-7.
- 29. Bob P, Susta M, Glaslova K, Boutros NN. Dissociative symptoms and interregional EEG cross-correlations in paranoid schizophrenia. *Psychiatry Res* 2010; 177:37-40.
- 30. Higashima M, Takeda T, Kikuchi M, Nagasawa T, Hirao N, Oka T, Nakamura M, Koshino Y. State-dependent changes in intra-

hemispheric EEG coherence for patients with acute exacerbation of schizophrenia. *Psychiatry Res* 2007; 149:41-7.

- 31. John JP, Khanna S, Pradhan N, Mukundan CR. EEG Alpha Coherence and Psychopathological Dimensions of Schizophrenia. *Indian J Psychiatry* 2002; 44:97-107.
- 32. Kubicki M, Styner M, Bouix S, Gerig G, Markant D, Smith K, Kikinis R, McCarley RW, Shenton ME. Reduced interhemispheric connectivity in schizophrenia-tractography based segmentation of the corpus callosum. *Schizophrenia Res* 2008; 106:125-1.
- 33. Friston KJ. Theoretical neurobiology and schizophrenia. *Brain Med Bull* 1996; 52:644-55.
- 34. Stephan KE, Friston KJ, Frith CD. Disconnection in schizophrenia: from abnormal synaptic plasticity to failures of self-monitoring. *Schizophrenia Bull* 2009; 35:509-27.

CHAPTER 5

THE CHANGES OF EEG CORRELATION SYNCHRONY AT DEPRESSIVE DEVIATIONS OF ADVANCED AGE

ABSTRACT

In this work we use the alternative method of assessing the EEG-synchrony which previously has proved its high sensitivity to the differentiation of psychopathological and functional states. The original recording of EEG had been performed in the state of quiet wakefulness with eyes closed for two groups of examinees/patients at the age of 49–82 years: a group of normal subjects ($n = 29$) and the group of subjects with depressive deviations of F43.21 category according to ICD-10 ($n = 51$). As a result of research, it is received the comprehensive picture of significant topographical, interhemispheric and regional differences between groups of norm and depression. One of basic features of the obtained integrated picture is existence at a depression of the extended zones of reduced EEG-synchrony covering the entire pre-medial region in the frontal-occipital direction, including intra-hemispheric connections as well as lateral frontal-temporal connections in both hemispheres. It testifies to the deep deprivation with depression frontal-occipital and interhemispheric interaction. As a compensatory reaction during depression the increase of synchrony in axial aimed intra-hemispheric pairs of derivations. It is noted the similarity of changes in EEG-synchrony topography of depression to those observed in schizophrenia. The used method has provided close to 100% reliability of the classification of the EEG norms and depressive deviations, which makes possible and promising its use as an auxiliary quantitative differential indicator.

Keywords: EEG, depressive disturbances, correlation of envelopes, coherence, discriminant classification, schizophrenia.

Among the large number of works devoted to differences in EEG in normal and depressive disorders, there are relatively few studies concerning differences in EEG synchronicity, as can be evidenced by a special review [9]. At the same time, the classification sensitivity of EEG synchronicity estimates is significantly higher compared to the amplitude of the spectrum, power [14; 15] and a number of other indicators [5, 6]. This is largely determined by the fact that the EEG synchronicity indicators are subject to significantly lower intra-individual variability, which, according to our estimates obtained from various experimental materials, the coefficient of variation is: 8-12% versus 23-41% for the average amplitude of the spectrum and 86-95% for power. Thus, according to EEG synchronicity estimates, it is possible to obtain the reliability of comparable differences in magnitude with smaller sample volumes and the reliability of smaller differences with comparable sample volumes.

The results obtained by different researchers are quite fragmentary and contradictory. In most cases, there is a decrease in coherence in depression, but in different localization: in the anterior and middle temporal zones of the α -, β_1 - and β_2 -ranges with an emphasis on the right, as well as in the frontal, central and parietal regions without noticeable asymmetry [10]; a decrease in interhemispheric coherence in the β range and intra-hemispheric coherence in the δ - and β -bands [13]; a widely distributed decrease in coherence in all ranges [15]; The focus of coherence reduction is in the left and right frontal and left parietal regions [161]; coherence decrease in Fp1-T3 and Fp2-T4 θ -band, in T3-P3 and T4-P4 α -band, in P3-O1 and P4-O2 β_2 -band with simultaneous increase in synchronicity in other pairs of leads [17]; decrease in interhemispheric coherence in the frontal area of the δ -band [18]. The opposite phenomena are also noted: an increase in coherence in the occipitoparietal pre-medial region, which is more pronounced in the δ - and θ -ranges [10]; an increase in coherence in the parietal region of the θ -range [18]; an increase in intra-hemispheric coherence in the frontal-parietal region in all ranges [19], an increase in coherence when taking antidepressants [14].

On the one hand, this situation may be caused by the fact that the coherence function is a rather unstable indicator of EEG synchronicity [7]. On the other hand, this may be due to the different etiology of depressive syndrome, and a number of studies [1; 3, 10; 12] reveal some local differences related to this. At the same time, the general ambiguity of the results of various studies, the uncertainty and blurriness of the situation makes it relevant to use alternative approaches to assessing the synchronicity of the EEG with a comprehensive identification and analysis

of differences between the norm and deviations of the depressive type.

METHODOLOGY

The study used background EEG recordings of 51 patients (group D, 11 men, 40 women) aged 49-82 years (67.45 ± 8.3 years) with a psychogenically provoked depressive reaction (bereavement reaction) to the death of close relatives (spouse, brother/sister, adult children), which meets the criteria of heading F43.21 according to ICD-10. The quantitative assessment of the severity of the depressive state in the dynamics of therapy was performed in the National Clinical Hospital of the Russian Academy of Medical Sciences individually for each patient using the Hamilton scale for depression HDRS-21, the average score for the group was HDRS = 22 ± 5.09 . The control group (group N, norm) without depressive disorders included 29 people aged 52-72 years (64.4 ± 4.6 years, 18 men, 11 women). The research protocol was approved by the local ethics committee of the Federal State Budgetary Institution "NCPZ" of the Russian Academy of Sciences. All the subjects signed an informed consent to participate in the research. EEG recordings in a state of calm wakefulness with closed eyes were performed for all patients who did not undergo drug therapy in derivations F7, F3, F4, F8, T3, C3, C4, T4, T5, P3, P4, T6, O1, O2 with respect to the ear referents A1 and A2, according to the 10-20% system, using the Neuro-KM hardware and software complex and the BrainSys computer program. The bandwidth of the amplifier is 0.6-35 Hz, the sampling frequency is 200 Hz. Non-abstract recording sections with a duration of 41 seconds (8196 time counts) were selected for analysis. The EEG synchronicity analysis was performed using CONAN and STADIA software packages in five standard frequency domains: delta (δ) – 0.5-4 Hz, theta (θ) – 4-8 Hz, alpha (α) – 8-13 Hz, beta1 (β_1) – 13-20 Hz, beta2 (β_2) – 20-30 Hz.

In the following, we will use the designations of groups D, N and the designations of the frequency ranges δ , θ , α , β_1 , β_2 .

METHODS OF ANALYSIS

In this study, an alternative approach was used to assess the similarity between the bioelectric activity of different regions of the cerebral cortex: the analysis of EEG correlation synchronicity (ACS), proposed by A.P. Kulaichev and described in detail in [5]. The author evaluates the degree of synchronicity of the EEG by the Pearson correlation coefficients between the envelopes of EEG recordings previously filtered in a given

frequency range. It is appropriate to emphasize here that since the envelope represents a change in the amplitude modulation of the EEG, the assessment of synchronicity based on it has a direct and important physiological meaning. Indeed, the amplitude of the EEG increases with increasing synchronicity of changes in postsynaptic potentials, therefore, the envelope correlation evaluates the degree of synchronicity in the change of such an intra-neural synchronism.

An ordered sequence of such correlations between nearby leads (in this case 36 pairs of leads) is called the synchronicity profile (PS) and it is profiles such as topographic patterns of EEG synchronicity (for groups of subjects - profile matrices) that are the starting material for further analysis. This method has already demonstrated its high effectiveness in differentiating between norm and mental pathology [5; 8], as well as various functional conditions [6].

The two-sample Wilcoxon criterion for non-normalized data, two-factor analysis of variance and discriminant classifying analysis were used to assess intergroup differences.

RESEARCH RESULTS

1. Discriminant classification

The results of a number of our studies (in particular [5, 6; 8]) have shown that the discriminant classification of groups of subjects meeting different nosologies, therapeutic effects, functional conditions, social, age and gender categories is an effective initial indicator of the prospects for further research. If such a classification within the framework of an initially specified grouping gives a significant number of errors (more than 20-30%), then such groups differ little in terms of EEG indicators or are strongly internally heterogeneous, therefore further detailed analysis of the differences is usually fruitless.

Percent of discriminant classification errors of records EEG at mental diseases and functional states in dependence of frequency domain

Experiments	δ	θ	α	$\beta1$	$\beta2$	Average
Depression-norm	0	0	0.8	1.5	0	0.44
Schizophrenia-1 (F20 F 25) - Norma-1 [5]	13.1	6	7.1	6	—	8.05
Schizophrenia-2 (F20 + F21)-Norma-2 [8]	4	4	2	3	1	2.8
5 sleep stages [6]	33.7	31.7	22.3	35.3	—	30.75

Therefore, we will carry out a direct discriminant classification of two groups of records D and N with a priori attribution to two different classes. The results of the classification according to the estimates of the correlation synchronicity of the EEG depending on the frequency range are shown in the table (top row). As can be seen from the table, the use of the frequency ranges δ , θ , $\beta2$ makes it possible to accurately separate the records obtained for depressed patients and for healthy people. A small number of errors are also obtained when using the frequency ranges α and $\beta1$ (0.8 and 1.5%). For comparison, the following rows of the table show the percentages of errors of similar classifications obtained by us when discriminating two different groups of adolescents with schizophrenia from healthy children, as well as with a 5-cluster classification of five different functional states (sleep stages). Based on the significantly lower average percentage of errors in the first case, it can be concluded that changes in the correlation synchronicity of the EEG in depressive disorders of category F43.21 according to ICD-10 are much more pronounced in comparison with the norm than in other considered cases. The result obtained is also significantly better than in the only similar study we found [15], where the discriminant classification of norm and depression records gave 8.7% errors when using spectral power and coherence estimates.

2. Topographic relations

To present a general detailed picture of the correlation synchronicity ratios of S in normal and pathological conditions, we calculate for each of the groups of records D, N the values of S in each pair of leads and consider first as a starting basis the topography of the distribution of estimates of S in group N (Fig. 1, A). Here the following draws attention: 1) the overall level of correlation synchronicity in the scalp (the average for all pairs of

leads) is approximately the same in the medium and low frequency ranges δ , θ , α (0.62, 0.61, 0.63), and then drops significantly in β_1 and β_2 (0.52, 0.47); 2) in the low and medium frequency ranges, the maxima of correlation synchronicity are manifested in most interhemispheric connections and in sagittal conjugate pairs of leads (both in pre-medial and lateral); 3) in high frequency ranges, on the contrary, maxima in interhemispheric connections are absent, but are preserved only in separate sagittal conjugate chains of pairs of leads; 4) there is no statistically significant manifestation of asymmetry for symmetrically arranged lead pairs in most frequency ranges, with the exception of two episodes of right-hemisphere asymmetry in the δ range: F8-C4 ($p = 0.002$), P4-O2 ($p = 0.03$), which cannot indicate any stable regular trend.

Let's move on to the topography of the differences in the average values of correlation synchronicity between the pairs of leads of the same name of the two analyzed groups and consider the intergroup relations of greater-lesser synchronicity (Fig. 1, B). In these topograms, the following first of all attracts attention.

1.1. An extensive zone of sharp decrease in depression of interhemispheric synchronicity in the forehead–center–crown–occiput region, which in the low frequency ranges (δ , θ) includes the occipital pair of O1–O2 derivations.

1.2. A similar decrease in synchronicity is observed in the sagittal directions, both lateral – F7–T3–T5, F8–T4–T6, and pre-medial – C3–P4, F4–C4–P4.

1.3. An increase in synchronicity in depression compared with the norm in axially directed intra-hemispheric connections: temporoparietal P4–T6, P3–T5, temporo–central C3–T3, C4–T4 (except in the δ domain) and in the frontal F7–F3, F8–F4 in the α domain;

1.4. In different frequency ranges, there are no fundamental changes in the overall topographic picture of decreasing– increasing synchronicity in depression compared to the norm, even in high-frequency ranges, where the overall level of EEG synchronicity is normally significantly reduced (Fig. 1, A).

It should be noted that conclusions 2.1, 2.2 may indicate significant violations of the interhemispheric and frontal–occipital relationships in depressive disorders.

3. Numerical ratios and statistical differences

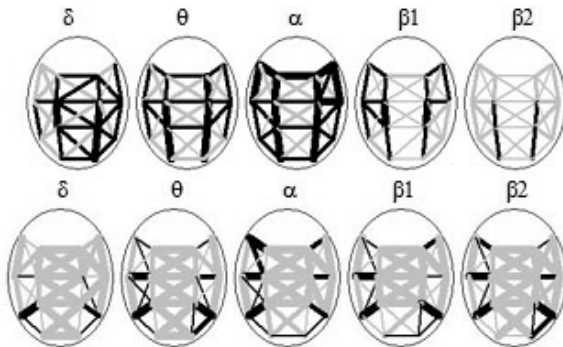


Fig. 1. The topography of EEG synchrony in control and depressive group in order of frequency domains: at top – average synchrony S in control group, line thickness and color indicates the synchrony value S : $0.4 < S < 0.5$ – grey; $0.5 < S < 0.6$ – grey; $0.6 < S < 0.7$ – black; $S > 0.7$ – black; at bottom – intergroup differences of averaged synchrony: the black color lines indicate the greater synchrony at depression compared with the control, gray lines indicate the lower overall synchrony, three gradations of increasing thickness point to the absolute value of difference in the average synchrony $|\Delta S|$ in order of its increasing: $|\Delta S| < 0.05$; $|\Delta S| < 0.1$; $|\Delta S| > 0.1$.

For a more detailed study of the correlation synchronicity relationships, it is useful to present the data obtained in the form of graphs separately for sagittal and axially arranged pairs of leads in the forehead–occiput order (Fig. 2). These graphs make it possible to clarify the topographic patterns discussed above (Fig. 1, B), the statistical justification of which is given below in paragraphs 3.1–3.3.

In paragraphs 3.1, 3.2, the reliability of intergroup differences is assessed by the method of two-factor analysis of variance with repeated measurements (repeated-measures design) for each frequency range separately: 1st factor – two groups being compared (intergroup factor); 2nd factor - the number of pairs of leads (intragroup factor) in which the trend is considered. The minimum, maximum and average values (in the analyzed frequency ranges) of the difference between the average synchronicities in the two groups are indicated in parentheses, as well as the maximum (in frequency ranges) level of significance of the 1st (intergroup) factor. To normalize the initial data before the analysis of variance, the Fisher preliminary Z-transform of EEG correlation synchronicity estimates r : $Z(r) = 0.5 \ln((1 + r)/(1 - r))$ was traditionally

used. In clause 3.3, the two-sample Wilcoxon criterion was used to identify statistical differences.

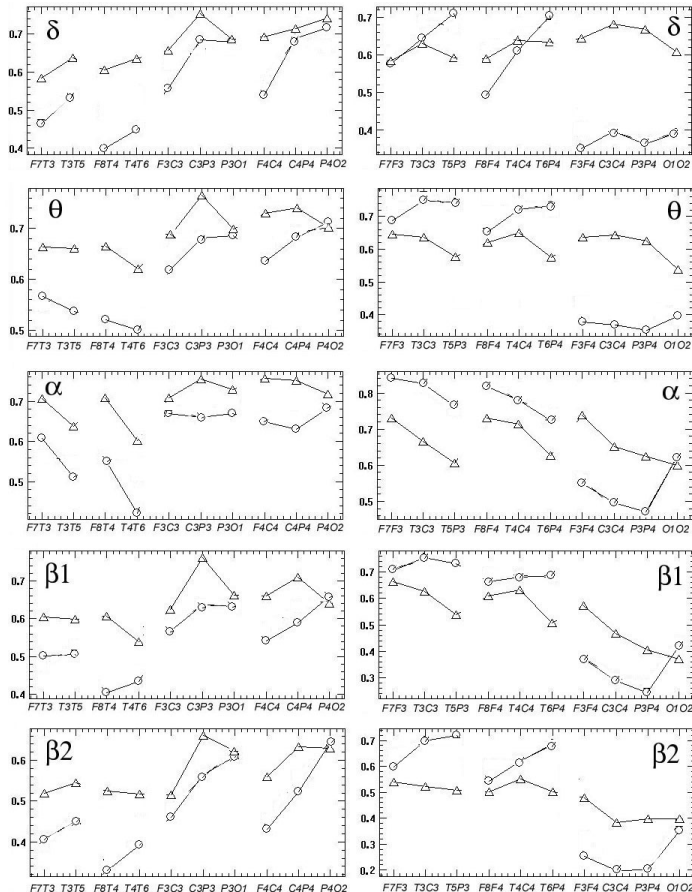


Fig. 2. The intergroup numerical ratios of synchrony in five frequency domains (from top to down). It shows the averaged synchrony for each derivation pair (at vertical axis) in order of derivation pairs (at horizontal axis). Markers of groups are: circles for depression, triangles for the norm. At top it shows the graphs of synchrony on sagittally located derivation pairs in order from forehead to occiput (from left to right), below it shows the graphs of synchrony on acsially located derivation pairs.

A sharp drop in synchronicity during depressions in all frequency domains occurs in interhemispheric connections (Fig. 2, B): F3–F4, C3–C4, P3–P4 (min = 0.155, max = 0.306, average = 0.223, $p < 10^{-14}$), which captures in the low frequency ranges δ and θ and the occipital pair O1–O2 (min = 0.141, max = 0.216, mean = 0.178, $p < 10^{-14}$), as well as in most sagittal intrahemispheric pairs of derivations (Fig. 2, A), both pre-medial left and right F3–C3, C3–P3, F4–C4, C4–P4 (min = 0.039, max = 0.207, mean = 0.11, $p < 10^{-5}$) and lateral left and right F7–T3, T3–T5, F8–T4, T4–T6 (min = 0.104, max = 0.306, average = 0.153, $p < 10^{-11}$). With the Bonferroni correction for a set of 15 hypotheses jointly tested here, $\alpha_{15} = 0.0033$ for the initial significance level $\alpha_1 = 0.05$. A significant increase in synchronicity during depression in domains α , α , β_1 , β_2 occurs in axially located intra-hemispheric pairs of derivations (Fig. 2, B): F7–F3, T3–C3, T5–P3, F8–F4, T4–C4, T6–P4 (min = 0.031, max = 0.21, mean = 0.111, $p < 10^{-8}$, $\alpha_5 = 0.01$).

The following changes in the ratios in adjacent pairs of leads in depression are also observed compared to the norm ($\alpha_{19} = 0.0026$, the ratios at the statistical trend level are marked with an asterisk below):

a) interhemispheric synchronicity (Fig. 2, B) increases in the direction P3–P4 → O1–O2 in all ranges ($p < 0.0008$) and especially strongly (up to 0.15–0.2 in magnitude) in the domains α , β_1 , β_2 ($p < 10^{-8}$), whereas normally there is a tendency to decrease synchronicity;

b) in the sagittal direction (Fig. 2, A):

- synchronicity increases C4–P4 → P4–O2 in the β_1 and β_2 domains, whereas normally there is mainly a tendency to decrease synchronicity ($p < 10^{-4}$); a similar trend is observed in the θ and α domains ($p = 0.018^*$, 0.044^*);
- in contrast, in symmetrical left pairs C3–P3 → P3–O1 in the domains δ , θ , β_1 , β_2 , there is a constant synchronicity, whereas normally there is a significant decrease in it ($p = 0.02^*$, 0.01^* , 0.004^* , 0.0039^*);
- c) in the axial direction (Fig. 2, B):
- in the δ -domain, synchronicity increases T3–C3 → T5–P3 ($p = 0.004^*$) and symmetrically T4–C4 → T6–P4 ($p = 0.003^*$), whereas normally there is a decrease or constancy of synchronicity;
- in similar pairs of derivations, there is a decrease in synchronicity in the θ domain ($p = 0.0024 \cdot 2 \times 10^{-8}$) and in the β_1 domain ($p = 0.022^*$, 0.0002) against the background of its relative constancy in the norm.

3. Hemispheric asymmetry

As noted above, interhemispheric asymmetry is not normally manifested globally in relation to the correlation synchronicity of the EEG. In depression, a slightly different picture is observed (Fig. 3). If in the low-frequency domains (δ, θ) there are only individual episodes of left-sided asymmetry, then in the medium-high frequency domains there is a single integral region of left-sided asymmetry, capturing the region of derivations F7-T3-T5-C3 (absolute values of statistically significant differences in symmetrical synchronicities are in the range of 0.04–0.18). This indicates a greater disintegration of processes in the right hemisphere, whose activity is associated with the predominance of negative emotions in depression [2; 11].

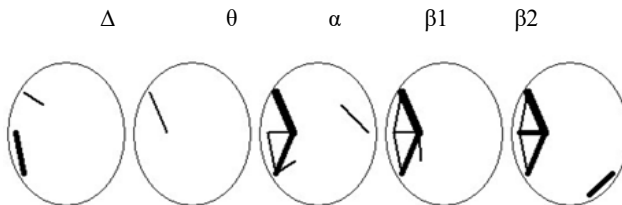


Fig. 3. Topography of interhemispheric asymmetry of EEG synchrony in depression group. It shows a pair of derivations in which the level of synchrony is higher than in symmetric pairs of derivations. Three gradations of lines thickness increasing indicate the level of zero hypothesis significance: $0.05 > p > 0.01; 0.01 > p > 0.001; 0.001 > p$.

DISCUSSION OF THE RESULTS

The results of the analysis revealed a complex picture of regional and interhemispheric differences in the correlation synchronicity of the EEG between the norm and depressive deviations, including different ratios of greater-lesser or identical synchronicity in the activity of different cortical zones [3]. Perhaps this determines the apparent inconsistency of the fragmentary results obtained by other researchers noted in the introduction.

One of the principal features of the resulting integral picture is the presence of extended zones of sharply reduced synchronicity of neurophysiological activation processes in depression, covering the entire pre-medial region in the forehead–occiput direction, including interhemispheric connections, as well as lateral connections in both

hemispheres. At the same time, a single topographic picture of changes in EEG synchronicity in depression is generally reproduced in all frequency domains. This indicates deep deprivation in depressions of frontal-occipital, frontotemporal and interhemispheric interactions throughout in the sagittal direction. These results and conclusions, with varying variations, are confirmed by a number of cited studies [10; 11; 13; 15; 16; 17].

A number of studies, as noted earlier [2-11], indicate greater activation in depression of the right hemisphere, which is consistent with modern ideas about the predominant role of the right hemisphere in the regulation of negative emotions and in the pathogenesis of depression [2]. At the same time, with regard to the correlation synchronicity of the EEG, its general decrease is observed in the sagittal directions with signs of left-sided asymmetry (Fig. 3), i.e. with a more significant decrease in the right hemisphere. This indicates that the increased activation of the right hemisphere, which causes the predominance of negative emotions in depression, may be enhanced by a greater discoordination of processes in the right hemisphere.

In addition (perhaps as a kind of compensatory reaction), depression revealed an increase in the correlation synchronicity of the EEG in a number of axially directed intra-hemispheric pairs of derivations, and above all – in the temporo-central and temporo-parietal, which may indicate an increase in systemic coordination between auditory and somatosensory sensitivity in both primary projection areas and in the associative posterior temporal and parietal zones. On the other hand, a decrease in synchronicity in sagittal anterior-posterior and central-parietal pairs of derivations may indicate a deprivation of systemic coordination between processes in the areas of primary projection of auditory and tactile analyzers and associative processes of integrated perception of the corresponding sensations. In relation to the primary and associative visual areas, such synchronization-desynchronization phenomena are not observed.

It should be especially noted that a similar picture of differences in norm and pathology was revealed earlier by us and in the study of two different groups of adolescents (8-15 years old) diagnosed with schizophrenia, F20 according to ICD-10 [8], where there was also (with certain numerical differences) an extended interhemispheric and pre-medial-sagittal zone of decreased synchronicity from the forehead to the occiput with a compensatory increase in correlation synchronicity in axially coupled pairs

of derivations. This indicates the similarity of changes in the synchronicity of neurophysiological activation processes in these two types of mental disorders.

This similarity of changes looks even more convincing considering that the topography of the distribution of correlation synchronicity in the group of healthy adolescents [8] had significant differences from the group of healthy elderly people (Fig. 1, A). This suggests that the method used gives stable results in the case of similarity of changes observed in different forms of pathology and in different age groups. This stability compares favorably with the heterogeneity of the results obtained when using the coherence function in studies of depression (noted in this paper) and schizophrenia (reviewed in [8]).

CONCLUSION

The results obtained regarding the disparate differences between the norm and depressive disorders in relation to the synchronicity of neurophysiological activation processes, as well as the high, close to 100% classifying reliability of the method used and the stability of its results in the analysis of two different diseases (depression and schizophrenia) and two age groups (adolescents and elderly patients) demonstrate, that EEG correlation synchronicity estimates may prove promising for use as additional quantitative indicators (in addition to ranked clinical expert indicators) for differentiating depressive disorders and schizophrenic abnormalities (as well as, possibly, for a number of other mental diseases and functional conditions that we have not studied) with a quantitative assessment of their individual severity by deviation from the norm the average statistical norm.

REFERENCES

1. Ivonin A.A., Tsitseroshin M.N., Kutsenko D.O., Shchepina A.M., Titova V.V., Shuvaev V.T. Features of violations of the processes of intercortical and cortical-subcortical integration in various clinical manifestations of neurotic depression. *Human physiology*. 2008. 34(6):10-22.
2. Iznak A.F., Zozulya A.A. Neurobiological foundations of depression. *Depression in general medicine*. Ed. Smulevich A.B. M.: MIA, 2001: 20-31.
3. Iznak A.F., Iznak E.V., Sorokin S.A. Changes in EEG and reaction time during the treatment of apathetic depression. *Journal of*

Neurology and Psychiatry. 2011. 7: 49–53.

- 4. Iznak A.F., Nikishova M.B. Electrophysiological correlates of psychogenic disorders. Human physiology. 2007. 33(2): 137-130.
- 5. Kulaichev A.P. The method of analyzing the correlation synchronicity of the EEG and its possibilities. Journal of Higher Education. the nerve. acts. 2011. 61(4): 485-498.
- 6. Kulaichev A.P. Comparative analysis of correlation synchronicity and amplitude ratios of EEG in night sleep. Journal of Higher Education. the nerve. acts. 2012. 62(1): 108-119.
- 7. Kulaichev A.P. On the informativeness of coherent analysis in EEG studies. Journal of Higher Education. the nerve. acts. 2009. 59(6): 766-775.
- 8. Kulaichev A.P., Gorbachevskaya N.L., Goryunov A.V., Sorokin A.S., Khromov A.I. Differences in the synchronicity of bioelectric activity on EEG in healthy and schizophrenic children and adolescents. Journal of Neurology and Psychiatry. 2012. 12: 55-62.
- 9. Melnikova T.S., Lapin I.A., Sirkosian V.V. Review of the use of coherent analysis in psychiatry. Soc. and klin. psychiatry. 2009. 19(1): 90-94.
- 10. Melnikova T.S., Lapin I.A. Coherent EEG analysis in depressive disorders of various genesis. Social and clinical. psychiatry. 2008. 18(3): 27–32.
- 11. Strelets V.B., Danilova N.I., Kornilova I.V. EEG rhythms and psychophysiological indicators of emotions in reactive depression. Journal of Higher Education. the nerve. acts. 1997. 47(1): 11-21.
- 12. Strelets V.B., Ivanitsky A.M., Ivanitsky G.M., Arceulova O.K., Novototsky-Vlasov V.Yu., Golikova Zh.V. Violation of the organization of cortical processes in depression. Journal of Higher Education. the nerve. acts. 1996. 46(2): 274-280.13. Armitage R., Hoffmann R.F., Rush A.J. Biological rhythm disturbance in depression: temporal coherence of ultradian sleep EEG rhythms. Psychol. Med. 1999. 29(6): 1435–1448.
- 14. Ford M.R., Goethe J.W., Dekker D.K. EEG coherence and power in the discrimination of psychiatric disorders and medication effects. Biol. Psychiat. 1986. 21(12): 1175–1188.
- 15. Knott V., Mahoney C., Kennedy S., Evans K. EEG power, frequency, asymmetry and coherence in male depression. Psychiat. Res. 2001. 106(2): 123–140.
- 16. Mann K., Maier W., Franke P., Ruschke J., Gdnsicke M. Intra- and interhemispheric electroencephalogram coherence in siblings discordant for schizophrenia and healthy volunteers. Biol. Psychiat.

1997. 42(8): 655–663.

- 17. Passynkova N.R., Wolf N.V. Seasonal affective disorder: spatial organization of EEG power and coherence in the depressive state and in light-induced and summer remission. *Psychiat. Res.* 2001. 108(3): 169–185.
- 18. Suhhova A., Bachmann M., Aadamsoo K., Võhma Ü., Lass J., Hinrikus H. EEG Coherence as measure of depressive disorder. *International Federation for Medical and Biological Engineering (IFMBE) Proc.* 2009. 22(6): 353–355.
- 19. Tsutomu T. EEG power and coherence analysis in major depressive disorder: analysis of drug-naïve patients. *J. Juzen Med. Soc.* 2005. 114(4): 62–68.
- 20. Yamada M., Kimura M., Mori T., Endo S. EEG power and coherence in presenile and senile depression. *Nihon Ika Daigaku Zasshi.* 1995. 62(2): 176–185.

CHAPTER 6

COMPARATIVE ANALYSIS OF EEG CORRELATION SYNCHRONISM AND EEG AMPLITUDE RELATIONSHIP IN ALL-NIGHT SLEEP

ABSTRACT

We used a new methodological approach to the evaluation of EEG synchronization based on correlation between amplitude modulation processes (EEG envelopes). There are revealed: the left-hemispheric dominance in all stages of sleep; the dominance of frontal regions over occipital; the differences in the ratio of synchronization relations on sleep stages in different frequency domains; the differences in change regularities of inter-hemispheric synchrony relations from frontal regions to occipital; topographical distributions of high synchronization localization in sleep stages and with respect to frequency domains. At the analysis of amplitude topography, it is also observed left-hemispheric dominance and revealed many significant differences in the relationships and change regularities in EEG activity during parasagittal chains of electrodes (meridians) both in terms of sleep stages and with respect to frequency domains. The combination of EEG synchrony estimates with the amplitude spectral estimates allows to perform a reliable discriminant recognition of five stages of sleep with errors not exceeding of 3-20%.

Keywords: sleep stages, EEG synchronism, envelope, topographical pattern, profile of synchronism, frequency domain, amplitude spectrum, hemispheric dominance, frontal-occipital relations, discriminant analysis, classification.

In the extensive literature devoted to sleep research, there are relatively few works related to the assessment of EEG synchronicity. Mainly, attention is drawn to the diversity and lack of consistency in research and their relation to particular, different, sometimes incomparable aspects: mentioning only selected stages of sleep, frequency domains and subdomains, selected brain regions and derivations [4, 6, 7, 9-11, 13-17, 27, 30]. The most common conclusion is an increase and proximity of EEG synchronicity in the three stages of sleep with an increase in slow-wave activity, as opposed to relaxed wakefulness [7, 9, 10, 16, 20, 23]. The greatest uncertainty and inconsistency relate to interhemispheric asymmetry in estimates of EEG synchronicity and power: both right-hemisphere dominance [12, 16, 21] and left-hemisphere dominance [15, 21, 24] are noted, as well as different dominance in different stages of sleep and areas of the scalp [1, 7, 26, 27] or the absence of asymmetry [11, 18]. A similar uncertainty concerns the increase or decrease of interhemispheric coherent bonds (see review [23]).

Therefore, it seems relevant to conduct a comprehensive study of this issue using a new approach outlined in [3]. In this study, in addition to the work [3], we further continue the applied development of the methodology of integrated system analytics, described in detail and illustrated in the monograph [2].

RESEARCH METHOD AND INITIAL DATA

The basis of our approach is the analysis of the correlation synchronicity of the EEG (ACS), which is described in detail in [3], and which shows its high efficiency and fruitfulness in relation to the differentiation of norm and schizophrenia. Therefore, in this article we will recall only the main provisions of the ACS method. The preliminary operations of this method include: 1) fast Fourier transform filtering in the selected frequency domain; 2) calculation of the envelope of filtered EEG recordings; 3) calculation of Pearson correlation coefficients between EEG envelopes of nearby lead pairs. The sequence of correlation coefficients between EEG envelopes ordered by lead pairs for nearby lead pairs is called the synchronicity profile, and these profiles are the source material for subsequent stages and directions of analysis. In particular, correlations between such profiles serve as estimates of the topographic consistency of EEG synchronism.

The initial data. As the source material, fragments of sleep recordings of 15 right-handed men (from 18 to 34 years old) were used, performed using

the 10-20% system for 16 off-center leads with a registration frequency of 200 Hz, filtering in the 0.5-40 Hz band (BioTop 6R12 amplifier, NEC, Japan, referent A2, these recordings have already been discussed in [5]). For each subject and each stage of sleep: REM (phase of rapid eye movements, rapid eyes movements), 1, 2, 3/4 and the stages of relaxed wakefulness with closed eyes (stage W, recorded before and immediately after sleep), there are five 20-second fragments of EEG recordings, visually evaluated according to the criteria of Rechtshafen—Kale and randomly selected from different sleep cycles, i.e. for each stage of sleep, the initial volume of the analyzed sample is 75 such records. For these stages and four standard frequency domains (delta, theta, alpha, beta1), 5.4×20 matrices of synchronicity profiles of EEG envelopes were calculated (columns — 43 pairs of nearby leads; rows — synchronicity profiles for 75 records). These matrices are the starting material for subsequent analysis.

Statistical estimates. Due to the often small volume of compared samples and the difference in their distributions from the normal, paired differences are identified using one- or the two-sample Wilcoxon criterion (significance levels below are indicated by p_w), and the assessment of factor effects is carried out using methods of single-factor nonparametric analysis of variance [2, p. 181-182]: Kruskal—Wallis (significance levels are indicated by p_{k-w}) or Jonkheer (with increasing/decreasing factor effects, significance levels are indicated by p_{jo}).

DATA CONSISTENCY ANALYSIS

The methodology. The initial data was previously analyzed for consistency. This technique [3] involves calculating the square correlation matrix of the synchronicity profiles of the EEG envelopes of all recordings with all. Using such a matrix, the average correlation value of the profile of each subject with the profiles of all other subjects is calculated and a variation series is constructed, according to which outliers are allocated, as well as a highly consistent and most representative group of records.

Discussion of the results. In such variation series (by sleep stages and frequency domains), most of the recordings of the three subjects turned out to be outside the highly consistent subgroups. Their visual analysis showed the absence of an EEG signal along one of the derivations in two subjects. The recordings of the third subject were characterized by abnormally low synchronicity in the frontal and temporal pairs of deri and in the right occipital region. Thus, consistency analysis has once again

shown its effectiveness in removing outliers and artifacts from the analyzed data. The records of the three identified subjects were not used in further analysis, i.e. the volume of the analyzed sample for each stage of sleep was reduced to 60 records.

The average correlation of the synchronicity profiles of the EEG envelopes differentially in frequency domains taking into account standard deviations, is: $\delta=0.304\pm 0.052$, $\theta=0.558\pm 0.034$, $\alpha=0.568\pm 0.052$, $\beta_1=0.537\pm 0.045$.: 1) relatively small standard deviations, indicating rather narrow confidence intervals of average estimates; 2) close levels of correlation in the theta, alpha and beta1 domains with the absence of paired differences at the significance level of $p_w = 0.14-0.38$; 3) a reduced level of correlation in the delta domain with differences relative to other domains at the significance level of $p_w < 0.006$. Thus, the individual variability of the topography of the EEG synchronism in the delta domain is quite large compared with other domains.

As for the average correlations by sleep stages, they are close in their values and amount to: REM=0.48, 1=0.46, 2=0.47, 3/4=0.51, W=0.54 with the absence of pairwise differences at the level of significance $p_w=0.07-0.34$. Thus, the individual variability of the EEG topography of synchronism in all the stages of sleep are approximately at the same level.

TOPOGRAPHY OF EEG SYNCHRONISM

Let us turn to the analysis of the topography of highly synchronous connections calculated by the ACS method (Section 1). To do this, we estimate the average synchronicity of the EEG envelopes for each pair of derivations (columns in the synchronicity matrices) differentially by frequency domains and sleep stages.

Table 1. The estimations of correlation synchronism averaged over EEG electrodes (\pm standard deviation), designations: REM - the stage of rapid eyes movements; 1, 2, 3/4 - sleep stages in order of its deepness; W - the stage of passive wakefulness.

Nº	Derivations	Delta	Theta
1	All	0.658 ± 0.084	0.648 ± 0.101
2	Left Hemisphere	0.690 ± 0.074	0.691 ± 0.086
3	Right hemisphere	0.636 ± 0.094	0.647 ± 0.110
4	Differences	$p=0.05$	$p=0.09$
5	Forehead	0.666 ± 0.084	0.684 ± 0.096
6	Crown – the back of the head	0.642 ± 0.087	0.607 ± 0.099
7	Differences	$p=0.16$	$p=0.01$
8	Sleep stage	Delta	Theta
9	REM	0.649 ± 0.093	0.642 ± 0.102
10	1	0.643 ± 0.084	0.649 ± 0.099
11	2	0.691 ± 0.087	0.656 ± 0.099
12	$\frac{3}{4}$	0.688 ± 0.091	0.628 ± 0.110
13	W	0.617 ± 0.119	0.664 ± 0.108

Nº	Derivations	Alpha	Beta1
1	All	0.656 ± 0.108	0.644 ± 0.091
2	Left Hemisphere	0.705 ± 0.089	0.712 ± 0.069
3	Right hemisphere	0.659 ± 0.112	0.639 ± 0.085
4	Differences	$p=0.1$	$p=0.006$
5	Forehead	0.701 ± 0.103	0.657 ± 0.095
6	Crown – the back of the head	0.607 ± 0.101	0.632 ± 0.093
7	Differences	$p=0.004$	$p=0.16$
8	Sleep stage	Alpha	Beta1
9	REM	0.627 ± 0.121	0.652 ± 0.096
10	1	0.649 ± 0.108	0.648 ± 0.092
11	2	0.675 ± 0.092	0.659 ± 0.088
12	$\frac{3}{4}$	0.687 ± 0.093	0.652 ± 0.091
13	W	0.639 ± 0.162	0.611 ± 0.116

The ratio of the areas of the scalp. The upper part of Table 1 shows the average values and standard deviations of such average estimates differentially by brain regions and frequency domains for all stages of sleep. First of all, the following draws attention to itself:

- left-hemisphere dominance in all frequency domains (Tables 1, lines 2, 4, sample size of 13 lead pairs) with differences in the delta and beta domains (Table 1, line 4); two-factor analysis of variance (factors: frequency domain and hemisphere) reveals the influence of the hemispheric factor at the level of significance $p<10^{-8}$; at the same time, left-sided dominance is observed not only in general, but also in each stage of sleep;
- higher synchronism in the frontal-central region compared with the parietal-occipital region (Tables 1, lines 5, 6, sample size 11 pairs of leads) with statistically significant differences in the theta and alpha domains (Table 1, line 7); two-factor analysis of variance reveals the influence of the frontal dominance factor at the level of the significance of $p<10^{-9}$;
- the average synchronicities in each group of leads in frequency domains are close in magnitude with no differences: $p_w=0.13-0.49$.

Ratios by sleep stages. The lower part of Table 1 shows similar estimates differentially by sleep stages (sample size — 43 pairs of leads). Here you can note the following:

- reduced synchronicity of EEG envelopes in the alpha domain and REM stage relative to other domains and stages ($p_w < 0.019$);
- almost identical synchronicity in stage 1 across all domains;
- increased synchronicity in the delta and alpha domains in stages 2 and 3/4 relative to other stages and domains without statistically significant differences;
- reduced synchronicity in the theta domain for stage 3/4 relative to other stages and domains ($p_w < 0.05$);
- decreased synchronicity in the delta and beta domains in stage W relative to other stages and domains ($p_w < 0.019$) with higher synchronicity in the theta domain for this stage ($p_w < 0.05$).

Thus, the general conclusion common in publications is an increase and proximity of EEG synchronism in the three stages of sleep compared with relaxed wakefulness. It is only partially confirmed, with the exception of the theta domain and stage 1 for the delta and alpha domains.

Interhemispheric connections. Let us now turn to the consideration of the ratios of nearby interhemispheric connections (Fig. 1, a) where the following patterns are revealed

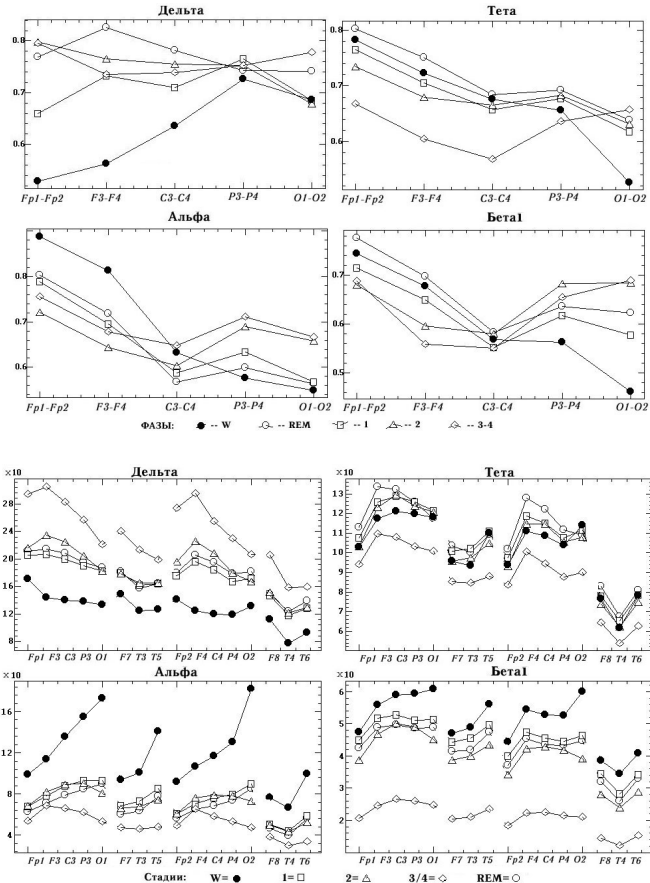


Fig. 1. The numerical dependencies of synchronicity estimates and spectral amplitudes at the top — the averaged interhemispheric correlation of the frequency domains depending on the stage of sleep, vertical axis — correlation values, horizontal axis — pairs of electrodes; below — the averaged normalized spectral amplitudes over frequency domains, electrodes and sleep stages, vertical axis — spectral amplitudes, horizontal axis — electrodes.

1. The delta domain differs significantly from other frequency domains: in the W stage, there is an increase in the interhemispheric synchronicity of the EEG envelopes from the forehead to the occiput ($p_{j0}<0.0002$) with less synchronicity in the frontal and central leads compared with the four stages of sleep ($p_w<0.04$), which do not have significant trends forehead to occiput ($p_{jo}>0.15$) and differ little from each other ($p_w>0.05$).
2. For other frequency domains, a consistent decrease in synchronicity from the frontal to the central leads ($p_w<0.00005$) is indicative, and for the theta domain (except stage 3/4) — and from the parietal to the occipital leads ($p_w<0.00001$).
3. A decrease in synchronicity in the central pair of leads, manifested in all 4 stages of sleep and especially vividly in stage 3/4: a) compared with frontal leads ($p_j<0.00003$); b) compared with parietal derivations in the alpha and beta domains ($p_w<0.03$); c) compared with occipital leads in the beta domain ($p_w<0.005$, except for stage 1); such trends may be associated with a decrease in motor activity and muscle afferentation.
4. A consistent decrease in synchronicity from the forehead to the back of the head in stage W ($p_{j0}<0.00001$). A similar pattern was found by us on a completely different experimental material [3]: adolescents 11-14 years old, two groups: norm and nosology autism, the "closed eyes" test. And this shows that the ACS method has sufficient accuracy and sensitivity to give the same results on fundamentally different experimental material.
5. A consistent decrease in synchronicity in the frontal region ($p_{j0}<0.0006$) and an increase in synchronicity in the parietal occipital region ($p_{j0}<0.0003$, except for the theta domain) both with deepening sleep and with respect to W and REM stages.

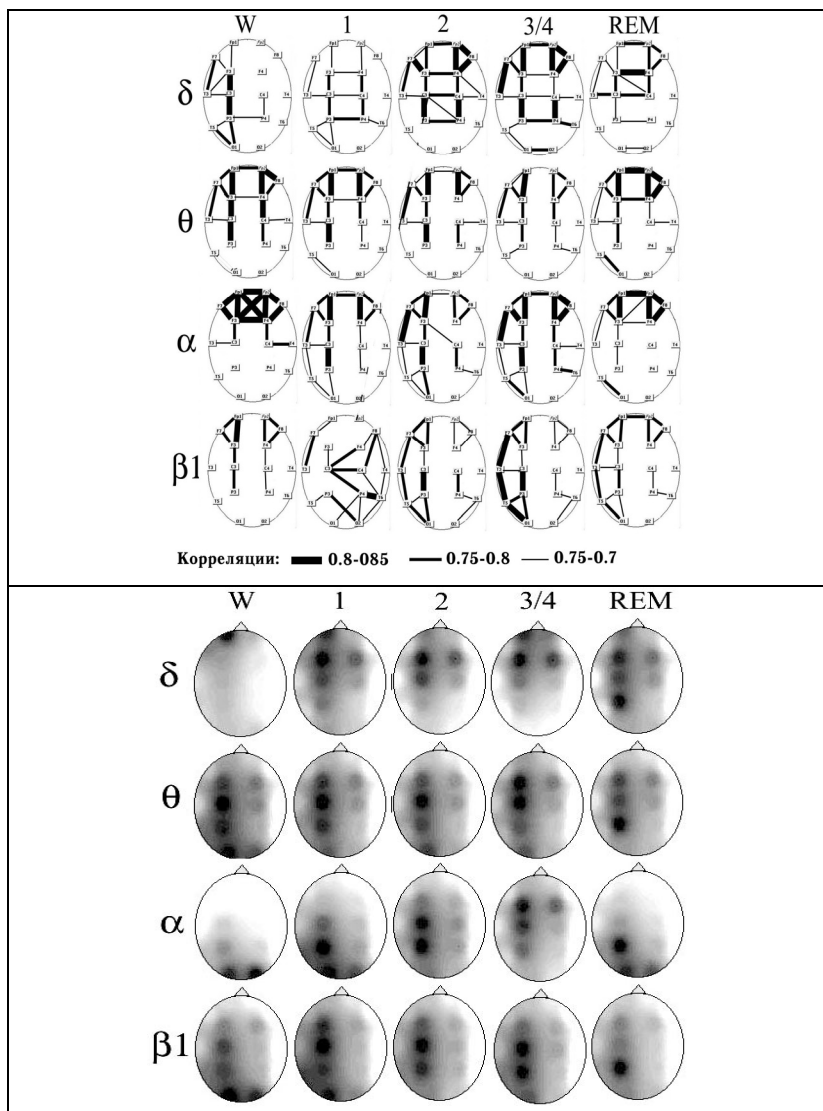


Fig. 2. The topographical relations over sleep stages and frequency domains. *at top* — the distribution of high synchronization links between pairs of electrodes; *at bottom* — the distribution of averaged spectral amplitudes.

Highly synchronous communications. At the end of this section, we turn to a comparative study of the topography of high average correlations (0.7-0.85) of EEG envelopes by frequency domains and stages of sleep (Fig. 2, a).

1. Delta domain. In the REM stage, interhemispheric synchronicity of the EEG envelopes and synchronicity in the frontal-central derivations prevail. In stage 1, the center of synchronicity shifts to the parietal zone with a slight predominance in the left hemisphere. In stage 2, this synchronicity distribution is enhanced. In stage 3/4, the topography of stage 2 extends to the temporo-occipital derivations with a slight dominance in the left hemisphere. In stage W, left-sided asymmetry dominates in most lead pairs in the absence of significant interhemispheric synchronicity.
2. The theta domain. For all stages of sleep, the topography of highly synchronous connections is close enough. It is characterized by the predominance of frontal-central parietal connections with little representation of interhemispheric connections and with slight left-hemisphere asymmetry.
3. Alpha domain. The REM stage is characterized by high synchronicity in the frontal derivations with some asymmetry in the left hemisphere in relation to the frontal temporal, frontal central parietal and temporal occipital derivations. Stage W is characterized by an abnormal increase in synchronicity in all frontal pairs of derivations, including rarely occurring diagonal connections in the absence of high synchronicity between the central, parietal and occipital derivations. Stages 1, 2 and 3/4 are quite close in terms of synchronism topography with some increase in overall synchronicity with deepening sleep. They are characterized by a small number of interhemispheric connections, the prevalence of parasagittal connections throughout the scalp with some left-hemisphere asymmetry.
4. Beta1 domain. Stages REM, 2, 3/4 have a close topography characterized by noticeable left-hemisphere asymmetry, parasagittal connections with small interhemispheric connections, and the absence of a predominance of frontal connections. In stage W, the asymmetry decreases, and the center of synchronicity shifts to the frontal and parasagittal frontal-central parietal connections. The localization of synchronicity in stage 1 is poorly expressed.

We note some similar patterns identified in some of the cited studies: high coherence in the delta and alpha domains of stages 2 and 3/4 [13], high coherence in the alpha domain of stage 3/4 and in the beta domain of stage

REM [16], minimum coherence in the beta domain of stage W, maximum coherence in the delta domain of stage 3/4 the prevalence of stage 2 coherence compared to stage 1 [22].

General characteristics. As general characteristics of the considered topographic pattern of synchronicity of EEG envelopes, it should be noted: 1) from Table 1, which coincides with the results: a) a decrease in interhemispheric synchronicity in the direction from the frontal to the occipital derivations (14 out of 20 topograms); b) increased frontal-central synchronism (10 out of 20 topograms); c) increased left-sided synchronization (12 out of 20 topograms); 2) reduced interhemispheric synchronicity (64 out of 100 correlations) compared to parasagittal connections; 3) low synchronicity between diagonal pairs of derivations (15 out of 320 correlations); 4) close topography of highly synchronous connections is observed: in the theta domain for all stages; in stages 2 and 3/4 for all frequency domains; in the alpha domain for stages 1, 2, 3/4; in the beta domain for stages REM, 2, 3/4; 5) the W stage is characterized by the greatest differences in all frequency domains.

It should be particularly noted that result 3 shows that when evaluating the synchronicity of the EEG by the ACS method, the effect of volumetric surface conduction of potentials, often mentioned in publications, is not revealed, otherwise, in the presence of highly synchronous sagittal and axial connections between the three derivations, diagonal connections would also be high.

AMPLITUDE TOPOGRAPHY-SPECTRAL ESTIMATES

The methodology. The above analysis of the highly synchronous connections of the EEG envelopes must be supplemented by an analysis of the topography of the amplitude characteristics of the EEG. Let's choose the most statistically stable indicator for this — the average amplitude of the spectrum in the frequency domain. The amplitude spectra are calculated for 16 derivations over the entire 20-second time interval of recordings, which gives a high frequency resolution of 0.05 Hz, and this ensures acceptable statistical stability of the averaged estimates, taking into account the presence of at least 80 spectral harmonics in each frequency domain. However, the average amplitudes of the spectrum in the frequency domains themselves are subject to significant interindividual variability (by 2-3.5 times), determined by the individual characteristics of the subjects' EEG and instrumental factors. To level it, we will normalize the average amplitudes of the spectrum: each value for a particular subject

is expressed as a percentage of the average amplitude for him over all derivations and all frequency domains.

Discussion of the results. Fig.1, b shows the average amplitudes of the spectrum, calculated differentially by frequency domains, derivations and sleep stages. It seems advisable to perform a comparative analysis of the results using longitudinal “meridians” or parasagittal electrode chains: two proximal Fp1, F3, C3, P3, O1 (the left meridian will be designated Fp1-O1) and Fp2, F3, C3, P3, O2 (the right meridian will be designated Fp2-O2) and two distal F7, T3, T5 (left meridian F7-T5) and F8, T4, T6 (right meridian F8-T6). It is these meridians that are highlighted in Fig. 1, b.

Numerical patterns. The meridian representation used makes it possible to clearly visually identify numerical ratios and patterns (both in parasagittal and axial directions, as well as by sleep stages and domains), which are then statistically verified.

1. Trends of a consistent increase in EEG amplitudes by sleep stages:

- in the delta domain: W, REM, 1, 2, 3/4 ($p_{k-w} < 10^{-5}$) with no differences in the stages of REM, 1, 2 ($p_{k-w} = 0.56$); in these ratios, the delta domain is opposite to the alpha and beta1 domains, as was the case with respect to interhemispheric synchronicity (Fig. 1, a);
- in the theta domain: 3/4, W, 1/2, REM ($p_{k-w} = 0.007$) with no differences in stages 1-2 ($p_{k-w} = 0.59$); in these ratios, the theta domain occupies an intermediate position, as was the case with respect to interhemispheric synchronicity (Fig. 1, a);
- in the alpha domain: 3/4, REM, 1, 2, W ($p_{k-w} < 10^{-5}$) with no differences in the stages of REM, 1, 2 ($p_{k-w} = 0.43$);
- in beta1 domain: 3/4, 2, REM, 1, W ($p_{k-w} < 10^{-5}$), differences in stages 2, REM, 1 are revealed taking into account the ordering of factor effects ($p_{jo} = 0.012$).

2. Left-hemisphere dominance, which is manifested in both pairs of meridians ($p_w < 0.00015$), but in terms of the relative ratio of amplitudes is especially pronounced in the distal meridians (the reverse ratio is observed only in the derivations O1, O2 for alpha domain W stage without significant differences $p_w = 0.15$).

3. The forehead-occiput ratio (except for the meridian F8-T6):

- sequential increase in amplitudes: in the alpha domain for all meridians ($p_{jo} < 0.013$), except stages 2 and 3/4; in the beta domain

for meridian F7-T5 ($p_{jo}<0.003$) and for meridian Fp1-O1 in stage W ($p_{jo}<10^{-9}$);

- sequential decrease in amplitudes (except for the Fp1, Fp2 derivations): in the delta domain ($p_{jo}<0.007$); in the theta domain for both proximal meridians in stages REM and 3/4 ($p_{jo} 0.01$); in the alpha domain for both proximal meridians in stage 3/4 ($p_{jo}<10^{-6}$).

4. The dominance of the proximal meridians over the distal ones ($p_w<0.013$).

5. Particular patterns: a) decrease in amplitudes in the derivations Fp1, Fp2 relative to F3, F4 ($p_w=0.02$); b) lower amplitudes in T4 compared to neighboring derivations of the meridian F8-T6 and a consistent increase in the amplitudes of the forehead - occiput in the meridian F7-T5 ($p_w<0.034$).

Topographic characteristics. Let's consider the topography of the average amplitudes of the EEG spectrum by sleep stages and frequency domains (Fig. 2, b, for better visualization of activity foci, each map is presented in its own black and white scale, therefore, to correlate activation levels, refer to Fig. 1. b). The following should be noted as general characteristics: 1) identical topography is observed in the non-REM sleep stages of the theta domain and in stages 2 and 3/4 of the delta and beta1 domains; 2) a significant difference in the topography of the REM stage and especially stage W from the non-REM sleep stages; 3) the general topographic differences increase sequentially in the order of frequency domains: theta, beta1, delta, alpha.

In the alpha domain, in the W stage, activity is localized in the occipital derivations, in the REM stage it captures the parietal derivations, and with deepening sleep it gradually shifts forward, capturing first the central and then the central frontal leads with a decrease in the activity of the occipital leads. This trend, although to a less pronounced extent, is manifested in the beta1 and theta domains, taking into account the greater spread of activity to the central and central frontal derivations. In the delta domain, in the W stage, the focus is localized in the anteroprontal leads, in the REM stage, activation covers a large area from the central frontal to the parietal derivations, and with deepening sleep, such widely distributed activation gradually shifts forward.

We note some similar patterns identified in some of the cited studies: the location of the focus of alpha activity in stage 1 in the left occipital region with its displacement to the central region in stage 2 [6], the maximum delta activity in stage 3/4 and beta activity in stage 1 [17], the difference

between stage 1 and stage REM with lower activity in the delta and theta domains and higher activity in the alpha and beta domains [14], the predominance of delta activity in the frontal-central region [30].

Table 2. Interhemispheric asymmetry calculated as $(left-right)/(left+right) \times 100\%$: mean values and standard deviations

Stage	<i>Fp1-Fp2</i>	<i>F7-F8</i>	<i>F3-F4</i>	<i>T3-T4</i>
REM	5.4±3.3	13.1±6.4	4.1±4.2	21.5±7.6
1	4.8±3.2	12.6±6.9	4.1±4	21.7±7.9
2	4.6±3.9	11.8±6.3	3.2±4.9	21.1±8.2
¾	5.4±3.7	12.5±6.7	3.7±4.3	22.2±8.8
W	4.9±3.3	11.4±6.5	3.6±4.4	20.7±7.2
General	5±3.5	12.3±6.5	3.7±4.4	21.4±7.9
Stage	<i>C3-C4</i>	<i>T5-T7</i>	<i>P3-P4</i>	<i>O1-O2</i>
REM	6.9±5.3	17.9±6.4	7.7±4	3.6±6.4
1	7.1±5.1	17.5±8	7.7±5.1	3±7.2
2	6.8±5	18±8.1	8±4.9	2.7±7.4
¾	6.9±5.2	16.8±7.3	7.7±5	2.2±7
W	6.6±5.5	15.8±8.1	6.8±4.8	1.9±6.4
General	6.8±5.2	17.2±7.6	7.6±4.7	2.7±6.9

Table 3. Percentage ratio of right-hemispheric asymmetry

Stage	<i>Fp1-Fp2</i>	<i>F7-F8</i>	<i>F3-F4</i>	<i>T3-T4</i>
REM	7.2	1.8	19.9	0
1	7.2	3.6	16.3	0
2	12.7	5.4	30.9	0
¾	5.4	3.6	16.3	0
W	3.6	5.4	16.3	0
Average	7.2	3.9	19.9	0
Stage	<i>C3-C4</i>	<i>T5-T7</i>	<i>P3-P4</i>	<i>O1-O2</i>
REM	10.9	0	5.4	23.6
1	7.2	0	7.2	27.2
2	7.2	1.8	5.4	21.8
¾	5.4	1.8	3.6	29
W	10.9	3.6	7.2	34.5
Average	8.3	1.4	5.8	27.2

Hemispheric asymmetry. Table 2 shows statistical estimates of interhemispheric asymmetry differentiated by sleep stages and symmetrical pairs of derivations. Similarly, Table 3 shows the percentages of cases of right hemisphere asymmetry. These data allow us to draw the following conclusions:

- for all stages of sleep and symmetrical pairs of derivations, left-hemisphere asymmetry dominates: right-sided asymmetry is observed on average only in 9.2% of cases (the average of “Average” in Table. 3), the global average value of the asymmetry is 8.9-5.4 (the average of the “Total” in the table. 2);
- in order of decreasing of left-hemisphere asymmetry of the symmetric pair of derivations can be ranked as follows: T3-T4, T5-T7 F7-F8, P3-P4, C3-C4, Fp1-Fp2, F3-F4, O1-O2;
- there are no trends of a regular or statistically significant change in asymmetry by sleep stages.

General patterns. The considered results of spectral analysis significantly complement the results of the analysis of synchronicity of EEG envelopes, but coincide in their following general characteristics: 1) left-hemisphere dominance; 2) significant topographic difference of stage W from other stages; 3) close topography is observed: in the theta domain for all stages; in stages 2 and 3/4 for all frequency domains.

DISCRIMINANT CLASSIFICATION

Classification according to synchronicity estimates. In order to automatically recognize the stages of sleep, we will conduct a general discriminant classification analysis [2, p. 365-370] of the synchronicity profiles of the EEG envelopes separately by frequency domains, when the class number is initially indicated for each stage of sleep. Table 4 (lines 1-4) shows the number of errors in this classification out of 60 synchronism profiles. It can be seen that the best results are obtained by using the alpha domain for all stages of sleep, although the average error rate of 22.3 is quite high here. Thus, the topography of synchronicity by sleep stages differs significantly less than in relation to norm and schizophrenia, where the minimum number of errors in discriminant classification was 1.5-6% [3]. In the direction of deterioration of recognizability, the sleep stages are ranked (by the total number of errors in four frequency domains: 63, 96, 95, 63, 52) in the following order: W, 3/4, REM, 2, 1 (with other indicators [28], the ranking order is close to the one considered: 3/4, W \square REM, 2, 1). Thus, the stages W, 3/4, REM differ markedly in the

topography of the EEG synchronism both among themselves and from stages 1, 2; at the same time, the highest differences occur for stage W.

Table 4. Errors in discriminant classification of sleep stages

Nº	Domain	Indicator	REM	1	2	3/4	W	Average percentage
1	Alpha	Synchronicity	12	15	20	12	8	22.3
2	Delta	-"-	17	32	23	13	16	33.7
3	Theta	-"-	14	25	28	16	12	31.7
4	Beta1	-"-	20	24	24	22	16	35.3
5	Alpha	Spectrum	16	24	27	2	10	26.3
6	Delta	-"-	25	31	21	4	1	27.3
7	Theta	-"-	26	44	27	18	28	47.7
8	Beta1	-"-	24	35	21	4	21	35.2
9	Alpha	Synchronicity + Spectrum	5	12	11	2	3	11.0
10	-"-	Control: discrimination	0	8	7	1	1	7.0
11	-"-	Control: classification	2	3	4	0	2	18.3

Classification by spectral estimates. Next, for comparison, we will classify the stages of sleep using spectral estimates. Here, the best results are also obtained for the alpha domain (Table 4, line 5), however, the use of synchronicity profiles (Table 4, line 1) is more effective both on average and for recognizing stages REM, 1, 2 and W, although spectral estimates give fewer errors when recognizing stage 3/4.

Combined classification. Now we will perform a discriminant analysis with expanded data matrices, when amplitude indicators are added to the synchronicity of the EEG envelopes. As can be seen from Table 4 (line 9), this gives an improvement in results with an average error rate of 11, while the classification errors of individual stages lie in the range of 3-20%.

Classification of new objects. To substantiate the stability of the results obtained, we will conduct a control classification, dividing the records of each stage of sleep of each subject into two groups in a ratio of 80 to 20%. Let's construct discriminant functions for the first group of records (training sample) and use them to classify records of the second group (classified sample). The results of the analysis (Tables 4, lines 10, 11)

demonstrate a small number of errors for the training sample (7%) and satisfactory recognition of sleep stages for the classified sample (18.3% of errors).

CONCLUSION

Quite detailed reviews of various approaches to automatic recognition of sleep stages are contained in [19, 28, 29]. Estimates of classification errors of various stages are: 10-42%, 5-37%, 15-25% [19], 6.9-12.5% [25], 7-39% [28], 18-21%, 12.3%, 23% [29]. It follows that over the past quarter century (since [19]), despite the introduction of many new computational methods, no significant progress has been achieved in this direction. In this comparison, the results we have obtained look undoubtedly promising. Thus, the combination of estimates of the correlation synchronicity of EEG envelopes with amplitude spectral estimates can be the basis for highly reliable automatic recognition of sleep stages and drowsy states both directly during the experiment and during post-experimental analysis of recordings. On the other hand, the numerous and multifaceted results discussed in sections 2, 3, 5 (in addition to the results of the work [3]) indicate the physiological validity, innovative effectiveness, fruitfulness and prospects of the proposed method for assessing EEG synchronicity. A similar conclusion based on the results of section 4 is valid for the proposed method of normalization of amplitude-spectral parameters.

REFERENCES

1. Zhavoronkova L.A., Trofimova E.V. Dynamics of EEG coherence and motor reactions during falling asleep in right-handed and left-handed people. *Human physiology*. 1997. 23(6):18-26.
2. Kulaichev A.P. Methods and means of complex data analysis. Textbook for classical university education. Moscow: FORUM—INFRA*M, 2006. 512 p.
3. Kulaichev A.P. The method of analyzing the correlation synchronicity of the EEG and its possibilities. *Journal of Higher Education. the nerve. acts.* 2011. 61(4): 485-498.
4. Kuraev G. A., Suntsova N. V. Interhemispheric relations at different stages of the human wakefulness-sleep cycle. *Human physiology*. 1998. 24(5):72-79.
5. Sulimov A.V., Maragey R. A. The study of sleep EEG as a nonlinear dynamic process: comparison of the global correlation dimension of human EEG and measures of linear dependence between channels. *Journal of Higher Education. the nerve. acts.* 2003. 53(2):151-155.

6. Sysoeva Yu.Yu., Verbitsky E.V. Investigation of the spatiotemporal organization of the EEG in the development of night sleep in persons with high and low anxiety. Materials of the 3rd conference "Sleep is a window into the world of wakefulness". Moscow. 2005. 97-98.
7. Shepovalnikov A.N., Tsitseroshin M.N., Rozhkov V.P., Galperina E.I., Zaitseva L.G., Shepovalenkov R.A. Features of interregional interaction of cortical fields at different stages of natural and hypnotic sleep (according to EEG data). *Human physiology*. 2005. 31(2):34-48.
8. Shishkin S.L., Kaplan A.Ya., Dorokhov V.B. Correlation between the amplitudes of the envelopes of the frequency components of the EEG as an additional tool for tracking the dynamics of sleep and drowsy states. Materials of the 1st conference "Sleep is a window into the world of wakefulness". Moscow, 2001. 157-158.
9. Achermann P., Borbely A. A. Coherence spectra of all-night sleep EEG. *Sleep Res.* 1997. 26:1.
10. Achermann P., Borbely A. A. Temporal evolution of coherence and power in the human sleep electroencephalogram. *J. Sleep Res.* 1998. 7 (Suppl 1):36-41.
11. Armitage R., Hoffmann R., Loewy D., Moffitt A. Variations in period-analysed EEG asymmetry in REM and NREM sleep. *Psychophysiology*. 1989. 26(3): 329-336.
12. Casagrande M., Bertin M. Night-time right hemisphere superiority and daytime left hemisphere superiority: a repatterning of laterality across wake-sleep-wake states. *Biol. Psychol.* 2008. 77(3):337-342.
13. Corsi-Cabrera M., Guevara M., Arce C., Ramos J. Inter and intrahemispheric EEG correlation as a function of sleep cycles. *Progr. Neuro-Psychopharmacol. Biolog. Psychiat.* 1996. 20(3):387-405.
14. Corsi-Cabrera M., Munoz-Torres Z., Del Rio-Portilla Y., Guevara M. Power and coherent oscillations distinguish REM sleep, stage 1 and wakefulness. *Int. J. Psychophysiol.* 2006. 60(1):59-66.
15. Duckrow H.P., Zaveri H.P. Coherence of the electroencephalogram during the first sleep cycle. *Clin. Neurophysiol.* 2005. 116(5):1088-1095.
16. Dumermuth G., Lehmann D. EEG Power and coherence during non-REM and REM phases in humans in all-night sleep analyses. *Eur. Neurol.* 1981. 20:429-434.
17. Dumermuth G., Langea B., Lehmann D., Meier C.A., Dinkelmann R., Molinari L. Spectral analysis of all-night sleep EEG in healthy adults. *Eur. Neurol.* 1983. 22(5):322-339.

18. Ehrlichman H., Antrobus J., Weiner M. EEG asymmetry and sleep mentation during REM and NREM sleep. *Brain Cogn.* 1985. 4(4):477-485.
19. Fell J., Roschke J., Mann K., Schaffner C. Discrimination of sleep stages: a comparison between spectral and nonlinear EEG measures. *EEG Clin. Neurophysiol.* 1996. 98(5):401-410.
20. Kaminski M., Blinowska K., Szelenberger W. Topographic analysis of coherence and propagation of EEG activity during sleep and wakefulness. *EEG Clin. Neurophysiol.* 1997. 102(3):216-227.
21. Kobayashi T., Madokoro S., Misaki K., Murayama J., Nakagawa H., Wada Y. Interhemispheric differences of the correlation dimension in a human sleep electroencephalogram. *Psychiat. Clin. Neurosci.* 2002. 56(3):265-266.
22. Kuraev G., Suntsova N., Chernoval L., Pavlov I. Interhemispheric relationships of the EEG activity during sleep-waking cycle in normal adults. *Sleep Res.* 1997. 26: 19.
23. Nielsen T., Abel A., Lorrain D., Montplaisir J. Interhemispheric EEG coherence during sleep and wakefulness in left- and right-handed subjects. *Brain Cogn.* 1990. 14(1):113-25.
24. Obermeyer W., Larson C., Yun B., Dolski I., Weber S., Davidson R., Benca R. Comparison of frontal activation in sleep and wake. *Sleep Res.* 1997. 26: 232.
25. Park Hae-Jeong, Oh Jung-Su, Jeong Do-Un, Park Kwang-Suk. Automated sleep stage scoring using hybrid rule and case-based reasoning. *Comput. Biomed. Res.* 2000. 33(5):330-349.
26. Pereda E., Gamundi A., Nicolau M., Rial R., Gonzales J. Interhemispheric differences in awake and sleep human EEG: a comparison between non-linear and spectral measures. *Neurosci. Lett.* 1999. 263(1):37-40.
27. Roth C., Achermann P., Borbely A.A. Frequency and state specific hemispheric asymmetries in the human sleep EEG. *Neurosci. Lett.* 1999. 271(3):139-142.
28. Susmakova K., Krakovska A. Selection of measures for sleep stages classification. *Proc. 7th Int. Conf. Measurement.* Smolenice. 2009:86-89.
29. Susmakova K., Krakovska A. Discrimination ability of individual measures used in sleep stages classification. *Art. Intel. Med. Arch.* 2008. 44(3):261-277.
30. Tanaka H., Hayashi M., Hori T. Topographic mapping of EEG spectral power and coherence in delta activity during the transition from wakefulness to sleep. *Psychiat. Clin. Neurosci.* 1999. 53(2):155-157.

CHAPTER 7

OPTIMAL CHOICE OF REFERENCE ELECTRODE FOR EEG RECORDING

ABSTRACT

During a "eyes closed" test, we looked at topographical differences in averaged EEG amplitudes in the alpha domain recorded in the 10–20 system. These discrepancies arose as a result of the usage of 13 different reference schemes: top and bottom of the chin (P1, P2); nose (N); top and bottom of the back of the neck (Sh1, Sh2); upper back (C); united electrodes at the base of the neck anteriorly and posteriorly (2Sh); united, ipsilateral, and individual ear electrodes (A12, Sym, A1, A2); vertex (Cz); and averaged reference (AR). Six experiments with grounded and ungrounded states of three distant fundamental references P2, C, and 2Sh were conducted for each of the ten subjects. On the proposed complex of three independent indicators with evaluative criterion, pairwise evaluations of topographic consistency of 13 reference schemes were carried out, followed by centroid-based clustering of the reference schemes and its discriminant verification. As a result, we've made some progress(1) that most coordinated topography is provided by the following reference electrodes—A12, P1, P2, Sym; (2) reference electrodes A1, Sh2, A2, Sh1, AR, Cz are characterized by individually varying topography, which may lead to contradictory conclusions obtained when they are used; (3) There have been no substantial reasons for assuming a grounded (neutral) state of reference electrodes, making the search for or mathematical construct of an indefinitely remote neutral reference electrode less important.

Keywords: EEG; reference electrode; infinitely remote reference electrode; neutral reference electrode.

INTRODUCTION

In electroencephalographic studies, despite a decade of debate, no consensus was found on the location of the reference electrode, which would be preferable for electroencephalogram (EEG) recording on the

scalp [1–3]. In the early 1950s, summarization of the preceding discussion showed [4] that the use of earlobes individually induced a decrease in the EEG amplitude due to their proximity to the temporal electrodes. The pathological activity in the temporal region is reflected on the data from the ear electrodes, and this affects results obtained from the other electrodes via the reference. The reference electrodes on the nose and face are sensitive to artifacts from eye movement. The placement of reference electrodes on the body leads to the appearance of ECG artifacts. The positioning of electrodes at the base of the neck anteriorly and posteriorly was proposed, which, when connected to scalp, results in approximately the same voltage but of the opposite sign, so this association provides unobtrusive secondary voltage. Later [2], the use of the following referents was discussed: the vertex (Cz), the united ear electrodes, united mastoid electrodes, ipsilateral or contralateral ears, nose tip, bipolar reference electrodes, the averaged reference (AR), weighted AR, and the reference of source derivation. Each of them has its advantages and disadvantages and can cause various distortions in the topographic pattern of EEG potentials distribution. More distant references located on the thumb, elbow, knee, shoulder, neck, chest, back, and nose are discussed in [5,6]. However, prospects of discovering a potential close to zero or the ideal reference electrode on the body at a large distance from the neural sources have repeatedly been questioned [1,7].

In addition, in recent years, mathematical methods of designing the inactive neutral reference have appeared: the reference electrode standardization technique (REST) [8], blind source separation (BSS) [9], minimum power directionless response (MPDR) [10], source density derivations (CSD) [11, 12], robust estimation [13], etc. These methods continue to be modified and support positive expectations [14], but they rather have the nominal and theoretical value than the actual use and verification in practice.

Thus, this problem is still far from a final solution, which determines the importance of new approaches to the subject, especially with regard to the comparison of actual physical reference electrodes.

MATERIALS AND METHODS

Ten right-handed men (age from 18 to 70 years old) took part in the study. Each subject performed three pairs of tests with two consecutive EEG recordings, each of these six tests began 2-3 minutes after the previous one. In these experiments, the recording from three basic remote and

minimally exposed to artifacts reference electrodes were carried out: chin bottom (P2), the first thoracic vertebra (C), and the united electrodes at the base of the neck anteriorly and posteriorly (2Sh). The state of the base reference electrode was different in each pair of experiments: (1) normal state (P2, C, 2Sh) and (2) grounded by an electrically independent earth (P2g, Cg, and 2Shg). The ground provided a constant zero potential on the reference electrode; i.e., it implemented the concept of an infinitely distant neutral referent. The 10–20 system, “eyes closed” test, sampling rate of 250 Hz, the band 0.5–32 Hz, duration of recording 32.77 seconds, and EEG amplifier NVX-52 (MKS, Russia) were used. All subjects gave their written informed consent to participate in the experiments.

Besides 21 scalp electrodes, separated ear electrodes (A1, A2), and remote electrodes—nose (N), top of the chin (P1), first cervical vertebra (Sh1), and seventh cervical vertebra (Sh2)—were used for recording. Each record was mathematically transformed to 13 reference schemes: P1, N, Sh1, Sh2, A1, A2, Cz, united ear electrodes (A12), ipsilateral ears (Sym), average reference (AR), and basic references (P2, C, 2Sh). The amplitude spectra from the scalp electrodes and their mean amplitudes (Amean) were calculated in the alpha domain for each record and reference scheme.

To compare the similarities and differences of EEG topography, three mutually orthogonal (independent) indicators were used:

- (1) Twelve Pearson correlation coefficients r_{ij} were calculated between Amean of scalp electrodes for each pair of i, j -references. The matrix of such mutual correlations was used to calculate the mean correlation $M_i(r_{ij})$ for each i -reference scheme along with all other reference schemes. These correlations were used to estimate the integral topographic differences.
- (2) The differences $\Delta Amean1$ of Amean1 in neighboring electrode derivations were calculated in the sagittal direction. Then, mean correlation between $\Delta Amean1$ were calculated as described above.
- (3) The differences $\Delta Amean2$ between Amean of symmetrical electrodes (asymmetry) were calculated. Then, mean correlations between $\Delta Amean2$ were calculated as described above.

The reference electrodes can be considered of similar topography if mean correlation $M_i(r_{ij})$ is strong for each indicator. Indeed, such reference electrodes show the topography similar to most of the other references. The topography of a reference electrode with low $M_i(r_{ij})$ value has little resemblance to the topography of the other references, and its use causes a

specific pattern of EEG potentials distribution. In the EEG derivations with an increase in amplitude for most reference schemes, a decrease in amplitude is observed in this particular reference scheme, and vice versa. In certain studies, it might lead to the conclusions contradicting studies with other reference schemes. We emphasize that these topographic relations are crucial to identify intergroup differences and differentiation of functional state, pathologies, sex, age, professional, social and other differences.

The classification of reference schemes in terms of their topographic coherency was carried out using the following method:

- (1) $Mi(r_{ij})$ estimates were transformed to uniform range by its ranking for better comparability;
- (2) The mean rank of each reference scheme was calculated for each subject;
- (3) Using the resulting matrix of mean ranks, the K-means cluster analysis of reference schemes was conducted;
- (4) The resulting classification is statistically verified by discriminant analysis.

RESULTS

Effect of the Base Reference Electrode Grounding

Fig. 4.1 shows the changes in Amean averaged over the scalp for three basic reference electrodes and their two states (grounded/ungrounded) in ten subjects with two consecutive records for each subject. Fig. 4.1 shows that the data are characterized by a strong inter-individual variability. It also demonstrates (when comparing two values for two consecutive records) the presence of intra-individual variability, which is significantly lower in comparison with the interindividual variability.

The analysis of the differences between grounded and ungrounded state of basic references requires considering that the raw data are not simultaneously recorded, so the intraindividual variability can affect the results of the comparison, and the extent of this influence should be assessed in advance. The presence of two successive records performed in each experiment helps to distinguish the correlations determined by the intraindividual variability and the influence of the grounding factor (GF). Three above-described primary topographical indexes Amean, Δ Amean1, Δ Amean2 are used separately as the raw data. The correlation between the

presence/absence of grounding was calculated for each parameter and ten subjects and for two consecutive recordings reflecting the impact of intra-individual variability.

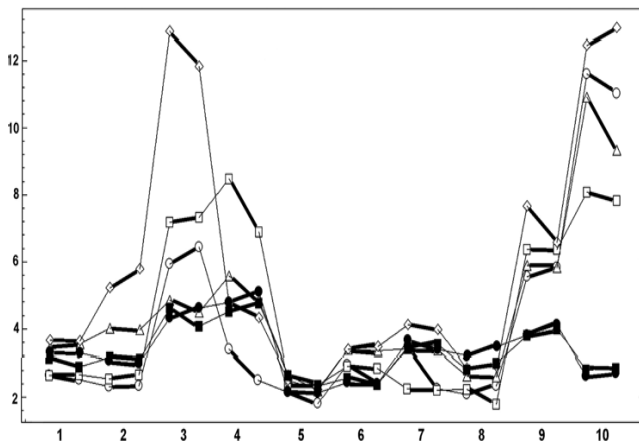


Fig. 4.1. Diagrams of mean spectral amplitudes [μ V] averaged over scalp [μ V] in the alpha domain in ten subjects (horizontal axis) in six experiments using three basic reference electrodes in two states (ungrounded and grounded): chin (P2, P2g—circles, squares), back (C, Cg—triangles, diamonds), united electrodes on the neck (2Sh, 2Shg—filled circles, filled squares). For each subject, two adjacent points on the diagrams (connected by bold lines) belong to two consecutive records. Thin lines play a supporting role for the connecting of points of each of the six diagrams

If the grounding actually has a significant effect on the topography change, topograms for grounded and ungrounded states would have greater differences than in the case of natural intra-individual variability (appearing as a random and less significant factor). Then, the correlations between the same primary topographical parameters would be repeatedly weaker than in the case of intra-individual variability. Therefore, the effect of GF can be detected by pairwise comparing the mean values in the samples relating to GF and intra-individual variability. For this purpose, three pairs of compared samples (correlations in the three primary parameters) of 60 values each (3 base references \times 2 consecutive recordings \times 10 subjects) were used.

Let us consider the descriptive statistics (mean \pm standard deviation) for the three pairs of samples:

0.9 ± 0.12 and 0.92 ± 0.09 (correlations with Amean); 0.82 ± 0.2 and 0.84 ± 0.15 (Δ Amean1); 0.67 ± 0.33 and 0.76 ± 0.21 (Δ Amean2). The mean values of the correlations related to GF, as expected, are slightly lower compared to intraindividual variability (2%, 2%, 14%) in all three cases. However, t-test for correlations with Fisher Z-normalization $Z(r)=0.5\ln((1+r)/(1-r))$ did not reveal significant differences between means at significance levels $p = 0.89, 0.67$, and 0.98 . Therefore, these three indicators were not affected by GF beyond the effect of intraindividual variability.

This is confirmed by cross correlations within the triad of the analyzed samples (related to Amean and Δ Amean1, Amean and Δ Amean2, Δ Amean1 and Δ Amean2) by GF 0.68, 0.63, 0.69, and 0.55 and the effect of intraindividual variability 0.55, 0.31, 0.54. As we can see, the former are repeatedly higher; i.e., GF correlations between the three pairs of samples are more coordinated than those related to intraindividual variability. Therefore, in this case, there is no reducing effect of the ground on the correlations.

Based on the results described above, grounded and ungrounded states of reference electrodes can be considered equivalent in terms of preserving the EEG topography.

Topographic Differences between References

Based on the identified equivalence, the recordings in this section were carried out with three conventional ungrounded basic reference electrodes. Unlike the previous section, the below comparisons were made within the same records arithmetically transformed to different reference schemes. This allowed us to obtain quantitative estimates of topographical differences caused by individual reference electrodes without the influence of intra- and interindividual variability. Fig. 4.2 shows diagrams of mean spectral amplitudes of chosen subject for 11 reference schemes at the base reference P2, where topographical differences at some of the reference electrodes were evident.

For quantitative verification of these differences, the reference patterns were classified according to the degree of their topographic similarity. Clustering into two, three, four, and five classes was tested. The only statistically significant ($p = 0$) classification included the three classes (table) in order of increasing topographic incoherence of reference schemes. The bottom lines of the table show the values of the Mahalanobis distance

$D2$ of each reference scheme to their cluster center and the significance p of the null hypothesis " $D2 = 0$," meaning "the reference scheme belongs to this cluster." All null hypotheses are accepted at the highest significance level. For quantitative comparison of reference schemes, averaged values of their ranks from ten subjects are shown in the table.

Thus, the following three classes of reference schemes were found:

- (1) Reference electrodes A12, P1, P2, and Sym (average ranks of 9.7, 8.6, 8.3, and 7.2) are characterized by the highest similarity of the topography with all other references.
- (2) Reference electrodes 2Sh, C, N, A1, Sh2, A2, and Sh1 (ranks 6.7, 6.6, 6.5, 5.4, 5.4, 4.9, and 4.6) are characterized by less coherent topography.
- (3) Reference electrodes AR and Cz (ranks 4.4 and 2.1) are characterized by the least coherent topography.

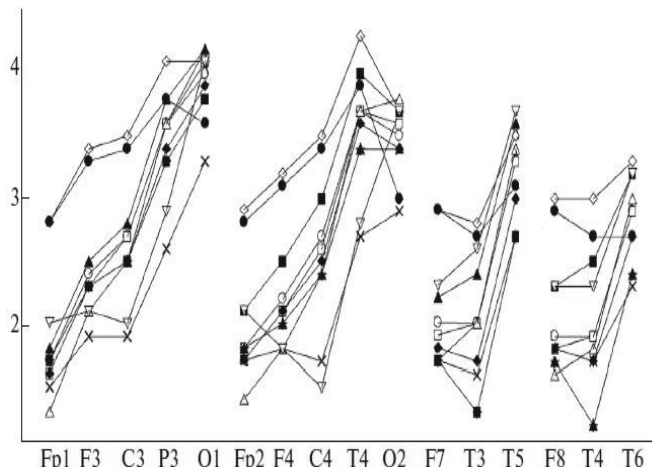


Fig. 4.2. Mean spectral amplitude A_{mean} [μV] in the alpha domain from scalp electrodes (horizontal axis) of a chosen subject in an experiment with an ungrounded base reference electrode at the bottom of the chin ($P2$). This recording was mathematically transformed to 11 reference schemes, whose A_{mean} are shown on 11 diagrams: base reference electrode (circles); upper chin $P1$ (squares), nose N (triangle up), bottom of the neck $Sh1$ (diamonds), top of the neck $Sh2$ (black circles), ear electrodes $A1$ (black squares) and $A2$ (black triangles), united ear $A12$ electrodes (black diamonds), ipsilateral ear electrodes Sym (crosses), averaged electrode AR (oblique crosses), vertex Cz (triangle down). The points are connected by lines on the diagrams according to the sagittal-meridian placement of the electrodes

DISCUSSION

Among the many publications on the subject, small numbers of studies are focused on the comparison of actual reference schemes used in research and clinical practice (it is discussed in [15, 16]). Most studies are concerned with general characteristics of the problem and discuss the views of previous authors and present new mathematical methods for the calculation of virtual reference electrodes that rather have theoretical research value than the actual use and verification in practice. They propose methods and compare them with other analogs and selected actual reference electrodes, mostly with AR, or rarely A12 [6,10,13,17,18] using the examples of simulation signals and selected EEG records [19]. The results are illustrated by examples of EEG records, the amplitude spectra, power spectra, and topographic maps, which in turn are compared and evaluated on the basis of visual inspection with a purely qualitative verbal assessments and conclusions [4,6,9,10,12,16,18,20]. Some studies implement quantitative assessment of correlations, means, and signal/noise ratio and illustrate them with timeline charts, scattering diagrams, and bar charts with standard errors [8,21] also discussed mainly with qualitative assessments. And only few papers present the statistical analysis of hypotheses, pairwise comparisons by Student's t-test and ANOVA [13,17,22], which, however, do not relate to differences of complex reference schemes but only their local aspects. Thus, despite the 65-year discussion of the problem, no quantitative criteria have been developed to compare and evaluate the benefits of using various EEG reference electrodes.

In contrast, our task was to assess the impact of existing reference electrodes used in research and clinical practice on the EEG topography. For comparison of the topographic proximity of reference schemes, we used three orthogonal parameters and a new classification technique. On this basis, the studied reference electrodes were divided into three classes according to their proximity and differences in the topography of distribution of the mean spectral amplitude on the scalp. The reliability of such a classification is statistically valid. In this study, we also investigated for the first time the effect of the grounded (electrically neutral) reference electrodes in order to identify the advantages of their use.

Table 4.1. Mean ranks of topographic coherency of 13 reference schemes in ten subjects with their clustering results and discriminant verification

Averaged correlations between references							
Basic reference Ch2 (bottom of chin)							
Reference	Ch2	Bc	2Nc	Ch1 N	Nc2	Nc1	A1
Δ mean	0.89			0.87 0.82	0.85 0.74	0.85	
$\Delta\Delta$ mean1	0.63			0.59 0.14	0.65 0.61	0.58	
$\Delta\Delta$ mean2	0.73			0.72 0.65	0.72 0.73	0.42	
Basic reference Bc (top of back)							
Δ mean		0.82		0.82 0.79	0.77 0.52	0.75	
$\Delta\Delta$ mean1		0.50		0.52 0.51	0.21 0.44	0.81	
$\Delta\Delta$ mean2		0.79		0.84 0.81	0.75 0.38	0.82	
Basic reference 2Nc (united neck)							
Δ mean				0.88 0.88 0.87	0.85 0.82	0.77	
$\Delta\Delta$ mean1				0.50 0.58 0.54	0.50 0.48	0.13	
$\Delta\Delta$ mean2				0.81 0.79 0.75	0.74 0.58	0.80	
Ranks							
Δ mean	11			9.5 4	7.5 2	7.5	
$\Delta\Delta$ mean1	9.5			7.5 4	7.5 9.5	2	

Averaged correlations between references							
Basic reference Ch2 (bottom of chin)							
Reference	Ch2	Bc	2Nc	A2	A12	Sym	AR
Δ mean	0.89			0.83 0.87	0.84 0.78	0.51	
$\Delta\Delta$ mean1	0.63			0.57 0.67	0.62 0.53	0.21	
$\Delta\Delta$ mean2	0.73			0.25 0.74	0.68 0.68	0.51	
Basic reference Bc (top of back)							
Δ mean		0.82		0.74 0.83	0.77 0.62	0.46	
$\Delta\Delta$ mean1		0.50		0.95 0.51	0.16 0.55	0.26	
$\Delta\Delta$ mean2		0.79		.78 0.84	0.82 0.69	0.63	
Basic reference 2Nc (united neck)							
Δ mean				0.88 0.84 0.88	0.83 0.70	0.51	
$\Delta\Delta$ mean1				0.50 0.25 0.55	.45 0.59	0.35	
$\Delta\Delta$ mean2				0.81 0.81 0.82	0.83 0.58	0.31	
Ranks							
Δ mean	11			5 9.5	6 3	1	
$\Delta\Delta$ mean1	9.5			1 11	5.5 5.5	3	

Reference electrode	<i>P2</i>	<i>C</i>	<i>2Sh</i>	<i>P1</i>	<i>N</i>	<i>Sh2</i>	<i>Sh1</i>	<i>A1</i>	<i>A2</i>	<i>A12</i>	Sym	AR	Cz
1	9.83	7.17	8.33	8.56	6.22	6.11	4.22	4.44	5.06	9.89	6.39	4.67	2
2	10.67	9.33	8.67	9.78	7.56	5.33	3.67	3.44	3.56	10.44	6.89	4.33	1.44
3	5.67	5.67	8	8.89	6.22	4.33	2.44	5.33	4.67	10.06	8.44	5.72	3.44
4	8.67	2.67	4.33	8.67	6.44	4.22	5.22	8	6.33	8.89	8.89	2.89	1.22
5	10.5	6.33	5	9.17	7.67	5.44	4.89	5.11	5	9.56	7.56	3	1.33
6	5.33	9.67	4.67	9	6.89	4.67	3.33	6.11	4.44	10.22	8.33	4.33	2.11
7	10	8	4.33	8	5.33	4	2.78	6.22	5.78	9.11	8.33	6.11	2.89
8	9	6	5.33	9.11	8.78	7	3.33	3.33	4.67	10	5.78	4.22	3
9	11	7.67	10	5.78	4.33	7.22	7.78	6.33	4.67	9.11	7.89	2.06	1.28
10	2.67	3.67	8	8.67	5.56	5.78	8.56	5.78	5	10.11	3.11	6.56	2.11
Mean	8.33	6.62	6.67	8.56	6.5	5.41	4.62	5.41	4.92	9.74	7.16	4.39	2.08
Cluster	1	2	2	1	2	2	2	2	2	1	1	3	3
D^2 Mahalanobis	7.5	8.57	8.57	7.5	8.57	8.57	8.57	8.57	8.57	7.5	7.5	5	5
<i>P</i>	0.68	0.57	0.57	0.68	0.57	0.57	0.57	0.57	0.57	0.68	0.68	0.89	0.89

CONCLUSIONS

- (1) We found no benefits in using either grounded or ungrounded basic reference electrodes. These conditions can be considered equivalent in terms of preserving the topography of EEG potentials that reduce the relevance of the tasks of searching and mathematical construction of an infinitely distant neutral reference electrode.
- (2) Reference electrodes *A1*, *Sh2*, *A2*, *Sh1*, AR, and Cz (in descending ranks order) are characterized by great topographic differences; thus, their use can lead to inconsistency of the results and conclusions.
- (3) The reference electrodes with the most coordinated EEG topography include *A12*, *P1*, *P2*, and Sym. Taking into account the first conclusion, we assumed that these reference electrodes provide the most adequate EEG topography. Regarding the most commonly used *A12* reference, the EEG correlations with proximal to *A1* and *A2* electrodes T3 and T4 are quite strong: approximately 0.75–0.8. However, the correlation with *A1*–*A2* is substantially weaker, approximately 0.35–0.45, and approximately 0.17–0.2 for the T3 and T4. Therefore, the combining of the ear electrodes does not lead to any significant distortions in the “true” topography of EEG potentials.

REFERENCES

1. Nunez, P.L., Electric Fields of the Brain: The Neuro- physics of EEG, New York: Oxford Univ. Press, 1981.
2. Teplan, M., Fundamentals of EEG measurement, *Meas. Sci. Rev.*, 2002, vol. 2, sect. 2, pp. 1– 11.
3. Schiff, S.J., Dangerous phase, *Neuroinformatics*, 2006, vol. 3, no. 4, pp. 315–318.
4. Stephenson, W.A. and Gibbs, F.A., A balanced non- cephalic reference electrode, *Electroencephalogr. Clin. Neurophysiol.*, 1951, no. 3, pp. 237–240.
5. Wolpaw, J.R. and Wood, C.C., Scalp distribution of human auditory evoked potentials. evaluation of reference electrode sites, *Electroencephalogr. Clin. Neuro- physiol.*, 1982, vol. 54, no. 1, pp. 15–24.
6. Hu, S., Cao, Y., Chen, S., Kong, W., Zhang, J., Li, X., and Zhang, Y., Independence verification for reference signal under neck of human body in EEG recordings, *Proc. 31th Chinese Control Conf.*, Hefei (July 25–27,2912), 2012, pp. 4038–4042.
7. Geselowitz, D.B., The zero of potential, *IEEE Eng. Med. Biol. Mag.*, 1998, vol. 17, no. 1, pp. 128–132.
8. Yao, D., A method to standardize a reference of scalp EEG recordings to a point at infinity, *Physiol. Meas.*, 2001, vol. 22, no. 4, pp. 693–711.
9. Madhu, N., Ranta, R., Maillard, L., and Koessler, L.A., Unified treatment of the reference estimation problem in depth EEG recordings, *Med. Biol. Eng. Comput.*, 2012, vol. 50, no. 10, pp. 1003–1015.
10. Hu, S., Cao, Y., Chen, S., Zhang, J., Kong, W., Yang, K., et al., A comparative study of two reference estimation methods in EEG recording, *Proc. Brain Inspired Cognit. Syst.*, 2012, pp. 321–328.
11. Hjorth, B., An on-line transformation of EEG scalp potentials into orthogonal source derivations, *Electroencephalogr. Clin. Neurophysiol.*, 1975, vol. 39, no. 5, pp. 526–530.
12. Carvalhaes, C.G. and Suppes, P., A spline framework for estimating the EEG surface Laplacian using the Euclidean metric, *Neural. Comput.*, 2011, vol. 23, no. 11, pp. 2974–3000.
13. Lepage, K.Q., Kramer, M.A., and Chu, C.J., A statistically robust EEG re-referencing procedure to mitigate reference effect, *J. Neurosci. Methods*, 2014, vol. 235, no. 30, pp. 101–116.
14. Kayser, J. and Tenke, C.E., In search of the Rosetta Stone for scalp EEG: converging on reference-free techniques, *Clin. Neurophysiol.*, 2010, vol. 121, no. 12, pp. 1973–1975.

15. Ng, S.C. and Raveendran, P., Comparison of different montages on to EEG classification, Proc. 3rd Kuala Lumpur Int. Conf. on Biomedical Engineering 2006, Biomed 2006, 11–14 Dec. 2006, Kuala Lumpur, Malaysia, Berlin: Springer, 2007, pp. 365–368.
16. Alhaddad, M.J., Common average reference (CAR) improves P300 speller, Int. J. Eng. Technol., 2012, vol.2, no. 3, pp. 451–463.
17. Qin, Y., Xu, P., and Yao, D., A comparative study of different references for EEG default mode network: the use of the infinity reference, Clin. Neurophysiol., 2010, vol. 121, no. 12, pp. 1981–1991.
18. Wang, B., Wang, X., Ikeda, A., Nagamin, T., Shiba- saki, H., and Nakamuraea, M., Automatic reference selection for quantitative EEG interpretation: identification of diffuse/localised activity and the active earlobe reference, iterative detection of the distribution of EEG rhythms, Med. Eng. Phys., 2014, vol. 36, no. 1, pp. 88–95.
19. Tenke, C.E. and Kayser, J., Reference-free quantification of EEG spectra: combining current source density (CSD) and frequency principal components analysis (fPCA), Clin. Neurophysiol., 2005, vol. 116, no. 12, pp.2826–2846.
20. Marzett, L., Nolte, G., Perrucci, M.G., Romani, G.L., and Del Gratta, C., The use of standardized infinity reference in EEG coherency studies, NeuroImage, 2007, vol. 36, no. 1, pp. 48–63.
21. Essl, M. and Rappelsberger, P., EEG coherence and reference signals: experimental results and mathematical explanations, Med. Biol. Eng. Comput., 1998, vol. 36, no. 4, pp. 399–406.
22. Hagemann, D., Naumann, E., and Thayer, J.F., The quest for the EEG reference revisited: a glance from brain asymmetry research, Psychophysiology, 2001, vol. 38, no. 5, pp. 847–857.

CHAPTER 8

SOFTWARE TOOLS FOR EEG COMPLEX GROUP ANALYSIS

ABSTRACT

The paper considers the possibilities and procedure for working with a freely distributed program Conan-EEG for Windows 7-10 that provides automatic group analysis of EEG recordings based on the most informative indicators of EEG amplitude and synchronicity with the removal of blinks and similar distortions.

Keywords: EEG synchronicity, EEG amplitude, blink artifacts, frequency domains, individual and group differences, depression, sleep stages, schizophrenia, factor analysis, cluster analysis, discriminant analysis.

The Conan-EEG program performs automatic group analysis of EEG recordings using indicators that are most effective for identifying intergroup and individual differences. It was created at Moscow State University and is a modification of the CONAN complex electrophysiological laboratory [1], which has been used in hundreds of Russian scientific and educational organizations since the early 90s.

The program implements the analysis of EEG correlation synchronicity, analysis of EEG amplitudes by derivations, removal of blink artifacts and similar distortions.

The program is distributed under the free license of The Free Software Definition and can be downloaded from the MSU website https://neurobiology.ru/res/ResourceFile/212/FILE_FILENAME/conan-EEG.zip.

At the beginning of the work, it is necessary to create the Blinks folder on disk C, into which to rewrite the EEG recordings files of examinees/patients intended for analysis in EDF format, which must meet

the requirements of the EDF+ standard and be accurately tested by EDF Checker and Polyman. All the results of working with the program will be placed in this folder.

The analysis of EEG correlation synchronicity

This method, created in 2010, has shown its high sensitivity in recognizing inter-individual and group differences (norm and schizophrenia, depressive disorders, sleep stages, etc. [2-5]), surpassing in this respect all known EEG indicators and ensuring the reliability of differentiation of the compared groups approaching 100%.

After starting the program, press the "2" key. After the message about the completion of the procedure, the AKS-Alpha.txt file will appear in the Blinks folder which includes the table "columns – file names, rows - pairs of derivations" with correlation synchronicity coefficients (values in % of 1) calculated for alpha or other current frequency range (AKS-Delta.txt, AKS-Teta.txt etc.).

The correct analysis of EEG amplitude

After starting the program, press the "4" key. After the message about the completion of the procedure, the DiapFiles.txt file will appear in the Blinks folder containing a matrix of results: rows – subjects, columns – EEG amplitudes by derivations. Recall that amplitude estimates are devoid of many errors inherent in frequently used EEG power estimates [6].

The correct removal of blinks and similar distortions [7]

Attention. There must be Fp1 or F3 derivation in the records. After starting the program, press the "0" key. After the message about the completion of the procedure, take the corrected files from the Blinks folder.

Before restarting the analysis, the text files of the results should be deleted from the Blinks folder.

Additional features:



Fig.1. EEG analysis menu

- **Selection of the frequency domains of the analysis.** Press the "1" key and in the EEG analysis menu (Fig.1), set the required domain according to the flip list **Диап= Alpha**, then cancel the menu. After that, the calculated synchronicities will be written to a file with the name of this range. The set range will be valid until the next change.
- **Changing frequency domains.** Press the "1" key and in the EEG analysis menu that appears, press the **А=Диапазоны** button. In the table that appears, change the number, names, and boundaries of the frequency domains. Using the write and read buttons, these settings can be archived and then read, if necessary, without manual adjustments. The set domains will be valid until the next change.
- **Changing the list of derivation pairs.** The calculation of synchronicity is performed according to a set list of derivation pairs. To create a new list, you should use any text editor to create a line-by-line list of derivation pairs separated by a space. Save the file in the program folder in text format (*.txt), then change its type to .csg (initially there are already three similar files and they can be viewed for review). To change the current list of pairs, press the "1" key, in the EEG analysis form that appears, perform

8=Синхронность then **Пары отведений** (Fig.2) and among the list of files of the type.csg select the desired one, then cancel the menu. The set pairs will be valid until the next change.

- **Analysis of a single record.** Press the "F3" key and read the desired EEG recording file from the list. Press the "1" key to open the EEG analysis form, in which two continuations are possible.

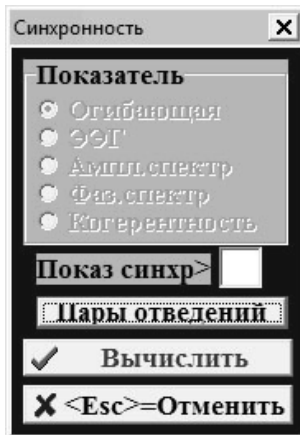


Fig.2. Synchronicity analysis menu

1. Press **8=Синхронность** button. and in synchronicity analysis menu (Fig.2) press **Вычислить** button then the diagram of synchronicities in the order of derivation pairs and the color map of the distribution of synchronicities on the scalp will be displayed (Fig.3). If you right-click on this diagram and select the **Экспорт в буфер обмена** item from the following list then the values X, Y will be transferred to the **Показ синхр>** clipboard. If in the right input field of synchronicity menu set some threshold value (less than 1, e.g. 0.5), then only over-threshold synchronicity estimates will be present on the diagram and map. To re-analyze the same record, you need to read its file again.

2. Press the **2=Диа** button and in the right half-

window you will see the diagram of average EEG amplitudes in frequency domains in the order of derivations and the color topographic maps of their distribution on the scalp (Fig.4). When you right-click in this half-window,

a context menu appears in which, by clicking the  button, the values of the column diagrams can be saved in a text file under the name of the read EEG record.

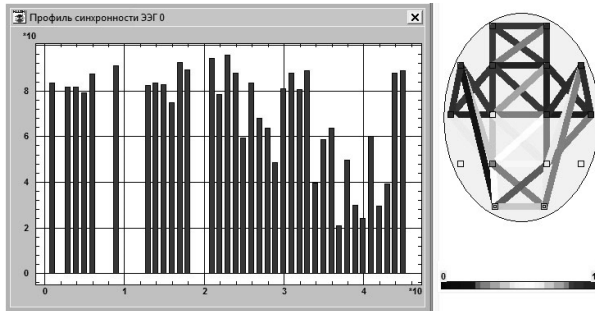


Fig.3. Results of synchronicity analysis

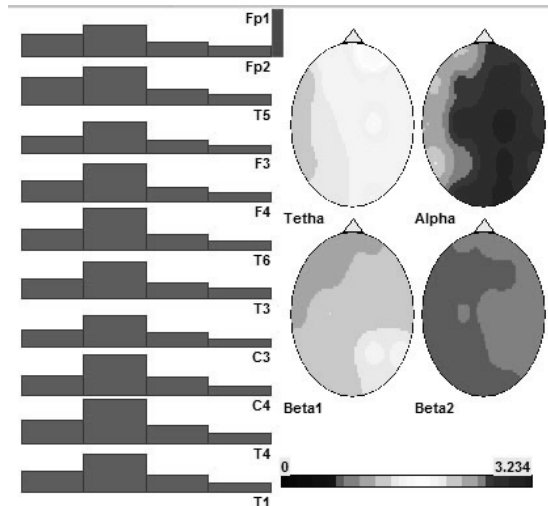


Fig.4. Results of amplitude analysis

Statistical analysis of results

So, as a result of the program, the matrices of the results of the examinees/patients-indicators are obtained. Researchers are usually interested in identifying differences (social, age, gender, ethnic, functional, clinical, etc.) between two groups of subjects.

The first step may be to identify paired differences between columns or rows according to known statistical criteria. Further, each file can be individually subjected to factor analysis, to study the main factors and the initial variables, mainly projected on them. On this basis, you can try to choose a meaningful interpretation of the main factors. It is also possible to visually study the projections of objects (subjects) on the plane of the main factors for the uniformity of their changes or the presence of some separate groupings. In the latter case, using a divisive cluster analysis strategy, you can try to divide objects into an estimated number of classes and verify this separation using discriminant analysis.

The total matrix with two groups of subjects can also be subjected to a discriminant analysis to verify its division into two groups. If such a classification turns out to be reliable and the number of incorrectly classified subjects is small, then this will be a convincing argument that the EEG synchronicity in the two groups as a whole differs significantly. In addition, the calculated discriminating function can be used to assign new indeterminate subjects to a particular group.

REFERENCES

1. Kulaichev A.P. Computer electrophysiology and functional diagnostics (textbook for classical university education). 5th ed. revised and supplemented. Moscow: INFRA-M, 2018. 469 p.
2. Kulaichev A.P. The new method of assessing EEG synchrony is the best instrument for identifying interindividual and intergroup differences. 2021. *Neurology & Neuroscience*. 2(3):1-7.
3. Kulaichev A.P., Gorbachevskaya N.L. Differentiation of Norm and Disorders of Schizophrenic Spectrum by Analysis of EEG Correlation Synchrony. *J.Exp.Integr.Med.*, 2013. 3(4):267-278.
4. Kulaichev A.P., Iznak A.F., Iznak E.V., Kornilov V.V., Sorokin S.A. Changes in EEG correlation synchronicity in depressive disorders of the psychogenic type. *Zh Vyssh Nerv Deiat Im I. P. Pavlova*, 2014, 64(2):1-9.

5. Kulaichev A.P. Comparative analysis of correlation synchronicity and amplitude ratios of EEG in night sleep. *Zh Vyssh Nerv Deiat Im I. P. Pavlova*. 2012. 62(1): 108–119.
6. Kulaichev A.P. Inaccuracy of Estimates of Mean EEG Amplitude in Frequency Domains Based on Amplitude and Power. *Spectrum. Int. J Psychol. Brain Sci.* 2016, (1) 2: 21-28.
7. Kulaichev A.P. Method of local, non-distorting EEG rhythm removal of blink artifacts. *Act.Probl.Hum.Nat.Sci.* 2018.11(117): 31-40.